DISCLAIMER

This report was prepared as an account of work sponsored by an agency of the United States Government. Neither the United States Government nor any agency thereof, nor any of their employees, makes any warranty, express or implied, or assumes any legal liability or responsibility for the accuracy, completeness, or usefulness of any information, apparatus, product, or process disclosed, or represents that its use would not infringe privately owned rights. Reference herein to any specific commercial product, process, or service by trade name, trademark, manufacturer, or otherwise does not necessarily constitute or imply its endorsement, recommendation, or favoring by the United States Government or any agency thereof. The views and opinions of authors expressed herein do not necessarily state or reflect those of the United States Government or any agency thereof.

PNL-5782
UC-66d

FIELD TESTS OF CORROSION AND CHEMICAL SENSORS FOR GEOTHERMAL POWER PLANTS

PNL--5782

DE86 008312

R. J. Robertus
D. W. Shannon
R. G. Sullivan
D. B. Mackey
O. H. Koski
F. O. McBarron
J. L. Duce
D. D. Pierce

March 1986

Prepared for
the U.S. Department of Energy
Under Contract DE-AC06-76RLO 1830

Pacific Northwest Laboratory
Richland, Washington 99352

MASTER

DISTRIBUTION OF THIS DOCUMENT IS UNLIMITED

DISCLAIMER

This report was prepared as an account of work sponsored by an agency of the United States Government. Neither the United States Government nor any agency Thereof, nor any of their employees, makes any warranty, express or implied, or assumes any legal liability or responsibility for the accuracy, completeness, or usefulness of any information, apparatus, product, or process disclosed, or represents that its use would not infringe privately owned rights. Reference herein to any specific commercial product, process, or service by trade name, trademark, manufacturer, or otherwise does not necessarily constitute or imply its endorsement, recommendation, or favoring by the United States Government or any agency thereof. The views and opinions of authors expressed herein do not necessarily state or reflect those of the United States Government or any agency thereof.

DISCLAIMER

Portions of this document may be illegible in electronic image products. Images are produced from the best available original document.

ACKNOWLEDGMENTS

First we would like to acknowledge the assistance of Gladys Hooper and Tony Adduci of the U.S. Department of Energy who helped with all the program management and administration. We gratefully acknowledge the financial support of the U.S. Department of Energy who financed this work under Contract DE-AC06-76RLO 1830.

The cooperation and assistance of the Magma Electric Company and its employees were instrumental in making the project happen. Special recognition goes to Russ Tenney, Dennis Downs, Michael Pierce, and Jeff Brown who donated time and equipment to the project.

The pH probe tests were made possible by the efforts of Bob Taylor from Leeds and Northrup Corporation and by Len Niedrach and Bill Stoddard from the General Electric Company.

SUMMARY

This report summarizes approximately two years of continuous monitoring of corrosion (and other variables that affect corrosion) in a 10-megawatt binary cycle geothermal power plant. The project goal was to develop methods for detecting adverse plant conditions soon enough to prevent equipment failures. The test procedures and instruments were developed by Pacific Northwest Laboratory[a] (PNL) for use in the 50-megawatt geothermal power plant at Heber, California.

The instruments tested were:

- Resistance-type corrosion probes (four in the brine system and four in the hydrocarbon system)
- Linear polarization corrosion probes (one at the plant brine inlet and one at the plant brine outlet). (All the corrosion probe locations contained weight-loss coupons, which provided a check on the probe readings.)
- Oxidation/reduction potential (ORP) probes for oxygen detection (one at the plant brine inlet and one at the plant brine outlet)
- High-temperature pH electrodes (several at the plant outlet with valving to monitor the plant inlet)
- Electrodeless conductivity cells for gas bubble detection (one at the plant brine inlet and one at the plant brine outlet).

The resistance corrosion probe elements are commercially available and have been built into a housing that can be inserted and retrieved under pressure. The linear polarization probes use commercial electronics with a high-temperature cell built at PNL. The others are prototype instruments still under development. Pacific Northwest Laboratory built most of the prototypes but actively sought commercial development of the designs.

---

[a] Pacific Northwest Laboratory located in Richland, Washington, is operated for the U.S. Department of Energy by Battelle Memorial Institute under Contract DE-AC06-76RLO 1830.

Some specific accomplishments include:

- The resistance corrosion probes were tested and shown to be useful indicators of corrosion in the brine system.
- Electrical problems on the linear polarization corrosion probes were solved; the latest high-temperature cells have over two years of successful operating experience.
- Methods for inserting/removing corrosion coupons and probes while the plant is on-line were perfected.
- The ORP probe was functional and responded to ppb levels of oxygen in the brine.
- The conductivity probe responded very well to changes in salinity and can be designed to detect gas bubble formation.

A qualitative evaluation of all the instruments is:

Instrument	Functionality	Reliability
Resistance Corrosion	Fair-Good	Fair
Linear Polarization	Good	Fair-Good
Oxidation Reduction Potential	Good	Fair[a]
High-Temperature pH (Ceramic)	Not Established	Poor
High-Temperature pH (Solid State)	Not Established	Not Established
Conductivity (For Salinity Changes)	Very Good	Very Good
(Gas Bubble Detection)	Fair[b]	Good

[a] Reference electrode life must be improved.

[b] One temporary design worked well.

CONTENTS

ACKNOWLEDGMENTS. iii

SUMMARY. v

1.0 INTRODUCTION 1.1

2.0 CONCLUSIONS. 2.1

3.0 DESCRIPTIONS 3.1

3.1 TEST FACILITY 3.1

3.2 DATA ACQUISITION SYSTEM AND SCHEDULE. 3.1

3.3 TEST PROCEDURES. 3.4

3.4 DATA PRESENTATION FORMAT 3.4

4.0 INSTRUMENT TEST RESULTS 4.1

4.1 CONTINUOUS CORROSION MONITORS 4.2

4.1.1 History of Some Resistance Probes 4.18
4.1.2 Linear Polarization Corrosion Probes 4.21

4.2 CORROSION COUPONS 4.23

4.3 pH 4.26

4.3.1 Ceramic pH Probe Testing Procedures and Results . . 4.30
4.3.2 Solid-State pH Electrode Testing 4.44

4.4 OXIDATION-REDUCTION POTENTIAL CELL (ORP PROBE). . . . 4.49

4.5 CONDUCTIVITY 4.57

5.0 REFERENCES 5.1

FIGURES

3.1.1	Instrument Test Loop	3.2
3.3.1	Monitoring Station on Brine System	3.5
4.1.1	Type of Linear Polarization Corrosion Probe	4.3
4.1.2	PNL High-Temperature Geothermal Linear Polarization Probe	4.4
4.1.3	Electrical Resistance Corrosion Probe With Coupons	4.5
4.1.4	Complete Monitoring System	4.6
4.1.5	Corrosion Probe Locations	4.8
4.1.6	Plant Brine Inlet Corrosion	4.9
4.1.7	Warm Brine Corrosion	4.10
4.1.8	Cool Brine Corrosion	4.11
4.1.9	Plant Brine Outlet Corrosion	4.12
4.1.10	Life of One Corrosion Probe at Plant Outlet	4.13
4.1.11	Cool Isobutane Liquid Corrosion	4.14
4.1.12	Hot Isobutane Liquid Corrosion	4.15
4.1.13	Hot Isobutane Vapor Corrosion	4.16
4.1.14	Cool Isobutane Vapor Corrosion	4.17
4.1.15	Linear Polarization Probe Response to Acidity Changes	4.24
4.1.16	"Instantaneous" Plant Inlet Corrosion	4.25
4.2.1	Coupon Corrosion Rates in Brine System	4.29
4.3.1	Schematic Diagram of Ceramic pH Sensor	4.31
4.3.2	Solid State pH Sensor	4.32
4.3.3	System for Evaluating Sensors With Simulated Geothermal Brines	4.33
4.3.4	PNL "Pumped" External Reference Electrode	4.36

4.3.5	Data From First Field Test of Ceramic pH Probes. . . .	4.38
4.3.6	Ceramic PNL pH Probe Responses	4.39
4.3.7	Response of Other PNL pH Probes	4.40
4.3.8	Response of Industrial (Y74-BJ) Ceramic pH Probe . . .	4.41
4.3.9	Response of Industrial (NGK-B4) Ceramic pH Probe . . .	4.42
4.3.10	Response of Industrial (NGK-E1-BJ) Ceramic pH Probe . .	4.43
4.3.11	pH Probe Response to a Calibration Sequence	4.45
4.3.12	pH Probe Response to Buffer Solutions	4.46
4.3.13	Structure of an Ion Sensitive Field Effect Transistor.	4.47
4.3.14	Schematic of ISFET Operation	4.48
4.3.15	Solid State pH Probe (1) Response	4.50
4.3.16	Solid State pH Probe (2) Response	4.51
4.4.1	Oxidation Reduction Potential Probe	4.52
4.4.2	ORP Probe Response to Oxygen Injection	4.53
4.4.3	Plant Inlet Oxidation/Reduction Potential	4.55
4.4.4	Plant Outlet Oxidation/Reduction	4.56
4.5.1	Submersible Electrodeless Conductivity Cell	4.58
4.5.2	High-Pressure/High-Temperature Electrodeless Flow-Through Conductivity Cell.	4.59
4.5.3	Literature and Experimental Conductivity Values . . .	4.60
4.5.4	Recorder Trace From Conductivity Cell	4.63
4.5.5	Plant Inlet Conductivity	4.65
4.5.6	Plant Outlet Conductivity	4.66

1.0 INTRODUCTION

The direct causes of geothermal plant failures are obvious when they occur--the pipe or heat exchanger has holes in it, the lines are plugged or the injection well will not accept waste brine. The problem that led to the failure is often not obvious; without data recording, it may not be possible to determine how the problem developed. In many cases, these types of failures in hydrothermal power plants have caused multimillion dollar repair costs and extensive down time. In addition to financial losses (over $100,000/day for a 55 MWe plant), these failures cause doubts about the economic viability of geothermal power.

In general, the causes of silica, calcite, and sulfide scaling are understood. Scaling results from operating choices made by the plant designer or operator who has regarded the brine as distilled water rather than a complex mixture of corrosive elements. Scale control involves understanding the behavior of minor elements in the brine--especially silica, calcium, and CO_2 and their interactions with brine temperature, pressure, and time after production. In Table 1.1, the chemistry of two wells at Cerro Prieto is given; one well scales up and one does not. The difference is the behavior of the CO_2 content of the brines at the steam separator operating pressures.

Uniform corrosion of carbon steel is also understood. Usually corrosion results from acidic (pH < 7) conditions or man-made air intrusions and the presence or absence of protective films on the metal. There are some conditions of nonuniform corrosion (e.g., pitting) where further research is needed to define the causes. The problems with plant failures due to corrosion or scaling are aggravated when a condition that developed over a period of time suddenly causes a plant shutdown. Operating personnel tend to look at the conditions at the time of failure rather than conditions that existed for some time.

TABLE 1.1. Geothermal Well Data, Cerro Prieto, Mexico[a]

Parameter	M30 "Does Not Scale"	M39 "Plugs in 3 Months"
pH at 25°C	8.00	8.05
Na^+, mg/ℓ	7,809	5,417
K^+, mg/ℓ	1,833	901
Ca^{+2}, mg/ℓ	596	404
Ba^{+2}, mg/ℓ	8	9
SiO_2, mg/ℓ	1,077	611
Fe^{+2}, mg/ℓ	0.5	0.6
SO_4^{-2}, mg/ℓ	13	8
HCO_3^-, mg/ℓ	31	148
Cl^-, mg/ℓ	15,173	10,181
CO_2, %	1.08	1.39
H_2S, %	0.15	0.29
Well Head, °C	175	166
Well Head Pressure, psig	113	90
Separator Pressure, psig	101 @ (170°C)	80 @ (162°C)
Total Flow, t/h	227	81
Steam Flow, t/h	57	14

[a] Mercado, Alfredo. Comision Federal De Electricidao Cerro Prieto Geothermal Field, Baja California, Mexico. Personal Communication, August 1977.

The in-line monitoring program at Pacific Northwest Laboratory (PNL) has been directed to developing in-line instruments and monitoring methods to provide continuous recording of important chemical parameters and corrosion. The objectives are:

- Develop methods to detect adverse plant conditions before failures occur,
- Determine what to measure and why,
- Determine where to measure, and
- Determine how to measure.

While such in-line chemical monitoring is common in the chemical and petroleum industries, every currently available commercial instrument we tested for geothermal service in hot brines failed to meet requirements. Clearly we are dealing with a need for technology beyond current commercial practice. Further study is needed to solve the problems. The National Materials Advisory Board (NAS-NAE) was asked by DOE to study these needs in 1978 and the PNL program was based on their findings (Shannon 1978 and NAS-NAE 1978).

An earlier report by Shannon, Elmore, and Pierce (1981) summarized the initial phases of the project. This report deals mostly with activities from 1982 through 1984.

2.0 CONCLUSIONS AND RECOMMENDATIONS

The monitoring program has defined the strengths and weaknesses of several in-line instruments for monitoring chemical, scaling, and corrosion parameters in geothermal brines. Findings include:

- Commercial resistance probes give useful indications of corrosion trends. Actual rates in mils/yr (MPY) compared favorably with coupon rates in the range 0.5 to 20 MPY.
- Commercial linear polarization probes fail rapidly in hot brines. A modified electrode design developed by PNL has worked for over two years without problems. The probe responds rapidly to any changes in corrosion rates. Indicated corrosion rates in MPY are higher than those indicated by either the resistance probes or coupons.
- The oxidation/reduction potential (ORP) probe is an excellent and sensitive detector of oxygen in brines. For commercial applications, a longer-lived and industrially durable reference electrode must be developed.
- High-temperature ceramic pH probes require mechanical and chemical modifications for useful application in geothermal brines. Better reference electrodes are also required.
- Solid-state pH electrodes require further research to solve seal problems. The concept appears promising and deserves further support. Commercial reference electrodes are required here, too.
- The electrodeless conductivity cell responds well to changes in salinity. Further work is needed to incorporate automatic temperature compensation. Significant effort is required to optimize the unit for bubble detection.

Ultimate success of the instrumentation program depends on transferring the technology to industry. Since the geothermal industry is small, other applications must be identified before commercial instrument manufacturers will be interested.

3.0 DESCRIPTIONS

3.1 TEST FACILITY

The instrument test loop is illustrated in Figure 3.1.1. Geothermal brine was collected through a 1/2-in.-diameter tube mounted on a flange through a 1-in. penetration on top of the main 12-in. brine pipe. The flow from the sample tube was routed to the 2-in. vertical pipe tees shown in Figure 3.1.1 where in-line sensors are installed. The vertical U-tube trap kept the electrodes wet with brine even if the main 12-in. line were drained. Clean-out plugs were provided to remove sand. A sample valve permitted connection of cooling coils for collection of brine and gas samples. After passing by the in-line sensors, the brine passed through a small orifice plate where the flow was measured. Generally flows were maintained between 6 and 10 gpm when geothermal brine was flowing in the loop. A second orifice, downstream of the flow measuring plate, was sized to take most of the pressure drop through the loop. This considerably increased the lifetimes of the flow control valves.

When instruments were calibrated, brine flow was stopped and calibration solutions were pumped through the loop. A back pressure control valve was used to maintain pressure on the system. Calibration solutions were generally recirculated with a high-pressure pump. These calibration solutions could be heated to brine inlet temperature using the combination of a brine-to-calibration fluid heat exchanger and an electrically heated pipe section. The electrically heated section was filled with steel spheres to increase the heat transfer area. The complete test facility consisted of the instrument test loop plus a data acquisition system.

3.2 DATA ACQUISITION SYSTEM AND SCHEDULE

The data acquisition system had several monitoring and storage devices. Technical details are omitted here since the components are no longer state-of-the-art and not necessarily recommended item by item. Philosophically, however, the system concept had many desirable features.

All the data were collected on a data logger. This included temperature and pressure measurements as well as outputs from the corrosion instruments (49 channels in all). From here data were sent at 15 minute intervals

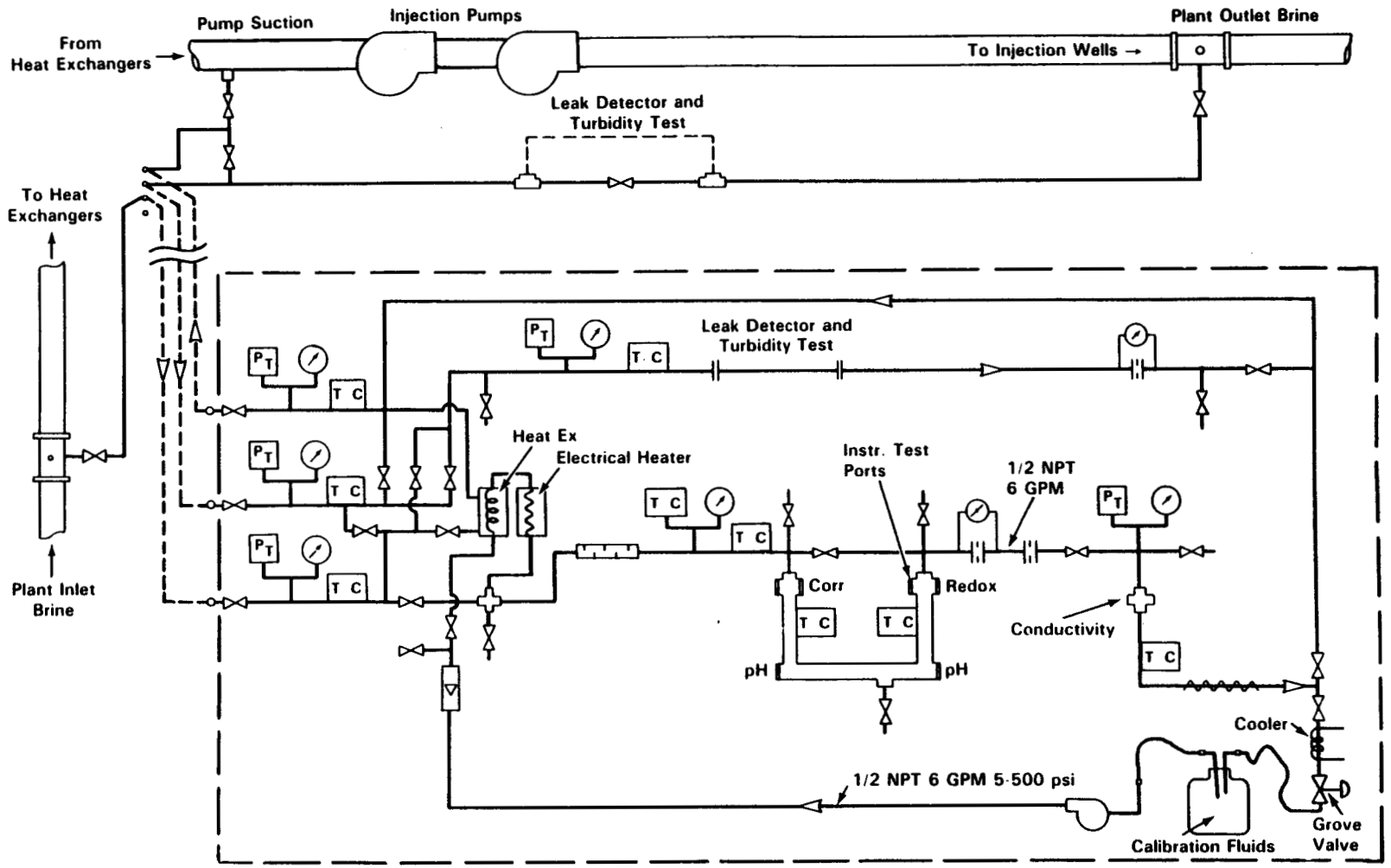

FIGURE 3.1.1. Instrument Test Loop

to a reel-to-reel magnetic recorder. The data were also transmitted to a desk top computer terminal with a cartridge-style magnetic tape. At any given time the terminal had in memory the twelve most recent data logger scans. It maintained a running statistical record of each channel's data (maximum, minimum, average, and standard deviation) for a given 24-hour period. That statistical information was available in memory for the previous day, also. Each day the statistical summaries were written to the tape. This terminal served as the remote interface device. It could be accessed by phone and all the in-memory information could be transmitted. This transmission occurred on a daily basis so we could spot malfunctioning instruments or trouble spots within the plant. The transmission was not automatic. It had to be initiated by someone at PNL's laboratories in Richland, Washington.

The reel-to-reel magnetic tapes were removed periodically and read on a computer at PNL in Richland. This computer generated the plots shown later in this report. Raw voltage data were reduced using appropriate formulas. Any particular time period could be analyzed with this program.

A microcomputer was dedicated to reading the resistance corrosion probes. It did this four times daily. Since signals from the resistance instruments were sent in digital form, the microcomputer also converted the signal to an analog output for the data logger. Each time the microcomputer received data from the resistance probes, it also read the other channels of temperature, pressure, etc. from the data logger. All the information was stored on floppy discs. This provided a third backup for storing information from the data logger. The microcomputer also generated one channel of information that provided a status check of the data acquisition system.

On several occasions one or more of the data storage devices exceeded storage limitations or otherwise malfunctioned. Having the backup systems allowed us to maintain a continuous record of plant events in spite of such problems.

All of the remote data acquisition instruments were powered by a noninterruptible power source. A battery package supplied power for short (up to 10 minutes) power outages. After that, a propane engine-driven generator kicked in automatically to supply power for up to two days.

3.3 TEST PROCEDURES

Test procedures varied depending on the instrument(s) involved. Details will be given as appropriate in the discussions of each instrument. In general, the instruments were first subject to laboratory testing. These tests used simulated brines in autoclaves to determine the temperature and pressure characteristics of the instruments. Prototype instruments that passed the autoclave tests were then subjected to field tests in actual geothermal brines.

The instruments were inserted in either the test loop described in Section 3.1 or in a monitoring station shown in Figure 3.3.1. These monitoring stations were located at the brine inlet to the plant and at the brine outlet from the plant. With the exception of the continuous corrosion probes, all the instruments were tested only in the brine. Instruments in the monitoring stations underwent long-term exposure tests. They could be removed as needed for repair or calibration.

All calibration tests in the field were done in the test loop described earlier. Calibration fluids varied with the instrument being tested, but the fluids were kept as close to the same as possible from one calibration to the next. Calibrations usually involved a matrix of conditions using temperature and solution composition as variables. All calibration solutions were continuously circulated in the test loop. During long calibration sequences, some solutions changed composition slightly. These changes were monitored by analyzing cooled samples of the fluid and were accounted for in the calibration procedure.

3.4 DATA PRESENTATION FORMAT

In general, for all the corrosion probes as well as supporting instruments, absolute readings are less important than changes which occur. More important is the ability to tie instrument readings to real plant events that can explain unusual outputs. Unfortunately, malfunctioning instruments can give responses that look like changing plant conditions. Malfunctions can mislead someone into believing an upset condition occurred. Being able to recognize equipment failure is a necessary part of using and understanding these instruments.

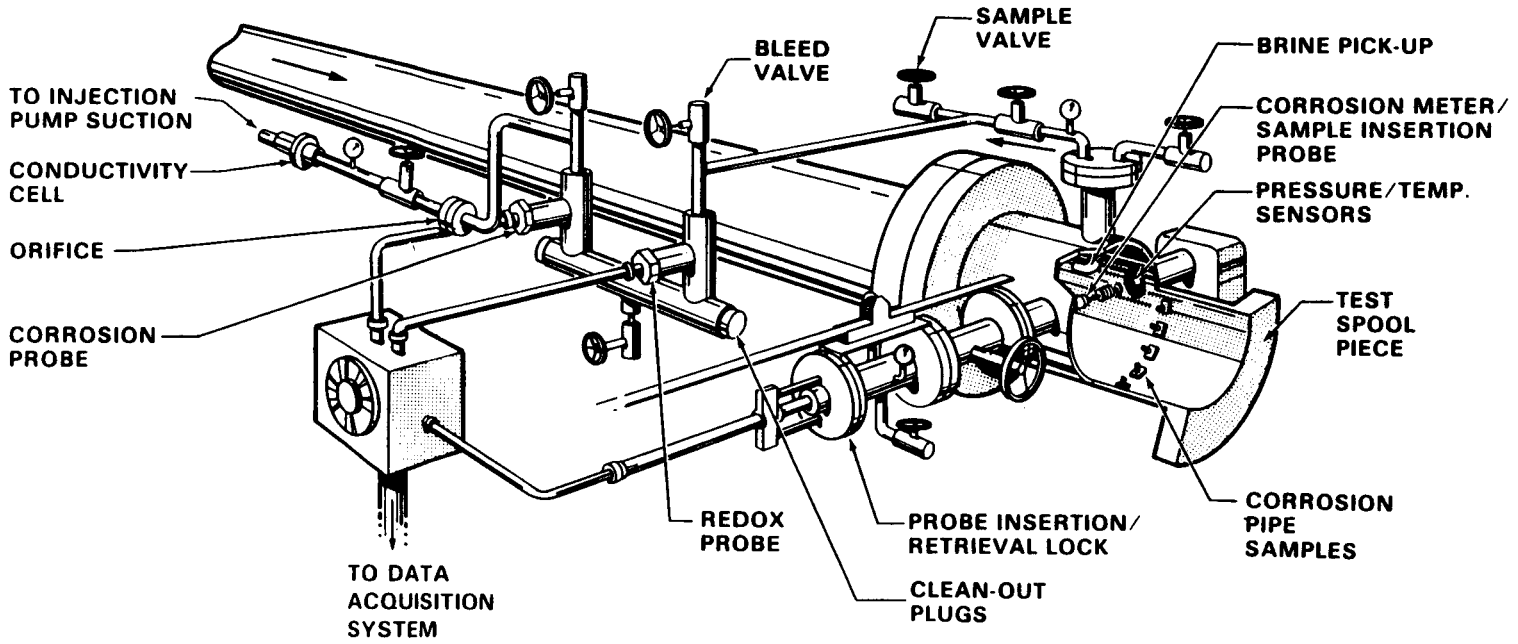

FIGURE 3.3.1. Monitoring Station on Brine System

A vital part of this program was determining the long-term reliability of the instruments. Valuable instruments earn that status by performing well enough and long enough so that plant operators trust the information they generate.

Instrument responses can change for a variety of reasons. A few are listed below:

- Real changes occur and the instrument senses them.
- Mechanical breakdowns cause erroneous readings.
- Electrical malfunctions cause unrealistic readings.
- An instrument is removed from service, so readings temporarily drop to zero.
- An instrument has a slowly deteriorating response.
- Automatic periodic calibration sequences are unrelated to plant upsets.
- The data acquisition system fails.
- No logical explanation exists.

All of the above reasons were needed to interpret the original complete plots for each of the instruments. Later in this report only a small segment of the total testing time for any given instrument is shown. The segments have been chosen to show some representative operating responses to normal events and abnormal events.

4.0 INSTRUMENT TEST RESULTS

One of the objectives of this work was to assist plant operators in diagnosing upset conditions which might increase corrosion rates in geothermal power plants. A part of this objective was to identify the equipment and procedures needed to provide reliable information. Some of those needs became clear as work proceeded. Unlike more traditional instrumentation, many of the devices being tested were unproven in the field. That fact complicated the requirements for usefulness. Still, the following list at least partially identifies characteristics of a good instrumentation system.

- duplicate indicators for the same phenomenon (coupons and resistance corrosion probes respond to long-term corrosion; instantaneous corrosion probes will respond to pH changes; pH and conductivity cells respond to gas breakout; corrosion and redox probes respond to oxygen infiltration)
- periodic calibration to maintain reliability (useful life for most of the instruments is not known)
- backup data acquisition system
- generated plots for selected time intervals (examining tabular data once per day misses slowly meandering responses indicative of some bad instruments)
- daily observation or inspection by someone familiar with the system (numerous unexpected things can happen to void all data for extended periods if not detected soon)
- good records regarding the individual instrument's history (calibration periods, repairs, and replacements must be documented)
- visual display of current data as well as selected other time periods
- remote accessibility by other personnel who need the information
- rugged, reliable, and easy operation.

The individual instrument sections that follow all show some test data which illustrates their usefulness and/or flaws in geothermal systems.

4.1 CONTINUOUS CORROSION MONITORS

In-line corrosion monitors of two commercial types have been tested. The first type used the linear polarization principle to apply a 10 mV potential to an electrode and, from the corrosion current, estimated a corrosion rate that was then displayed in MPY. The polarization probe gave a rapid response (within minutes after conditions changed). These probes worked well in cooling water systems at the test site and were instrumental in detecting several potentially serious events (Shannon et al. 1981). One of the most serious occurred when a cooling water acid injection pump failed to shut off as expected, resulting in the pumping of concentrated sulfuric acid into the condenser system. Because of the corrosion alarm, no damage was done.

However, in high-temperature brine the commercial linear polarization probe failed rapidly. Unfortunately, the mode of failure was to indicate a very low corrosion rate 10 to 100 times below the actual rate. The problem was traced to buildup of iron sulfide corrosion scale on the electrode where it threaded onto the stud as shown in Figure 4.1.1. This introduced a high electrical resistance into the circuit, which led to very low corrosion currents being measured. Various gasket materials were tried to prevent H_2S entry to this threaded region, but under high pressures we decided a more reliable solution was to eliminate the threaded stud and use a solid metal electrode as shown in Figure 4.1.2. This design worked for over two years and has been built into the Heber Binary Demonstration Plant. Standard commercial electronics can be used with the PNL cell if the surface areas of the modified electrodes are the same as the commercial ones.

A second type of commercial probe, one in which the electrical resistance of a thin metal tube changes as it corrodes, was also tested in both brine and hydrocarbon systems (Figure 4.1.3). This probe was installed in a custom-built probe holder with coupons added and was quite useful for long-term monitoring. The measured corrosion rates agreed reasonably well with coupon data except in regions of very low (<0.5 MPY) or very high (>20 MPY) corrosion rates. This may be due to hydrodynamic conditions around the probe or possibly metallurgical differences between the annealed 1018 carbon steel probe material and piping steels. A drawing of the pressure lock system that permits probe insertion and retrieval is shown in Figure 4.1.4.

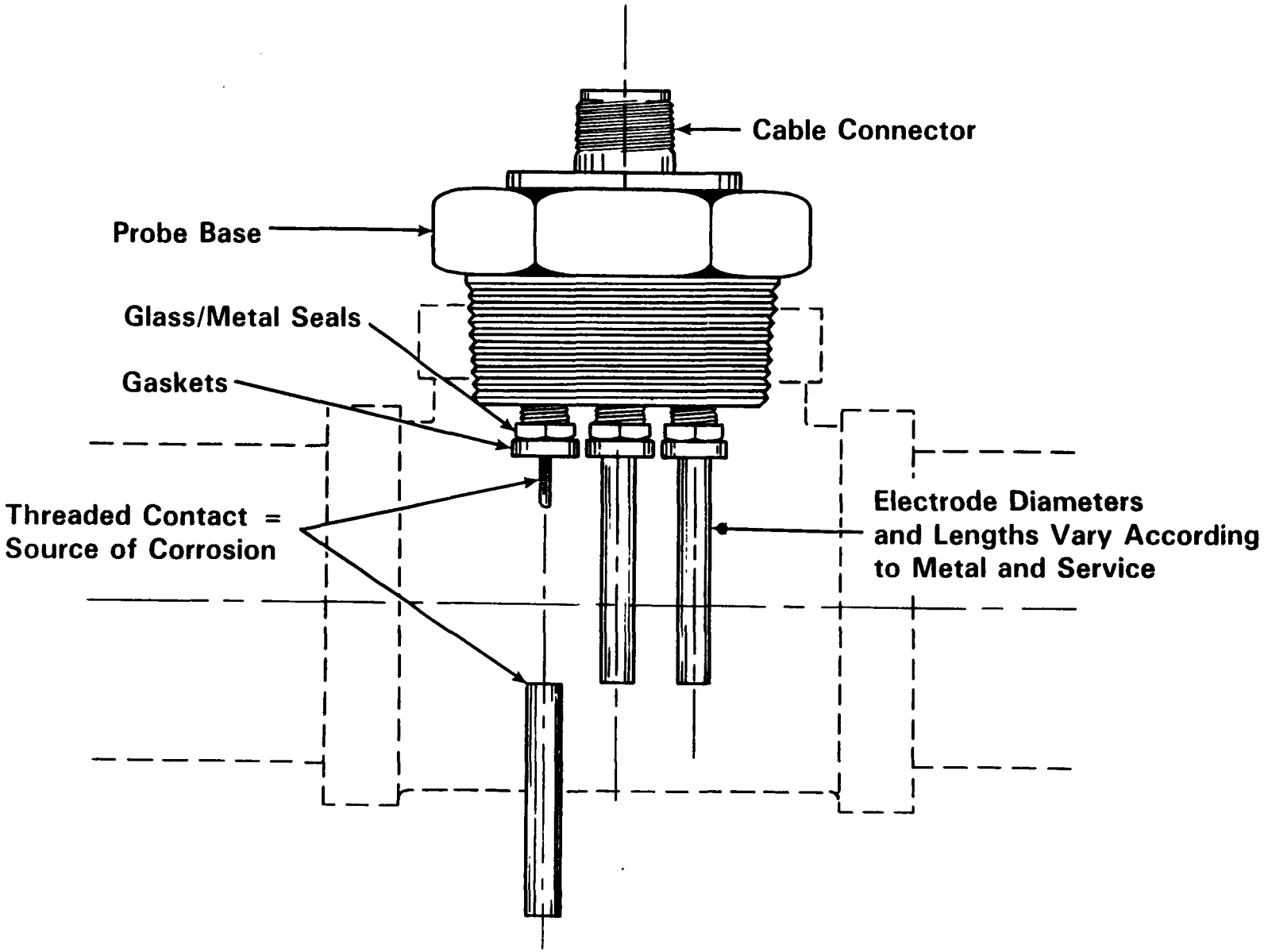

FIGURE 4.1.1. Type of Linear Polarization Corrosion Probe

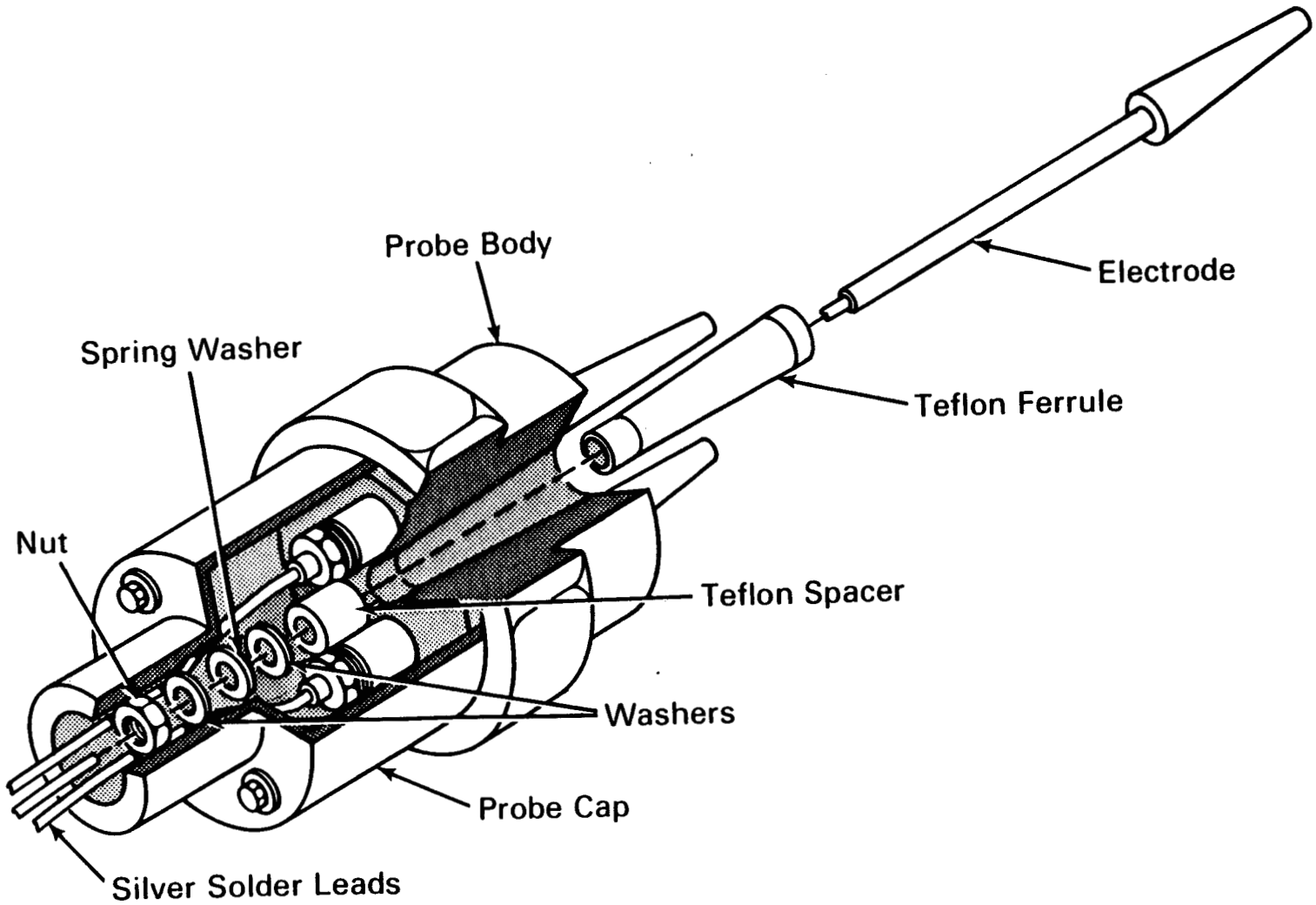

FIGURE 4.1.2. PNL High-Temperature Geothermal Linear Polarization Probe

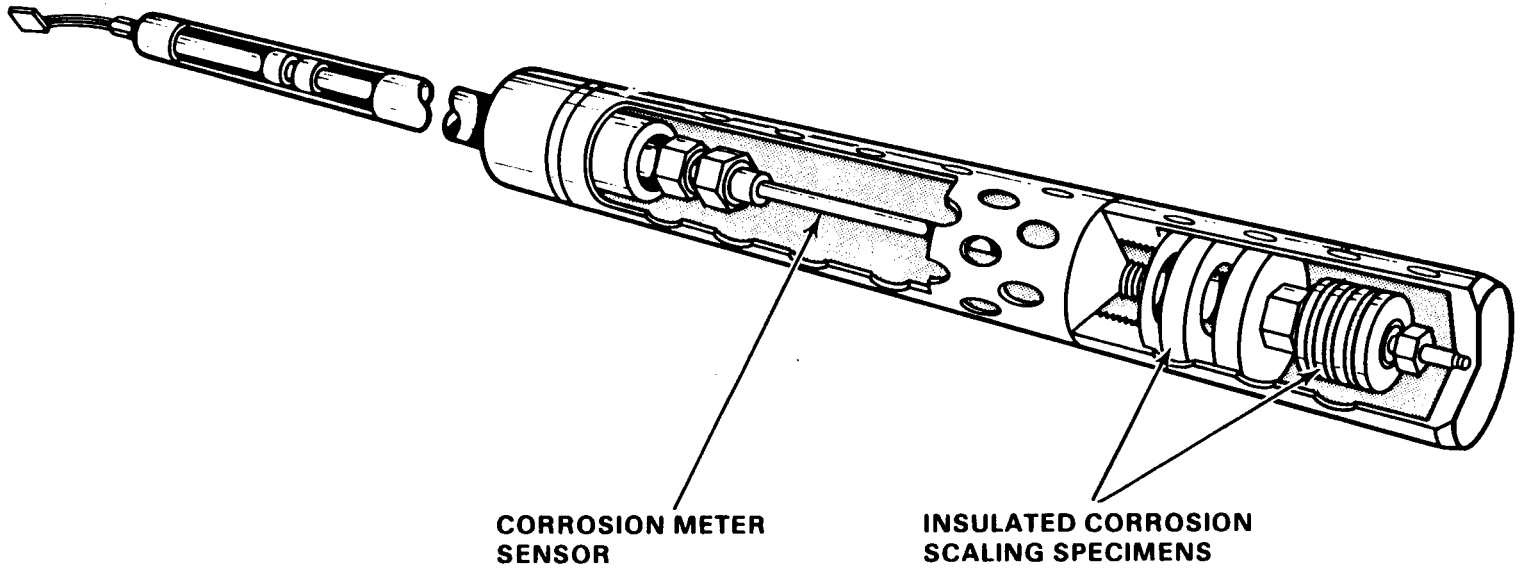

FIGURE 4.1.3. Electrical Resistance Corrosion Probe With Coupons

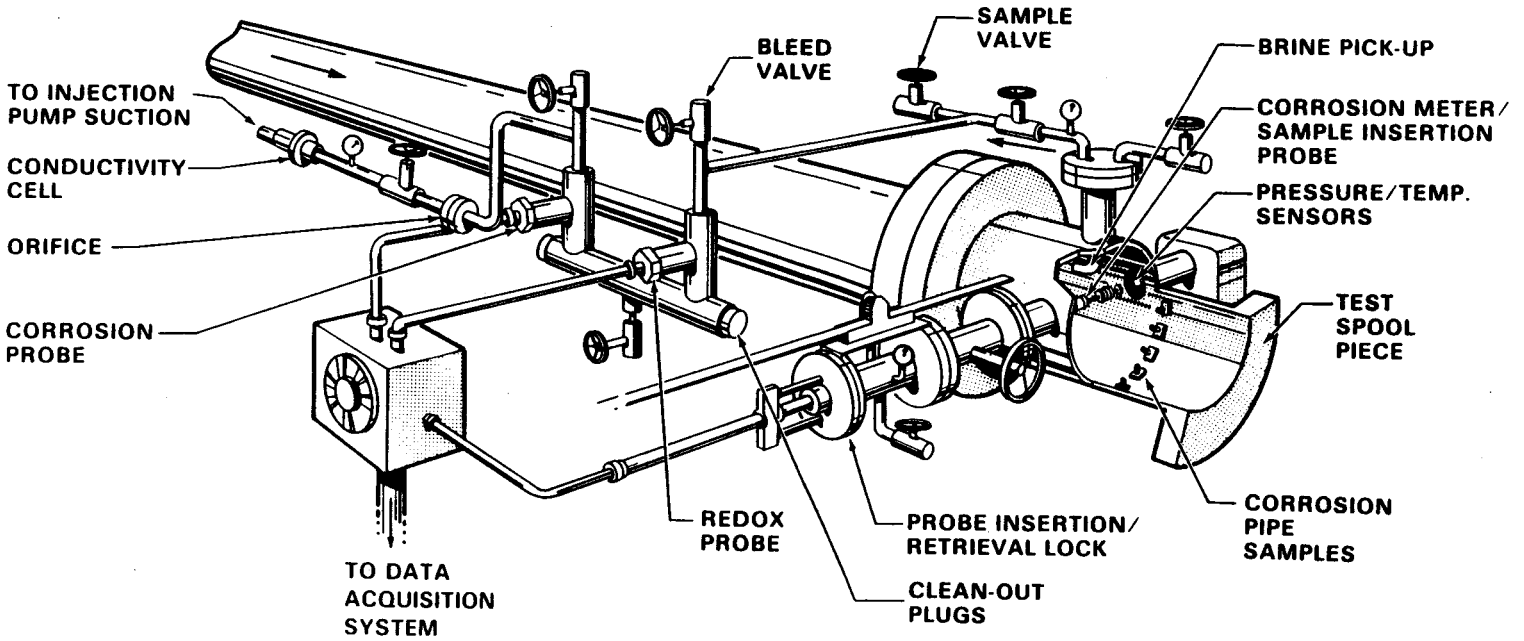

FIGURE 4.1.4. Complete Monitoring System

Previous plant experience provided incentive for monitoring corrosion in the hydrocarbon system. Corrosion on tubes from an earlier heat exchanger design revealed attack on the hydrocarbon side. It was known that water and air had contacted the hydrocarbon side of the tubes for short intervals, primarily during shutdowns. Still, there was some possibility that the hydrocarbon stream itself could be corrosive because of the trace quantities of degradation products it contains. To answer the question, a corrosion monitoring study was initiated.

A total of eight resistance-type corrosion probes were installed in the power plant; four monitored corrosion in the hydrocarbon system and four measured corrosion in the brine system. Locations for the probes are shown in Figure 4.1.5.

The hydrocarbon stations were chosen to monitor cool liquid (1), hot liquid (2), hot vapor (3), and cool vapor (4) in the system. Since no previous work had been done on corrosion in hydrocarbon systems of binary cycle geothermal plants, the effect of temperature was unknown and was investigated in this study. The brine was monitored at the plant inlet (A), the plant outlet (PC2), and two intermediate points (B, C). If problems had been noticed at any particular probe, manual sampling stations could have been used to pinpoint which particular exchanger was the source.

All the isobutane probes had 5 mil useful life (1 mil = 0.001 inches) resistance elements. These thin elements provided good sensitivity to corrosion phenomena but still gave reasonably long lifetimes. Operationally, the probes measure the resistance of a metal element. As metal corroded away, the element's resistance increased and provided a direct measure of the corrosion that had occurred. The probes responded only to uniform corrosion, however, and were not very useful for detecting pitting corrosion (severe pitting is interpreted as uniform). Because brine side corrosion rates were expected to be higher than those for isobutane, elements with 10 mil useful life were used in Locations A, B, C, and PC2.

Table 4.1.1 compares some of the probe and coupon values. Each coupon value is an average of at least three coupons. Example resistance probe readings are shown in Figures 4.1.6 through 4.1.14.

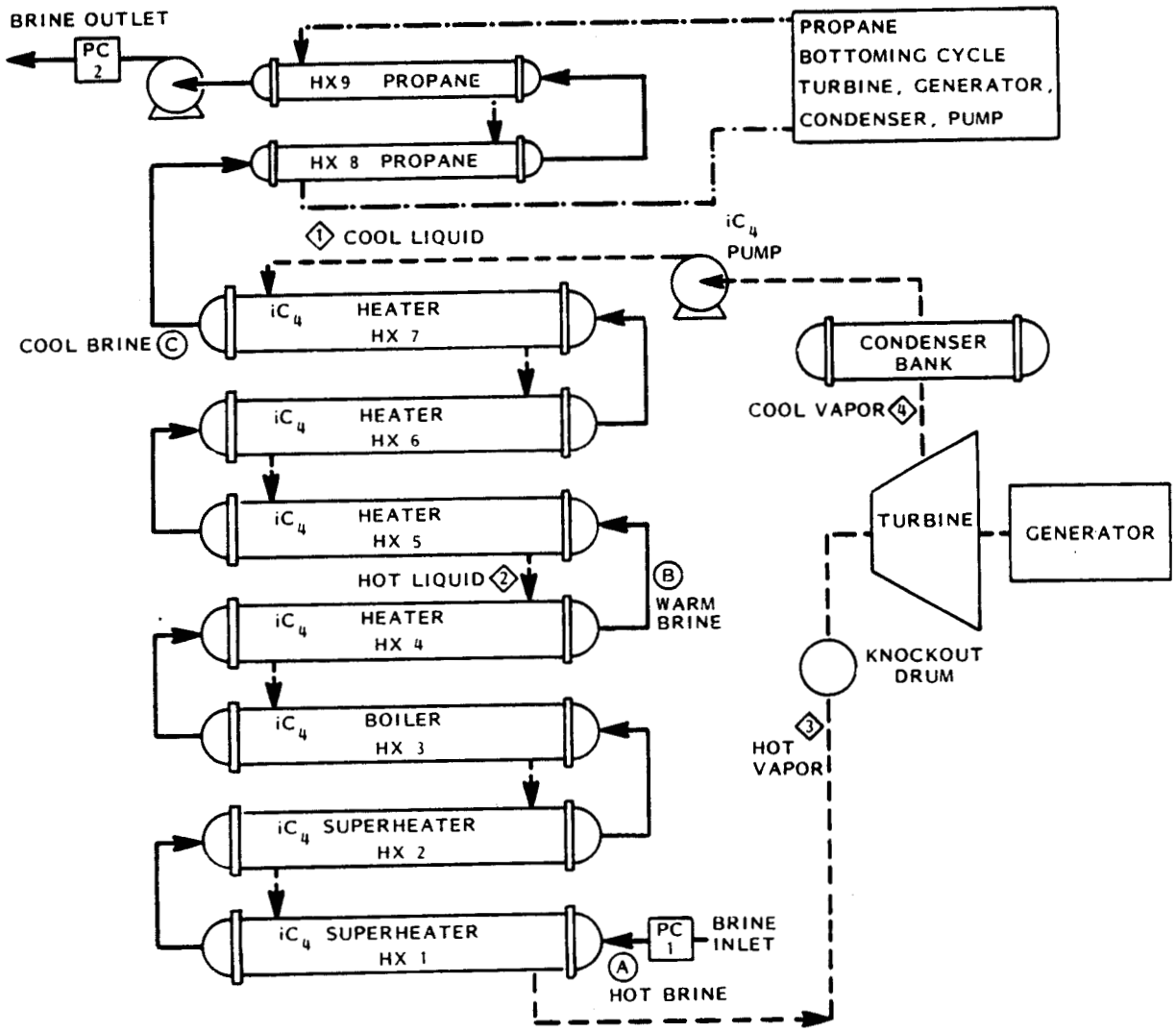

FIGURE 4.1.5. Corrosion Probe Locations

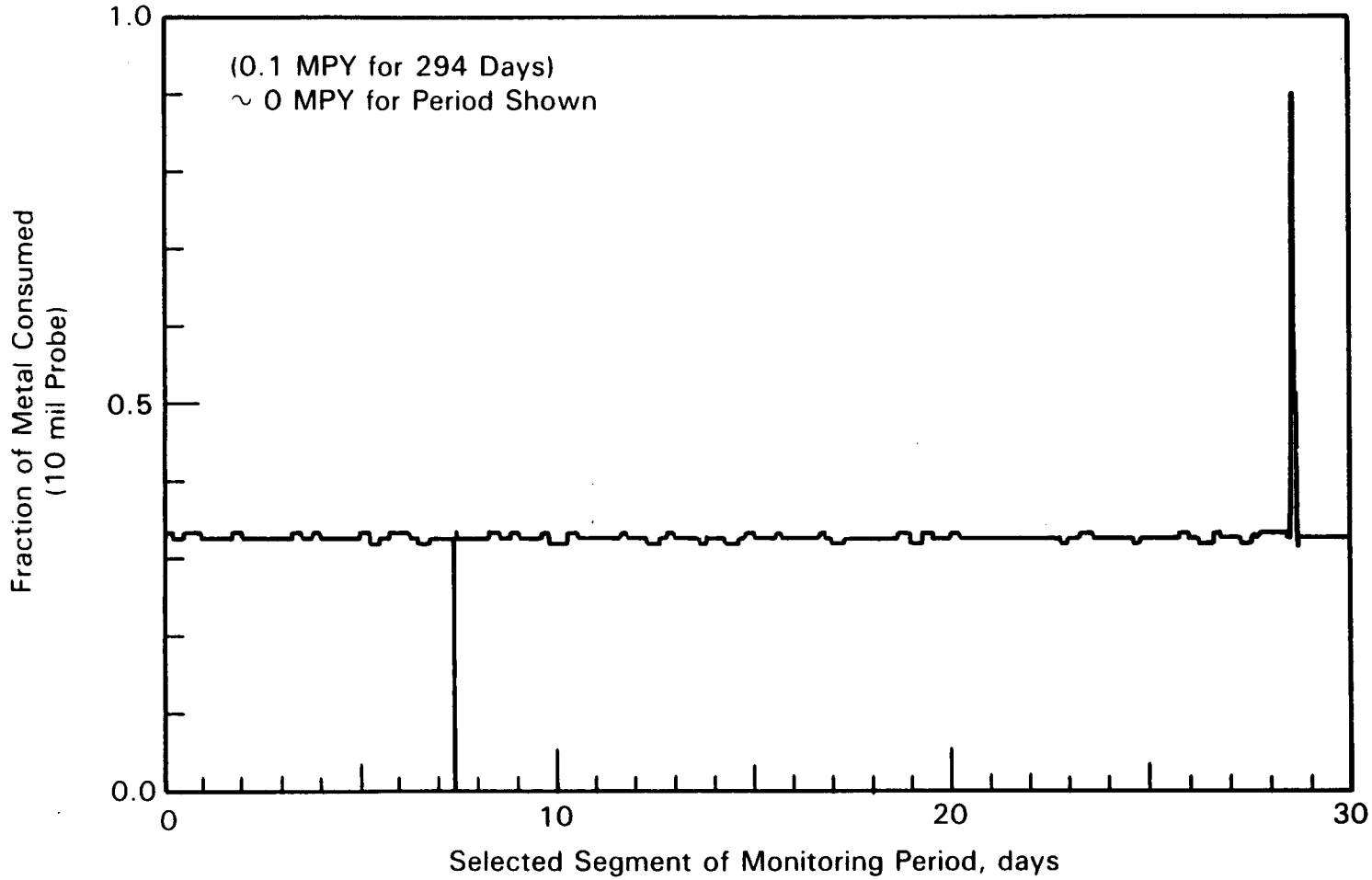

March 14, 1983

FIGURE 4.1.6. Plant Brine Inlet Corrosion

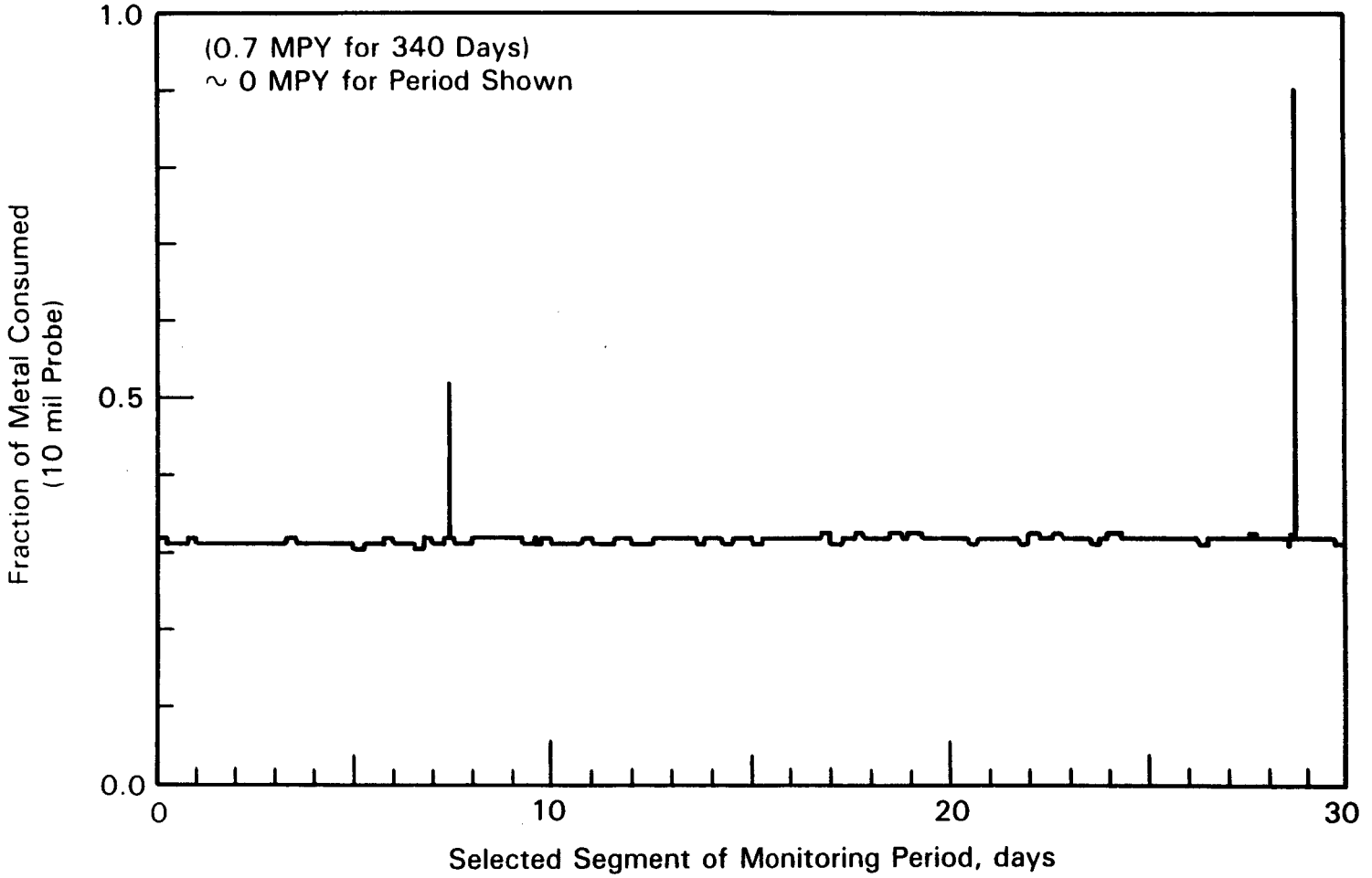

March 14, 1983

FIGURE 4.1.7. Warm Brine Corrosion

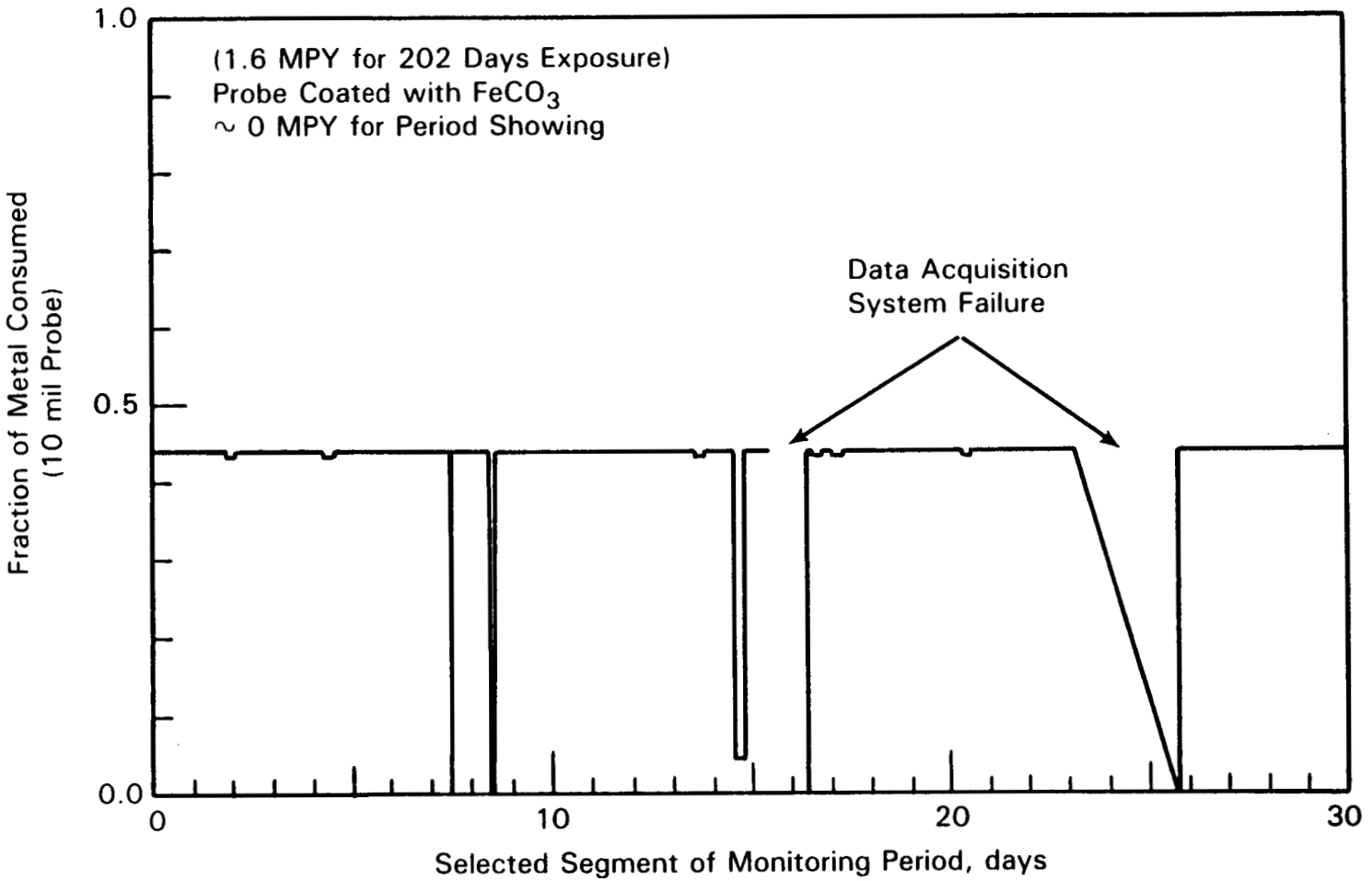

November 25, 1982

FIGURE 4.1.8. Cool Brine Corrosion

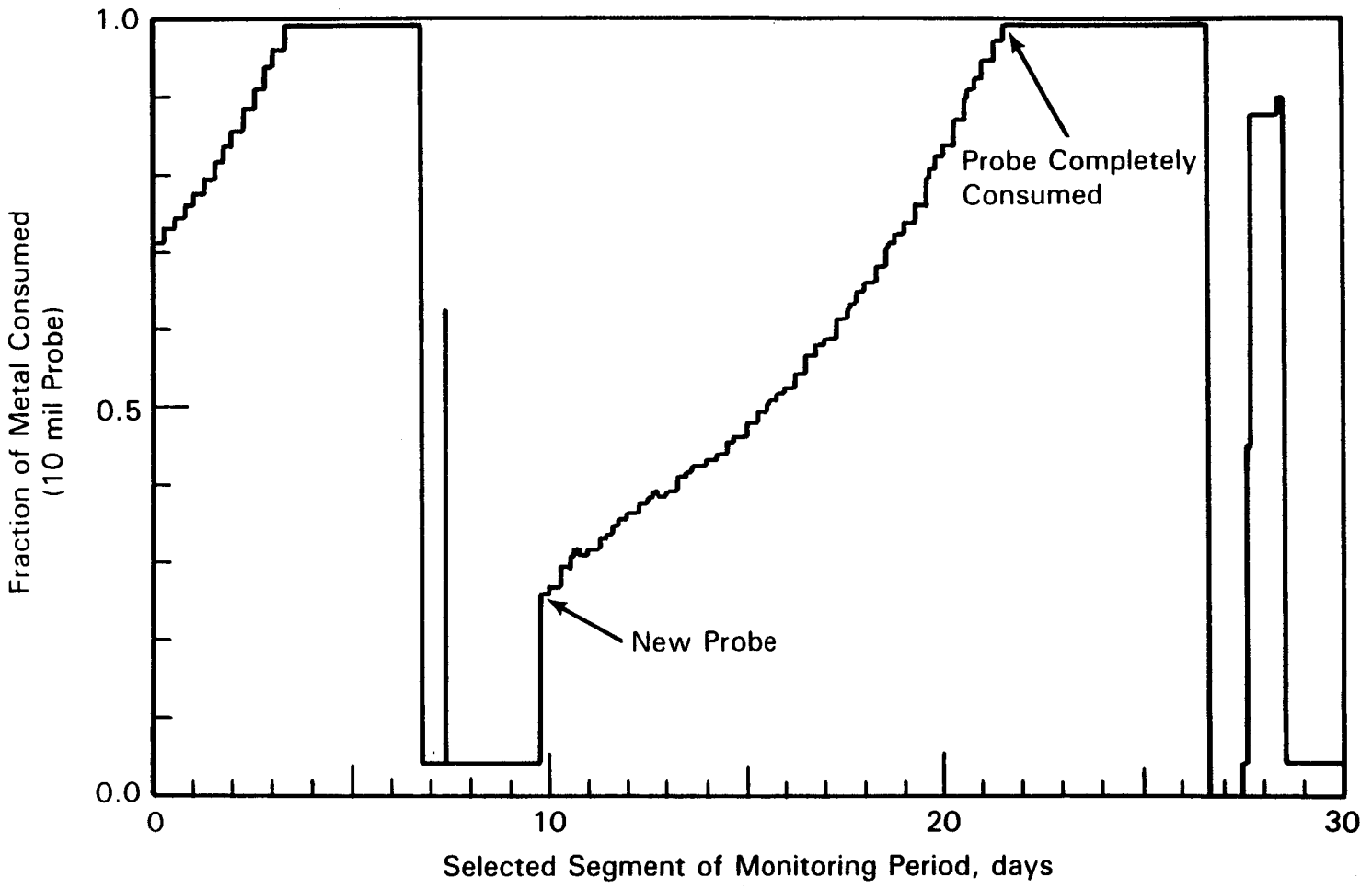

March 14, 1983

FIGURE 4.1.9. Plant Brine Outlet Corrosion

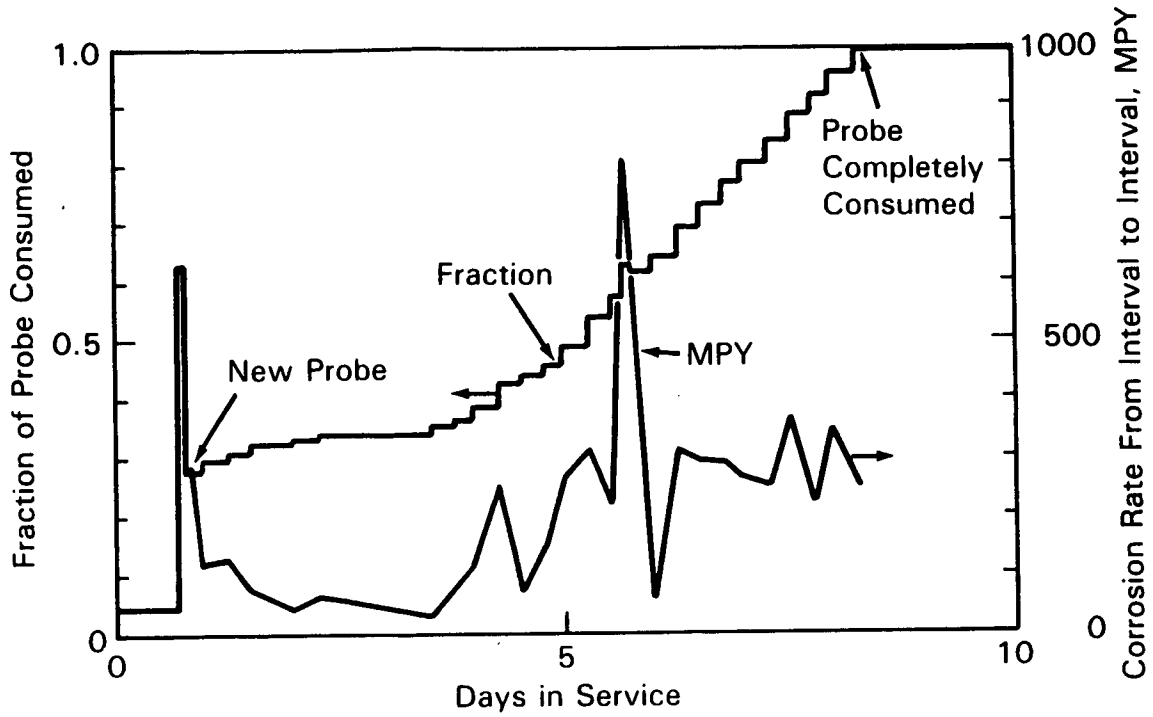

February 11, 1983

FIGURE 4.1.10. Life of One Corrosion Probe at Plant Outlet

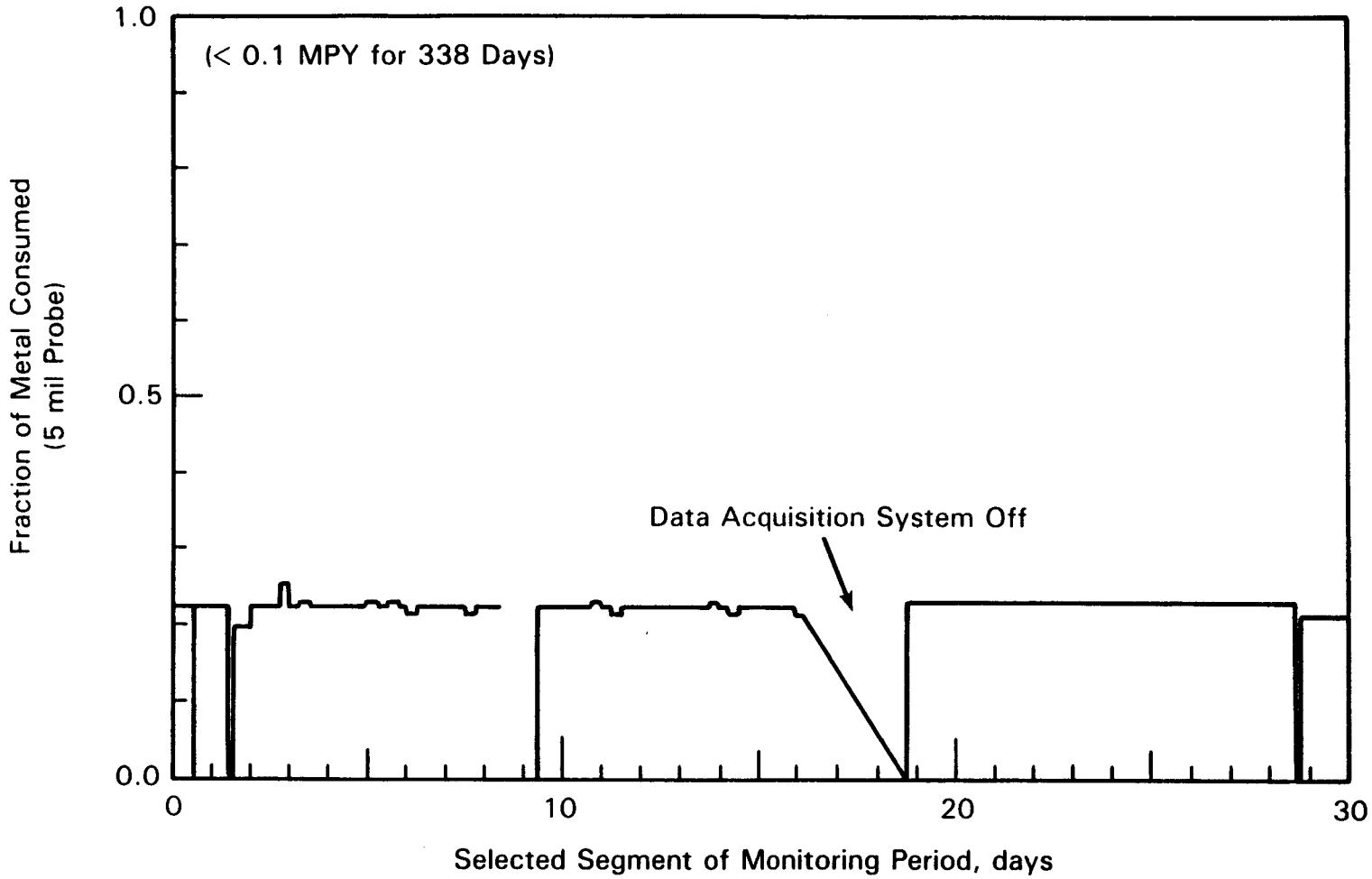

December 2, 1982

FIGURE 4.1.11. Cool Isobutane Liquid Corrosion

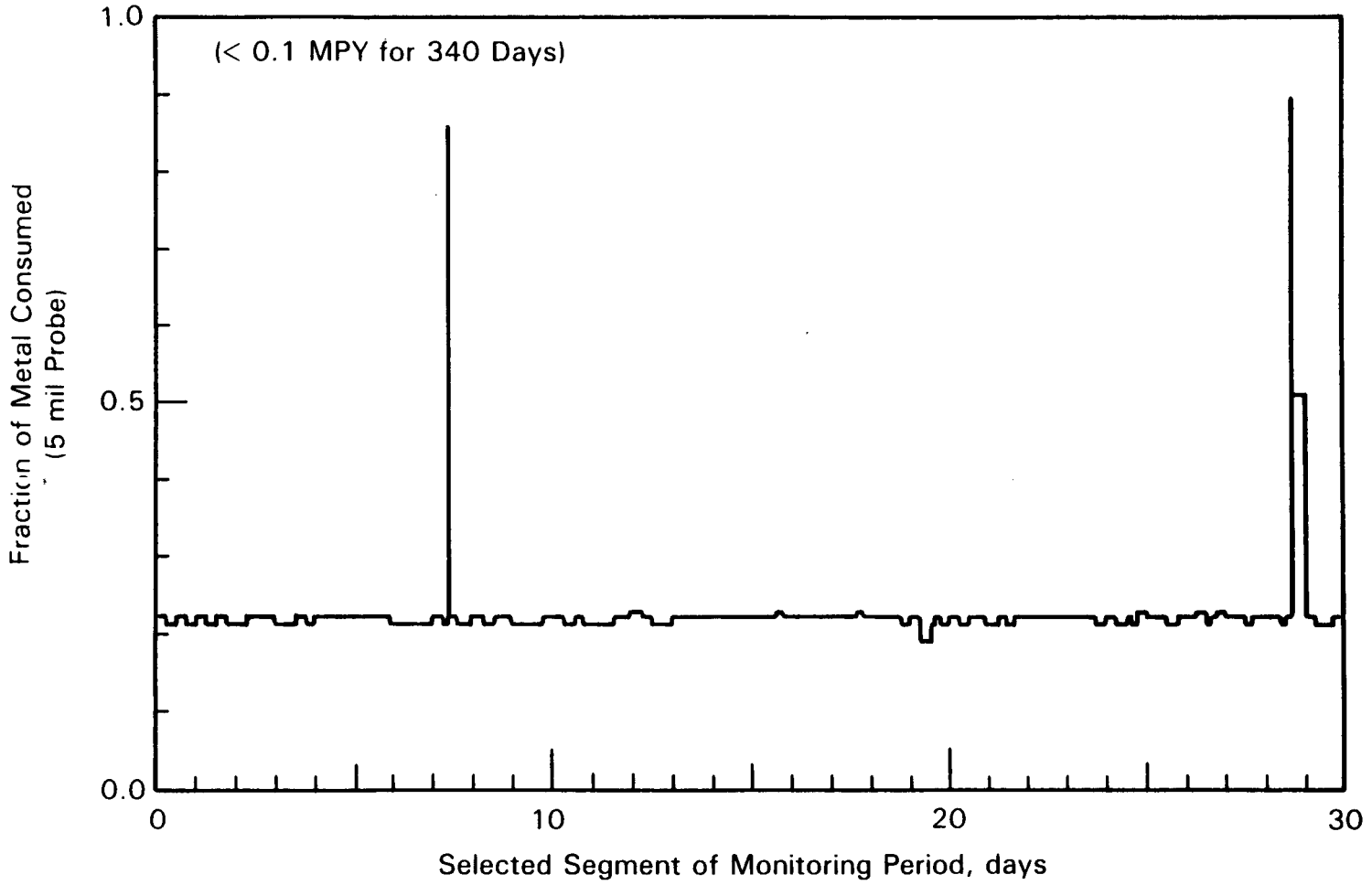

March 14, 1983

FIGURE 4.1.12. Hot Isobutane Liquid Corrosion

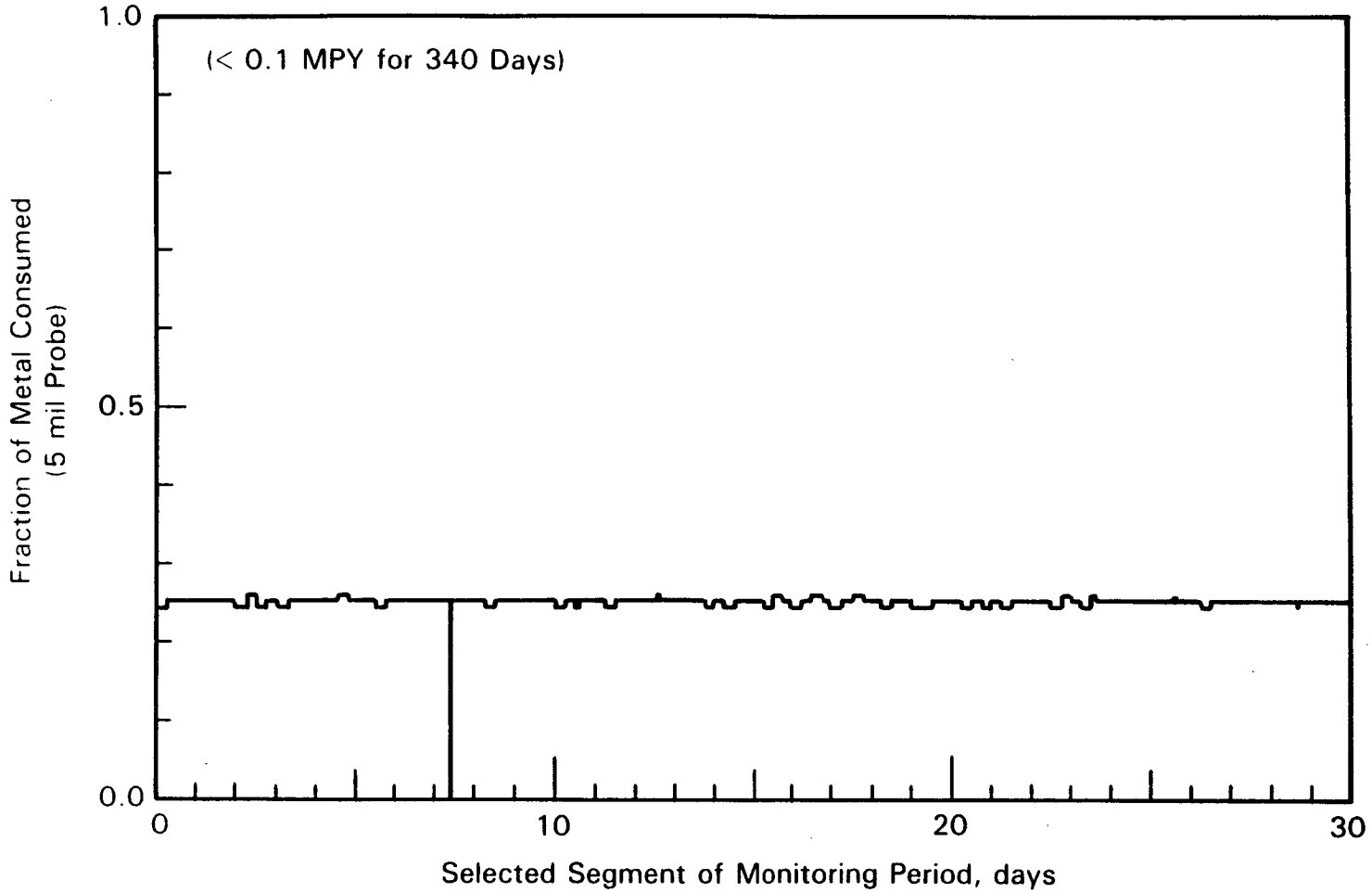

March 14, 1983

FIGURE 4.1.13. Hot Isobutane Vapor Corrosion

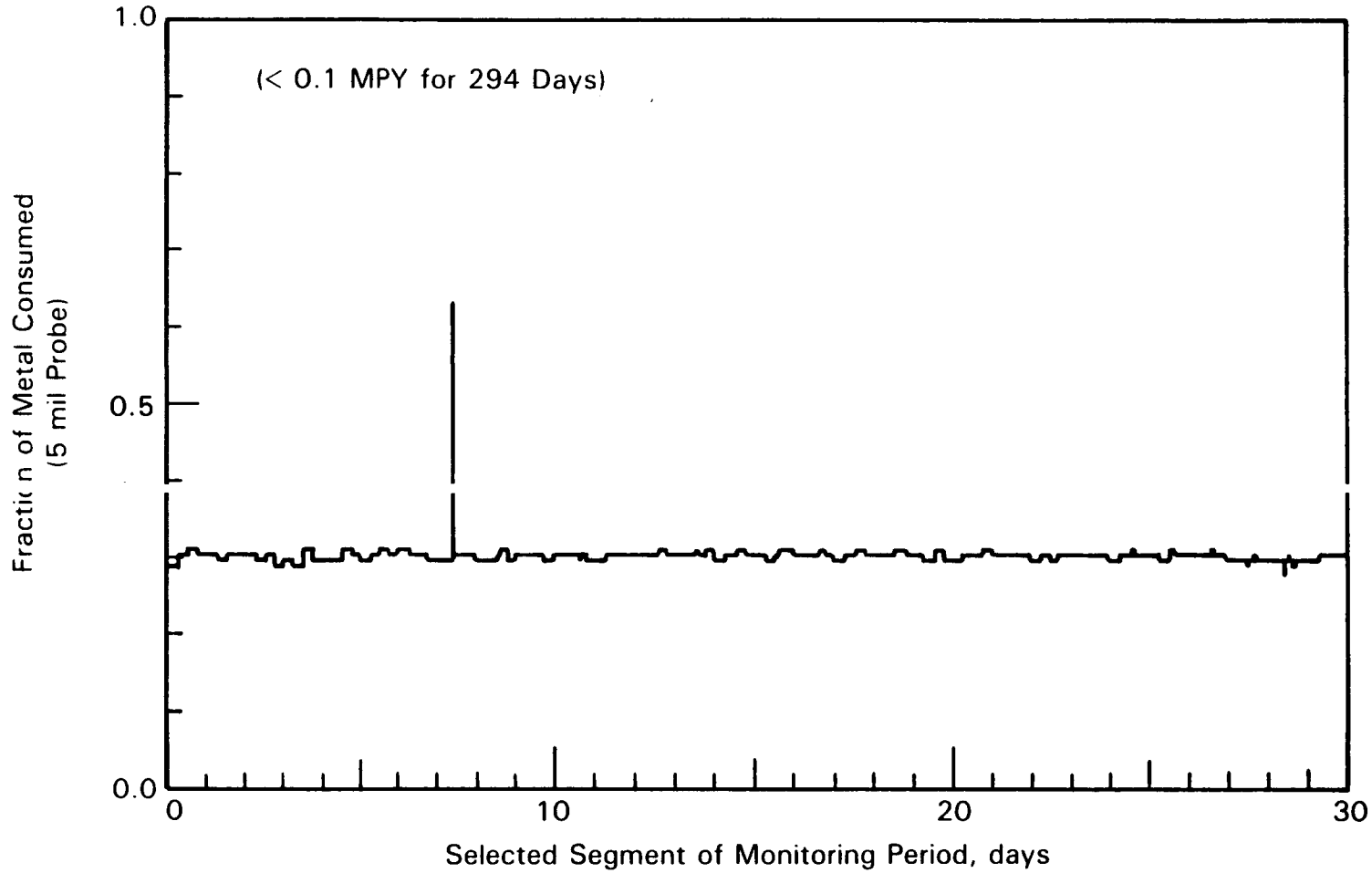

March 14, 1983

FIGURE 4.1.14. Cool Isobutane Vapor Corrosion

TABLE 4.1.1. Corrosion Probe Data Summary

Sample Location	Test Days	Corrosion Rate, MPY Resistance Probes	Coupons
Hydrocarbon System			
Cold Liquid	338	<0.1	0.08
Hot Liquid	340	<0.1	0.07
Hot Vapor	340	<0.1	0.05
Cool Vapor	294	<0.1	0.05
Brine System			
Hot Inlet Brine	294	0.1	0.9
Warm Brine	340	0.7	1.1
Cool Brine	202	1.6	2.0
Plant Outlet Brine	296	see text	4.7

The total corrosion which occurred in the hydrocarbon system was so low as to be almost not detectable even with the coupons. For the size coupons used and a 340 day exposure, 0.05 MPY corresponds to only 10 mg weight loss. As a practical matter, the limit of detection for the resistance probes used was about 0.1 MPY.

4.1.1 History of Some Resistance Probes

No single probe was in satisfactory operation at the plant outlet more than two months. Service dates for the probes installed in the plant outlet are tabulated below. For some, failure occurred several days before manpower was available to remove them.

Probe	Date In	Date Out	Comments
PC2A	11/01/83	01/18/83	Pinhole leak in holder
PC2B	01/19/83	02/09/83	Second pinhole leak
PC2C	02/11/83	02/23/83	5 mil probe
PC2D	03/01/83	03/21/83	10 mil probe
PC2E	03/24/83	04/10/83	10 mil probe
HX7A	04/14/83	06/14/83	Old probe from Heat Exchanger 7
PC2F	06/14/83	08/22/83	Presoaked probe in hot brine

Plant was shut down from July 1 through August 22, 1983.

Readings from Probes PC2A and PC2B were quite erratic. Leaks in weld seams on the probe holder allowed water to short across some electrical leads.

After the leaks were fixed, new probes disappeared very rapidly. Figure 4.1.9 shows the last days of Probe PC2D and the short life of PC2E; both probes had 10 mil useful lives. Figure 4.1.10 shows that corrosion did occur on a new probe even though brine was not flowing. The brine was stagnant for the first 3+ days. When brine flow started, the indicated corrosion rates exceeded 200 MPY. Initially there was no logical explanation for the rapid corrosion. In April, a probe was taken from one of the last heat exchangers (Number 7) and inserted in the plant outlet. The probe had shown no change in corrosion rates in that heat exchanger for the previous two months. In the plant outlet brine, it again showed no corrosion occurring for about six weeks; then a pinhole developed at a weld seam on the probe itself. This allowed brine to short parts of the sensor and made all other readings meaningless.

This test plus unpublished data from corrosion experiments in an unrelated project suggest that formation of protective films is essential to prolong the life of the elements or any piping in geothermal systems. At low temperatures this film does not form rapidly enough to be protective. At temperatures seen in plant inlet brines, a protective coat will form rapidly and will retard corrosion rates. The film is protective even through temperature cycling due to plant start up and shutdown.

To verify this hypothesis, the last probe was first "filmed" in the plant inlet brine for 24 hours. It was then inserted in the plant outlet brine. The corrosion rates observed at the plant outlet with this probe were indeed much lower than for "unfilmed" ones used earlier.

The only probe used in the plant inlet operated 294 days and still had significant metal left. Similarly, the probe in the warm brine operated 340 days with more than half its useful life remaining. The probe originally placed in the cool brine operated there for 202 days; then it was transferred to the plant outlet. There it failed from pitting corrosion on a weld seam (rather than gross uniform corrosion). These facts suggest that early in the plant's start up history all the probes were subjected to high-temperature brine long enough to form a very protective film. The same film likely formed in the heat exchangers and connecting piping, also. Performance of the many

probes at the plant outlet showed that without this protective film, corrosion rates are quite high (over 100 MPY in some cases). The film on corrosion coupons and linear resistance probes was identified as $FeCO_3$. X-ray diffraction provided the crystalline identification. An electron microprobe on a scanning electron microscope confirmed the composition.

The first brine side probe at Heat Exchanger 7 was installed and operated for 202 days. After 100 days of operation, readings from the probe were virtually constant. This meant corrosion rates were too low to be measured or that the probe and associated instrumentation were faulty. Since observed corrosion rates were very high at the plant outlet, this probe was removed from the heat exchanger and installed at the plant outlet. As previously mentioned, it showed no change in corrosion at the plant outlet. When this old probe was moved to the plant outlet, a new one was installed in Heat Exchanger 7. This new probe disappeared from general corrosion in 75 days of operation. That translated to a corrosion rate of 36 MPY. Although that rate was somewhat lower than probe readings at the plant outlet, it was much higher than the original probe was indicating.

This instance further supports our "protective film" theory. The original probe at Heat Exchanger 7 was installed just before a plant start up. That plant start up passed hot brine over the probe and filmed it with $FeCO_3$. The $FeCO_3$ retarded further corrosion even when the probe was installed at the plant outlet.

The second probe at Heat Exchanger 7 was installed while the plant was operating normally. During normal operation, the probe at Heat Exchanger 7 sees only cool brine. Protective films develop very slowly and corrosion rates are high.

Figures 4.1.6 through 4.1.14 provided the numerical data for the probes in Table 4.1.1. Small blips seen on many of the plots are not actual corrosion rate changes. The oscillations show limits of resolution of the digital to analog conversion required by the data acquisition system. The limit is <0.1 MPY for test periods longer than 10 days.

The figures show what fraction of the metal has been removed from the probe by corrosion. The corrosion rate in MPY is calculated as follows:

$$\text{MPY} = \frac{\text{Fraction Removed At End Date} - \text{Fraction Removed At Start Date}}{(\text{End Date}) - (\text{Start Date})} \times \frac{365\ \text{Days}}{\text{Year}} \times \left(\begin{array}{c}\text{Useful Life}\\ \text{In Mils Of}\\ \text{Probe}\end{array}\right)$$

NOTE: End Date - Start Date = Exposure Days.

The important conclusion from the resistance probe testing was that the probes will give readings nearly equal to corrosion coupon data in geothermal brines. That conclusion is valid only if the coupon and probe have the same exposure history.

4.1.2 Linear Polarization Corrosion Probes

The resistance corrosion probes are gross indicators of corrosion rates and relatively insensitive to short-lived increases in rates. Also needed is a corrosion rate monitoring system that 1) responds to rapidly changing corrosion conditions and 2) is easily available for installation by the plant operator. Part of this testing was concerned with determining whether commercial corrosion measuring equipment using the polarization resistance (PR) method can be easily adapted for use in the geothermal environment.

In general, the technique is able to predict corrosion rates in the laboratory within a factor of two (Callow, Richardson, and Dawson 1976). In the field, where the interplay of the corrosion rate determining variables is more complex, the prediction if actual corrosion rates may be less accurate. The theoretical relationships for the PR technique are shown here (Danielson and Koski 1979a).

$$I_{corr} = B \cdot 1/R_p \tag{4.1}$$

where

$$B = \beta_a \beta_c / 2.30(\beta_a + \beta_c) \tag{4.2}$$

and

$$1/R_p = \Delta I / \Delta E \tag{4.3}$$

The corrosion current density, I_{corr}, is linearly related to the reciprocal of the polarization resistance, R_p. When the system is polarized a few millivolts from the corrosion potential ($\Delta E < 20$ mV), the measured current, ΔI, permits the calculation of R_p. The proportionality constant, B, is related to the anodic and cathodic Tafel slopes, β_a and β_c, respectively. Although the Tafel slopes vary widely, the B value is relatively constant and, for carbon steels and stainless steels, falls within the range of 10 to 45 mV and 18 to 41 mV, respectively (Callow, Richardson, and Dawson 1976) and (Danielson and Koski 1979a). Commercial PR instrumentation is designed to make use of Equation 4.1 by polarizing the corroding specimen ±10 mV or ±20 mV, measuring the current, and directly reading out the corrosion rate in mils per year. Equation 4.1 applies only under the following conditions:

1. The mixed potential theory applies, and the corrosion potential of the system is >50 mV from the reversible potential of either the anodic or cathodic reactions (Danielson and Koski 1979a).
2. Both the anodic and cathodic reactions are activation controlled.

Both of these conditions are often found in the corroding environment. However, when the cathodic reaction is under mass transport control (such as when oxygen enters the system), Equation 4.1 no longer applies. The PR relationship under conditions when the corrosion rate is controlled by mass transport of the cathodic process is shown here

$$I_{corr} = (\beta_a/2.3)(1/R_p) \qquad (4.4)$$

One of the unresolved problems with PR methods is the difficulty of recognizing whether Equation 4.1 or Equation 4.4 applies, since there can be a large difference between B and β_a (especially if the metal is partially passivated).

The problem of the linearity of $(\partial I/\partial E)$ near E_{corr} has been extensively examined in the PR literature (Fontana and Staehle 1970). This is because I_{corr} is proportional to $(\partial I/\partial E)_{Ecorr}$ only at the corrosion potential, and any nonlinearity of $I = f(E)$ could lead to an error in $(\partial I/\partial E)_{Ecorr}$ obtained by extrapolation from ±10 or ±20 mV. Laboratory studies have revealed that $I = f(E)$ is often nonlinear, but that the error is not significant when E_{corr} is greater than RT/F (R = gas constant; T = Kelvin temperature scale; and F = Faraday's constant) from both equilibrium potential of the corrosion

reaction and the reduction reaction. Conditions for a small error are usually encountered.

Earlier PNL tests evaluated the use of the PR technique at 150°C and 250°C in 3 and 20 percent brines, with and without oxygen. In general, the agreement between weight-loss coupons and the PR technique was good. Details of the electrochemical measurements and results are given by Danielson and Koski (1979b). That analysis showed that good comparison with corrosion coupon data required experimental determination of B values for a given probe. The "hardwired" B value in commercial electronics is within a factor of two of his experimental value. That may be close enough for many applications, provided the probe material matches the corroding material of interest.

Field tests showed the average corrosion rates from the polarization probes agreed reasonably well with the resistance probes and coupon data. The polarization readings were generally high by a factor of two and sometimes more. Infrequently, stable readings erred by a factor of five higher than the resistance probes.

The real value of the polarization probes was their response to "instantaneous" phenomenon. Figure 4.1.15 shows response of one probe to pH changes during a period when pH probes were being calibrated. It is worth noting that once the polarized surface is disturbed, some time is required to get back to initial background readings. Experience says this can sometimes require a few days.

The polarization probe also responds to oxygen infiltration into the brine because oxygen will increase corrosion rates significantly. Figure 4.1.16 illustrates what are believed to be possible oxygen-caused spikes. The time period shown corresponded to a plant start up where frequent (but short duration) interruptions to the brine flow had occurred. Response of the probes is somewhat flow dependent, but the magnitude of some of the spikes indicates other phenomena are also occurring. Speculation is that air leaked into the system during the flow disturbances.

4.2 CORROSION COUPONS

The primary mode of monitoring corrosion in the plant was with the linear resistance probes. However, at each location, at least 10 disc-shaped corrosion coupons were installed to get some intermediate corrosion rates and

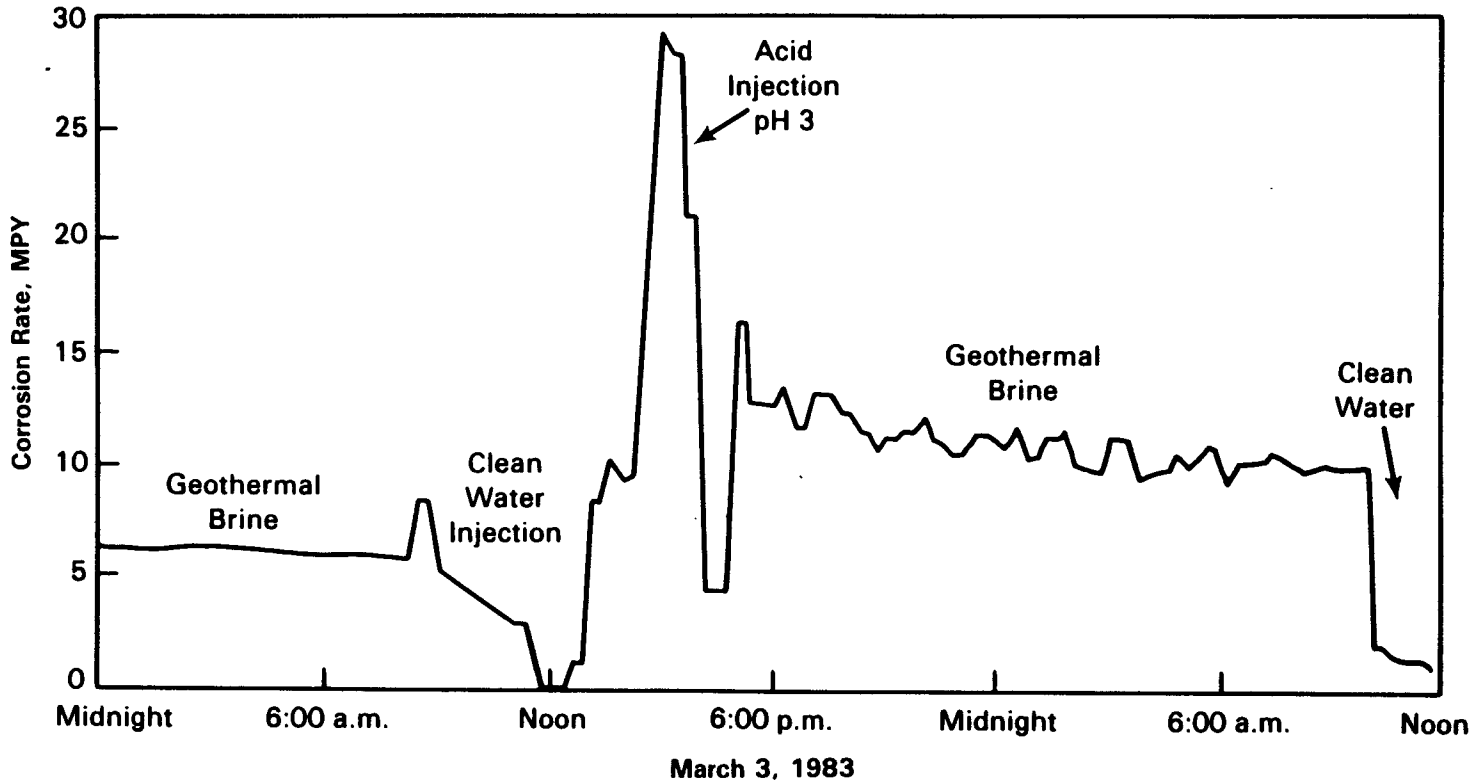

FIGURE 4.1.15. Linear Polarization Probe Response Acidity Changes

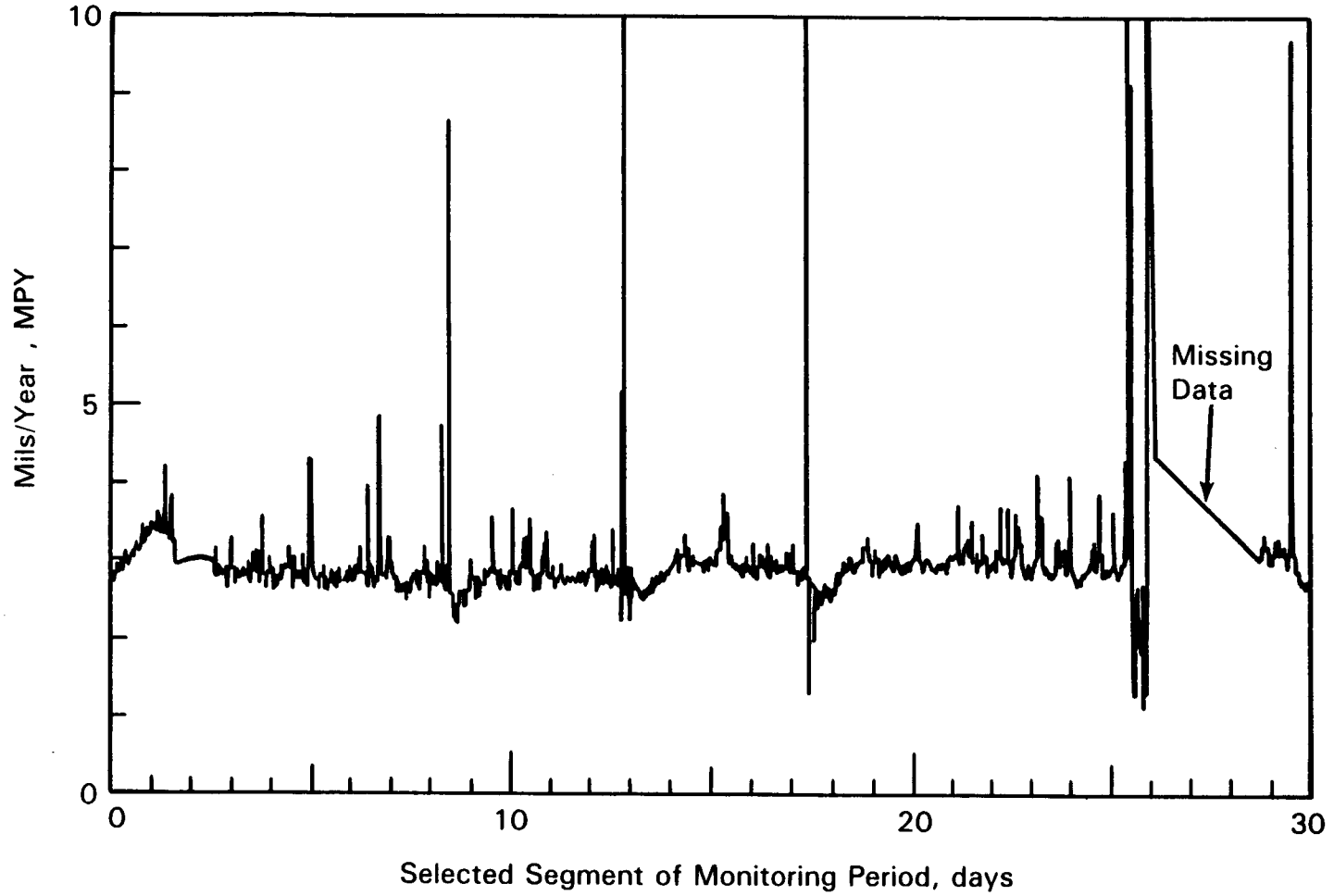

November 22, 1982

FIGURE 4.1.16. "Instantaneous" Plant Inlet Corrosion

check on the continuous readings. Table 4.2.1 details the corrosion coupon exposure data at each location. Material codes are:

- MA = pipe segments (ASTM A53B carbon steel) cut from pipe used in the plant inlet piping
- MF = 1010 carbon steel sheet
- ME = DHP copper 1/16-in.-thick sheet.

Location codes were pictured in Figure 4.1.5 and are described below:

- B1PC = hot brine at plant inlet
- BHX1 = warm brine out of first heat exchanger
- BHX7 = cool brine out of seventh heat exchanger
- BPC2 = cool brine at plant outlet
- IHX7 = cool isobutane liquid into heat exchanger train
- IHX5 = hot isobutane liquid out of fifth heat exchanger
- IKOD = hot isobutane vapor into the knockout drum
- ITO = cool isobutane vapor out of the turbine.

Figure 4.2.1 shows average coupon corrosion rates as a function of exposure time. Rates are averages of at least three coupons and generally six or more. In general, cooler brines cause faster corrosion than hot brines. Scatter in the plant outlet is explained by the protective film theory. Coupons with the high corrosion rates were inserted into the brine at times when they could not form the $FeCO_3$ film because temperatures were too low. The coupons with lower rates were exposed to high-temperature brines early in their exposure history. Thereafter, they resisted corrosion even as the brine cooled. Films were physically observed to be thickest on the coupons exposed to high-temperature brines. A few coupons at the plant outlet collected almost no film.

The protective film theory seems to explain corrosion phenomena observed in this test. The theory is still incomplete because it cannot yet predict how long the film remains intact after it forms. Given sufficient time at the low temperature, the film might dissolve.

4.3 pH

The pH of a fluid is a measure of the acidity and is probably one of the most important chemical parameters affecting mineral scaling, corrosion, and

TABLE 4.2.1. Corrosion Coupon Data

Material	Loc Code	Fluid	Exposure Days	Area (dm^2)	Corrosion Rate MPY
MF 1010 CS	B1PC	Hot Brine	67	0.0887	6.25
MF 1010 CS	B1PC	Hot Brine	67	0.0897	4.70
MF 1010 CS	B1PC	Hot Brine	67	0.0888	5.66
MF 1010 CS	B1PC	Hot Brine	225	0.0851	1.02
MF 1010 CS	B1PC	Hot Brine	225	0.0827	1.14
MF 1010 CS	B1PC	Hot Brine	225	0.0854	1.00
MA A53B	B1PC	Hot Brine	294	0.5358	2.11
MA A53B	B1PC	Hot Brine	294	0.5382	0.51
MA A53B	B1PC	Hot Brine	294	0.5315	0.55
MF 1010 CS	BHX1	Warm Brine	147	0.0821	1.60
MF 1010 CS	BHX1	Warm Brine	147	0.085	1.58
MF 1010 CS	BHX1	Warm Brine	193	0.0851	0.95
MF 1010 CS	BHX1	Warm Brine	193	0.0858	0.88
MF 1010 CS	BHX1	Warm Brine	193	0.0861	0.97
MF 1010 CS	BHX1	Warm Brine	193	0.0843	0.90
MF 1010 CS	BHX1	Warm Brine	193	0.0845	0.80
MF 1010 CS	BHX1	Warm Brine	340	0.0829	0.93
MF 1010 CS	BHX1	Warm Brine	340	0.0894	0.91
MF 1010 CS	BHX1	Warm Brine	340	0.0817	1.16
MF 1010 CS	BHX7	Cool Brine	64	0.0852	11.67
MF 1010 CS	BHX7	Cool Brine	64	0.0895	1.30
MF 1010 CS	BHX7	Cool Brine	64	0.0827	11.87
MF 1010 CS	BHX7	Cool Brine	68	0.0898	3.13
MF 1010 CS	BHX7	Cool Brine	68	0.0893	3.13
MF 1010 CS	BHX7	Cool Brine	68	0.0897	3.11
MF 1010 CS	BHX7	Cool Brine	80	0.086	0.98
MF 1010 CS	BHX7	Cool Brine	80	0.0912	0.97
MF 1010 CS	BHX7	Cool Brine	122	0.086	0.93
MF 1010 CS	BHX7	Cool Brine	122	0.0847	1.52
MF 1010 CS	BHX7	Cool Brine	133	0.0899	0.62
MF 1010 CS	BHX7	Cool Brine	133	0.0899	0.62
MF 1010 CS	BHX7	Cool Brine	202	0.0883	2.05
MF 1010 CS	BHX7	Cool Brine	202	0.0885	1.80
MF 1010 CS	BHX7	Cool Brine	336	0.0907	1.17
MF 1010 CS	BHX7	Cool Brine	336	0.0887	1.31
MF 1010 CS	BHX7	Cool Brine	336	0.0887	1.32
MF 1010 CS	BPC2	Outlet Brine	13	0.0854	9.14
MF 1010 CS	BPC2	Outlet Brine	13	0.0829	10.37
MF 1010 CS	BPC2	Outlet Brine	17	0.0847	7.17
MF 1010 CS	BPC2	Outlet Brine	17	0.0833	7.05
MF 1010 CS	BPC2	Outlet Brine	25	0.0843	17.13
MF 1010 CS	BPC2	Outlet Brine	25	0.0824	16.33
MF 1010 CS	BPC2	Outlet Brine	25	0.0851	17.23
MF 1010 CS	BPC2	Outlet Brine	33	0.086	7.86
MF 1010 CS	BPC2	Outlet Brine	33	0.0839	7.28
MF 1010 CS	BPC2	Outlet Brine	69	0.0895	6.10
MF 1010 CS	BPC2	Outlet Brine	69	0.0896	6.23
MF 1010 CS	BPC2	Outlet Brine	69	0.0897	5.84
MF 1010 CS	BPC2	Outlet Brine	102	0.0831	4.66
MF 1010 CS	BPC2	Outlet Brine	102	0.0831	3.31

TABLE 4.2.1. Corrosion Coupon Data (Continued)

Material	Loc Code	Fluid	Exposure Days	Area (dm²)	Corrosion Rate MPY
MF 1010 CS	BPC2	Outlet Brine	129	0.0883	4.38
MF 1010 CS	BPC2	Outlet Brine	129	0.0887	5.09
MF 1010 CS	BPC2	Outlet Brine	130	0.0825	11.08
MF 1010 CS	BPC2	Outlet Brine	134	0.0881	2.52
MF 1010 CS	BPC2	Outlet Brine	167	0.0829	3.39
MF 1010 CS	BPC2	Outlet Brine	167	0.0883	3.62
MF 1010 CS	BPC2	Outlet Brine	227	0.0854	6.19
MF 1010 CS	BPC2	Outlet Brine	227	0.0854	5.62
MF 1010 CS	BPC2	Outlet Brine	296	0.0843	3.73
MF 1010 CS	BPC2	Outlet Brine	296	0.0885	4.08
MF 1010 CS	BPC2	Outlet Brine	296	0.0885	4.52
MF 1010 CS	BPC2	Outlet Brine	296	0.0887	4.79
MF 1010 CS	BPC2	Outlet Brine	296	0.0845	4.60
MF 1010 CS	BPC2	Outlet Brine	296	0.0854	4.48
MF 1010 CS	IHX5	Hot iC4 Liquid	84	0.0839	0.09
MF 1010 CS	IHX5	Hot iC4 Liquid	84	0.0827	0.04
MF 1010 CS	IHX5	Hot iC4 Liquid	256	0.0825	0.03
MF 1010 CS	IHX5	Hot iC4 Liquid	256	0.0817	0.02
MF 1010 CS	IHX5	Hot iC4 Liquid	256	0.0854	0.01
MF 1010 CS	IHX5	Hot iC4 Liquid	340	0.0883	0.02
MF 1010 CS	IHX5	Hot iC4 Liquid	340	0.0883	0.02
MF 1010 CS	IHX5	Hot iC4 Liquid	340	0.0883	0.02
MF 1010 CS	IHX5	Hot iC4 Liquid	340	0.0827	0.03
MF 1010 CS	IHX5	Hot iC4 Liquid	340	0.0849	0.03
MF 1010 CS	IHX7	Cool iC4 Liquid	338	0.0823	0.06
MF 1010 CS	IHX7	Cool iC4 Liquid	338	0.0827	0.06
MF 1010 CS	IHX7	Cool iC4 Liquid	338	0.0847	0.07
MF 1010 CS	IHX7	Cool iC4 Liquid	338	0.0827	0.08
MF 1010 CS	IHX7	Cool iC4 Liquid	338	0.0825	0.07
MF 1010 CS	IHX7	Cool iC4 Liquid	338	0.0825	0.05
MF 1010 CS	IHX7	Cool iC4 Liquid	338	0.0909	0.06
MF 1010 CS	IHX7	Cool iC4 Liquid	338	0.0825	0.06
MF 1010 CS	IKOD	Hot iC4 Vapor	340	0.0829	0.04
MF 1010 CS	IKOD	Hot iC4 Vapor	340	0.0833	0.04
MF 1010 CS	IKOD	Hot iC4 Vapor	340	0.0881	0.04
MF 1010 CS	IKOD	Hot iC4 Vapor	340	0.0851	0.05
MF 1010 CS	IKOD	Hot iC4 Vapor	340	0.085	0.04
MF 1010 CS	IKOD	Hot iC4 Vapor	340	0.0831	0.05
MF 1010 CS	IKOD	Hot iC4 Vapor	340	0.0833	0.05
MF 1010 CS	IKOD	Hot iC4 Vapor	340	0.086	0.04
MF 1010 CS	ITO	Cool iC4 Vapor	80	0.0843	0.11
ME DHP Cu	ITO	Cool iC4 Vapor	80	0.1034	0.02
MF 1010 CS	ITO	Cool iC4 Vapor	80	0.0898	0.13
MF 1010 CS	ITO	Cool iC4 Vapor	214	0.0843	0.03
MF 1010 CS	ITO	Cool iC4 Vapor	294	0.0856	0.04
MF 1010 CS	ITO	Cool iC4 Vapor	294	0.0823	0.03
MF 1010 CS	ITO	Cool iC4 Vapor	294	0.0831	0.03
MF 1010 CS	ITO	Cool iC4 Vapor	294	0.0821	0.05
MF 1010 CS	ITO	Cool iC4 Vapor	294	0.0885	0.06

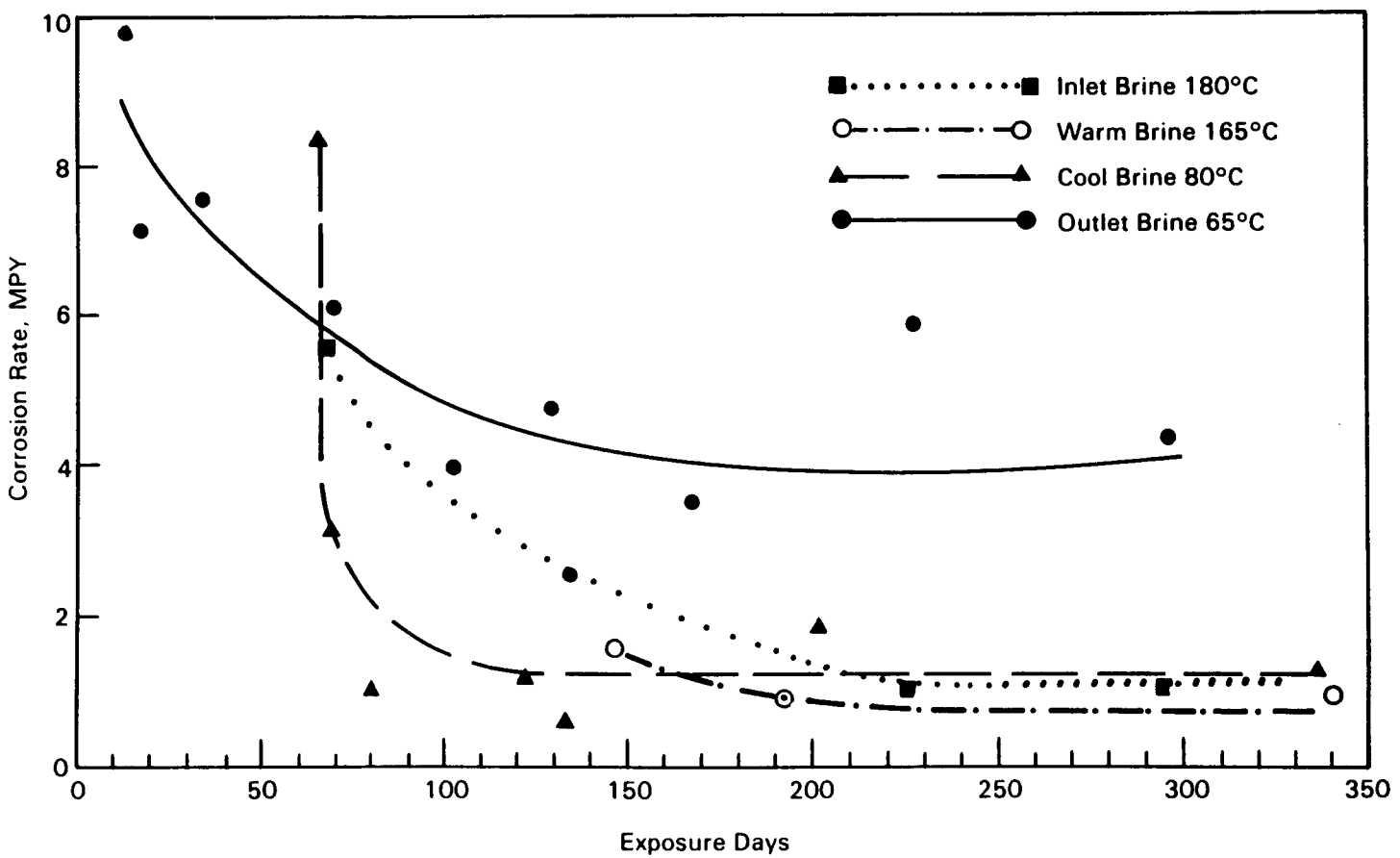

FIGURE 4.2.1. Coupon Corrosion Rates in Brine System

brine treatment processes. The pH can be measured simply in any laboratory when low-temperature, in-line cells are available. However, since CO_2 pressure in the brine is a major determinant of the actual pH, measurements on depressurized samples are of dubious value. Also, pH changes with temperature; what is needed is a pH cell to operate at hot, pressurized conditions. Unfortunately, commercial pH cells fail rapidly. In geothermal brines, glass electrodes chemically dissolve in a few days even at modest temperatures (150°C).

Some of the nation's leading manufacturers of pH electrodes were subcontracted by PNL to build high-temperature probes. Two different approaches were tried. The first tested several ceramic materials. A typical ceramic pH electrode is shown in Figure 4.3.1. The second used Ion Sensitive Field Effect Transistors (ISFET) to detect hydrogen activity. Figure 4.3.2 gives a cross-sectional view of the solid-state sensor.

The ceramic probes worked well in laboratory tests and gave fair response at 260°C in geothermal brines. Two factors hinder their acceptance in the geothermal industry: 1) low-temperature response (below 100°C) is poor and gets worse with temperature cycling and 2) physically, the probe is very fragile and must be handled very carefully. Many probes failed mechanically before they could be reliably tested in the field.

The ISFET models respond well at both high and low temperatures. However, a major problem surfaced during the field testing of these units. Electrical leads inside the probes broke during temperature cycling. The sealing material and wires have significantly different thermal expansion coefficients, and rapid cooling seen in the field caused the leads to fail. Total duration of the field tests was too short to uncover any other problems. A more detailed description of the probes and their testing follows.

4.3.1 Ceramic pH Probe Testing Procedures and Results

Autoclave testing of the probes was done by each of the contractors in their own laboratories. All the ceramic probes were made using stabilized zirconia tubes. Industry tested the ceramic probes they produced in the system shown in Figure 4.3.3 (Niedrach and Stoddard 1983). The system was fabricated of titanium and glass. Provision was made for pumping water, acid, base, and simulated brines containing carbonate buffers and sulfides into the heated and pressurized titanium autoclave, which had a capacity of one liter. It was also possible to introduce aliquots of concentrated acid or base to bring about more rapid changes in pH. All streams that entered the autoclave

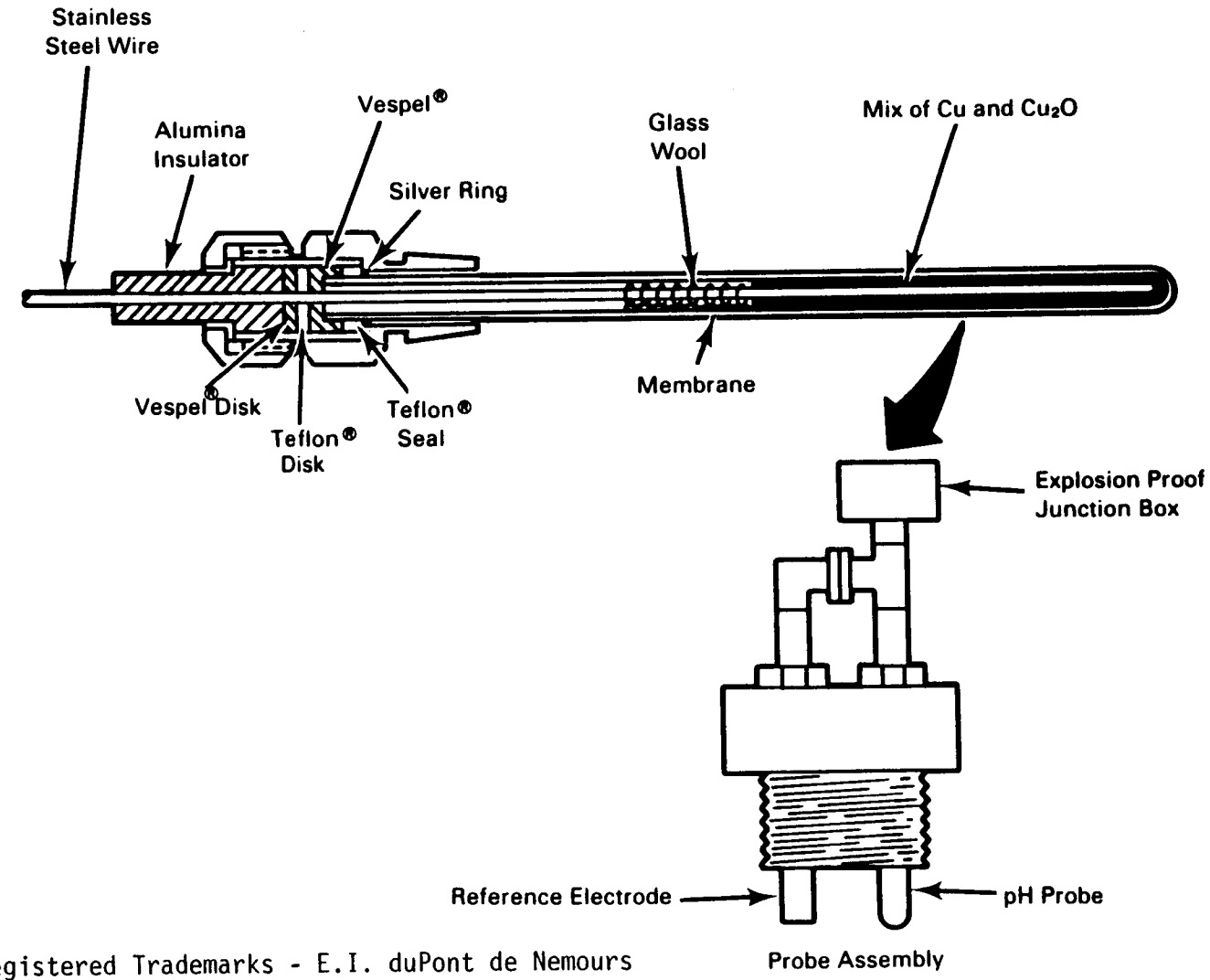

Registered Trademarks - E.I. duPont de Nemours and Company, Wilmington, Deleware

FIGURE 4.3.1. Schematic Diagram of Ceramic pH Sensor

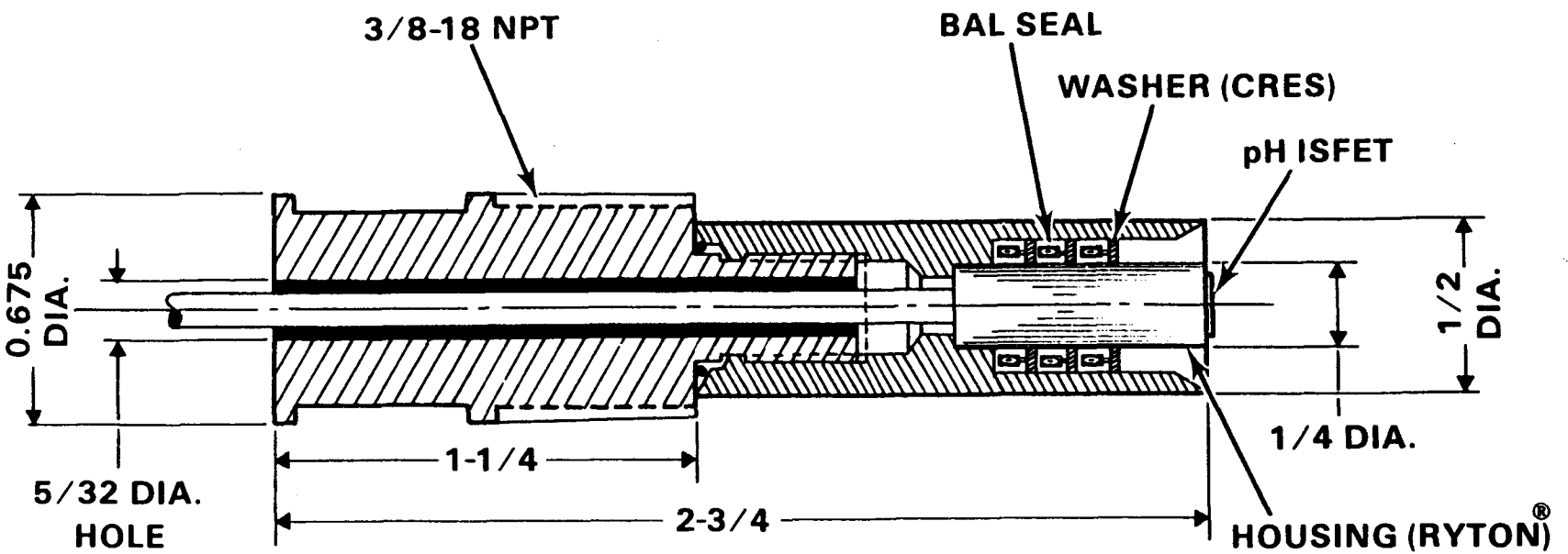

Registered Trademark - E.I. duPont de Nemours and Company, Wilmington, Deleware

ALL DIMENSIONS IN INCHES

FIGURE 4.3.2. Solid State pH Sensor

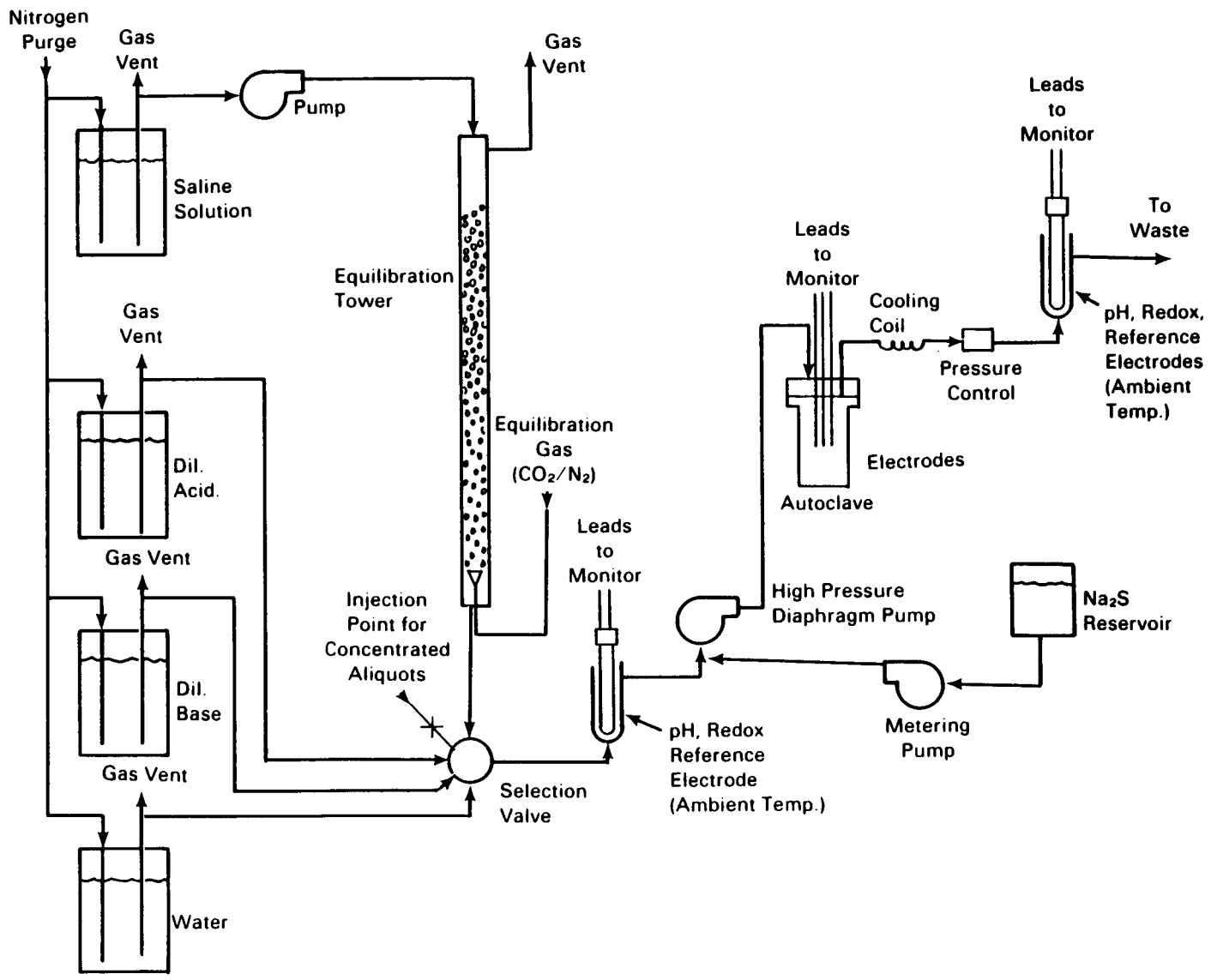

FIGURE 4.3.3. System for Evaluating Sensors With Simulated Geothermal Brines

were purged with nitrogen to reduce the oxygen concentrations to low levels. Brine solutions were contacted with carbon dioxide-nitrogen mixtures in a packed column to control their pH. Appropriate temperature, pressure, and analytical information were recorded to be sure the autoclave solutions remained constant for each test. Most of the testing was done at 285°C between pH 3 and pH 9. A limited amount of testing was done at lower temperatures: 95, 150, and 225°C. Details of these tests are provided by Niedrach and Stoddard (1981, 1983, 1884). Several of the probes tested showed good repeatability at 285°C. Very few survived temperature cycling between 90°C and 285°C for any length of time. The best of the probes in terms of repeatability and time of service were shipped to the field test site for further evaluation.

Field evaluation involved a combination of monitoring the plant inlet and plant outlet brines (at alternating intervals) coupled with calibration testing. The calibration fluids were as follows:

pH 3 = .015 M $NaH_2PO_4 \cdot H_2O$
.0022N HCl

pH 5.5 = .01 M $B(OH)_3$

pH 7 = .01 M K_2HPO_4
.01 M $NaH_2PO_4 \cdot H_2O$

pH 8 = .01 M $B(OH)_3$
.001 M LiOH

pH 10 = .01 M Na_2CO_3
.01 M $NaHCO_3$

Ambient temperature pH's of each buffer were measured with glass electrodes before and several times during each test.

Most laboratory testing was done using an Ag-AgCl reference electrode housed in a ceramic tube similar in dimensions to the pH probe itself. The reference electrode appears conceptually in Figure 4.3.1 and in more detail in Figure 4.4.1. The reference electrodes were filled with 0.5 N KCl and then sealed with ceramic cement before testing. Lifetime for the best of the reference electrodes was about three months. Brine eventually contaminated the electrolyte and altered the reference potential. At that point pH measurements became meaningless. This style of reference electrode was used only periodically during field testing of the pH probes. It was used almost exclusively in the oxidation-reduction potential probe field tests. (Frequent replacements were required.)

In the field the pH probes were coupled to a quasi-reference electrode shown in Figure 4.3.4, and mv readings between the two were recorded. That reference electrode is described in detail by Danielson (1979). It was developed at PNL for use with both oxidation-reduction potential (ORP) probes and pH probes. The reference was developed to be resistant to H_2 and H_2S in the brine solution. The probe required a continuous flush (albeit at very slow rates near 6 ml/h) of 0.5 molal KCl electrolyte solution. Special high-pressure pumps were needed for this refreshment. The reference electrode remained stable as long as the pumps operated.

The reference electrode itself was external to the flowing brine stream and remained at ambient temperature; hence, it suffered from a thermal liquid junction and thermodiffusion potential. Much work was done to show that the thermal liquid junction potential stabilizes rapidly (Danielson 1979). Thermodiffusion was extremely slow to develop when KCl was used as the electrolyte. Consequently, the potential of the reference electrode could be placed on the hydrogen scale and could function successfully as a truly thermodynamic model.

The first field test suffered from lack of temperature control in the test loop (described in Section 3.1). The primary pump for circulating calibration fluids had broken and a secondary one did not have sufficient capacity to keep the test loop full of hot fluid.

During the first field test, two ceramic pH sensors were each paired with their own quasi-reference electrode. In spite of the operational difficulties, some encouraging data were obtained. The results are summarized in Table 4.3.1 and Figure 4.3.5. A third sensor was tried but failed early, so data from it are not presented. The two sets of data in Table 4.3.1 come from a volt meter connected directly to the probes with only local output and from a line-powered volt meter tied to the datalogging system.

The temperature trace in Figure 4.3.5 shows oscillations between 120 and 170°C; the target was 140°C. Sensor 3 was at the outlet of the test section and showed a response lower than theoretical. Since Sensor 3 was a few degrees cooler than Sensor 1, some difference in the slopes of the respective millivolt (mV) versus pH plots could be expected. Observations after the test showed that the reference for Sensor 3 had lost electrolyte flow sometime

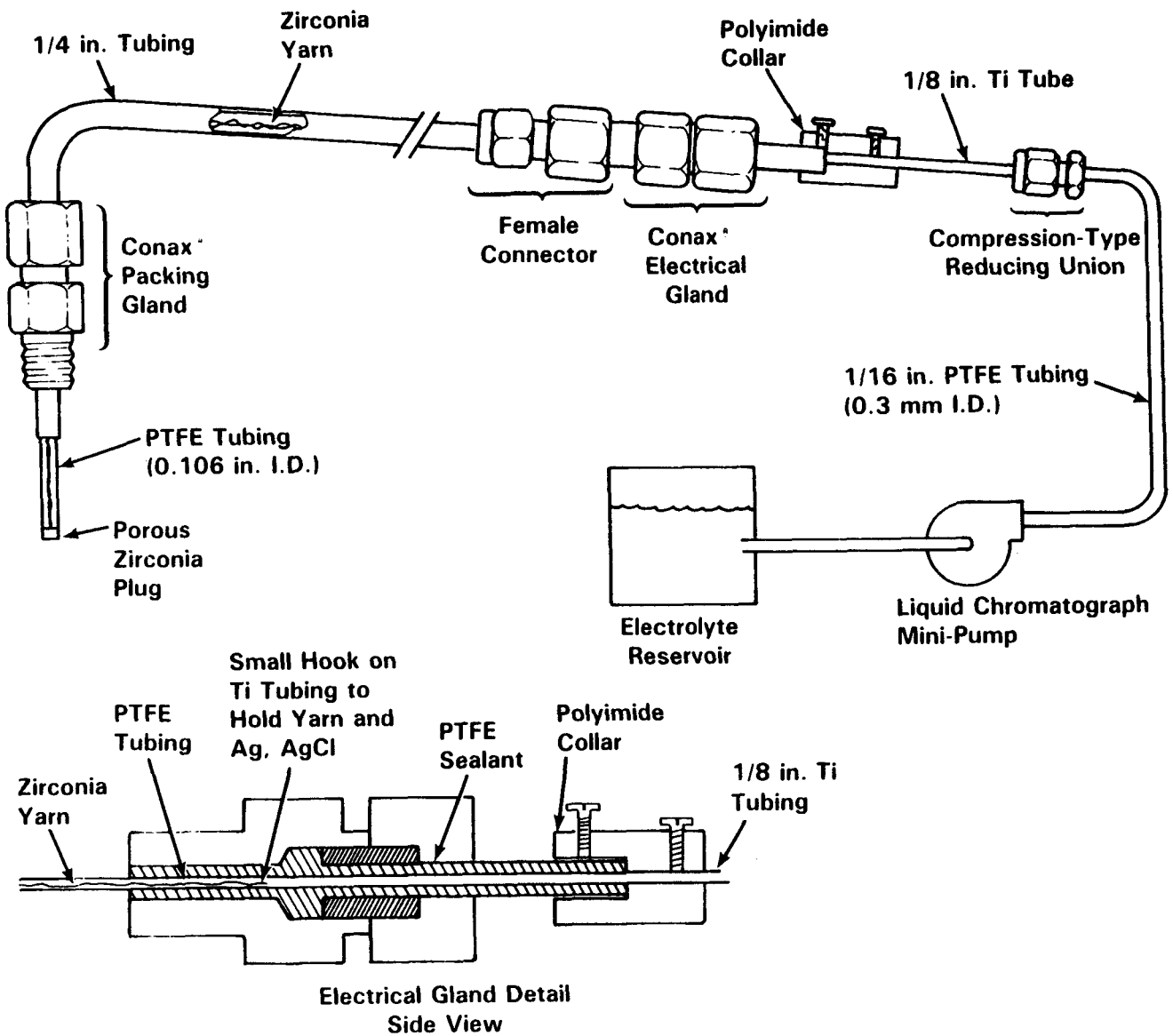

FIGURE 4.3.4. PNL "Pumped" External Reference Electrode

TABLE 4.3.1. Response Data for Selected Ceramic pH Sensors

Sensor	Reference Electrode	Measuring System	Calc pH	Response: mV/pH Unit	Response: % of Theory[a]
1 (Japanese Manufactured)	1	Battery Powered Portable Voltmeter	3.3	95	116
			7.3	--	
			9.4		
1 (Japanese Manufactured)	1	Line Powered Voltmeter (In Instrument Panel)	3.3	90	110
			7.3	-164	--
			9.4		
3 (USA Manufactured)	2	Battery Powered Portable Voltmeter	3.3	54	66
			7.3	--	
			9.4		
3 (USA Manufactured)	2	Line Powered Voltmeter (In Instrument Panel)	3.3	53	65
			7.3	(59)	(72)
			9.4	70	85

[a] Based on 82 mV/pH unit at 140°C.

during the tests. This could explain a part of the discrepancy between the two sensors.

After this initial field test, several other ceramic probes were installed in the test loop to monitor the pH of geothermal brines with time. Figures 4.3.6 through 4.3.10 show responses for several probes as solutions changed from real geothermal brines to pH calibration solutions and back again. The probes designated OHK were supplied by PNL; others were supplied by industry. The test period is the same for all the figures, and the annotated comments describe what was happening. There is no "standard manufacturing procedure" for the ceramic tubes. Consequently, the differences in absolute voltage readings between the probe pairs is to be expected.

The temperature of fluid in the test loop is superimposed on the plots to show that none of the ceramic probes performed well at temperatures close to

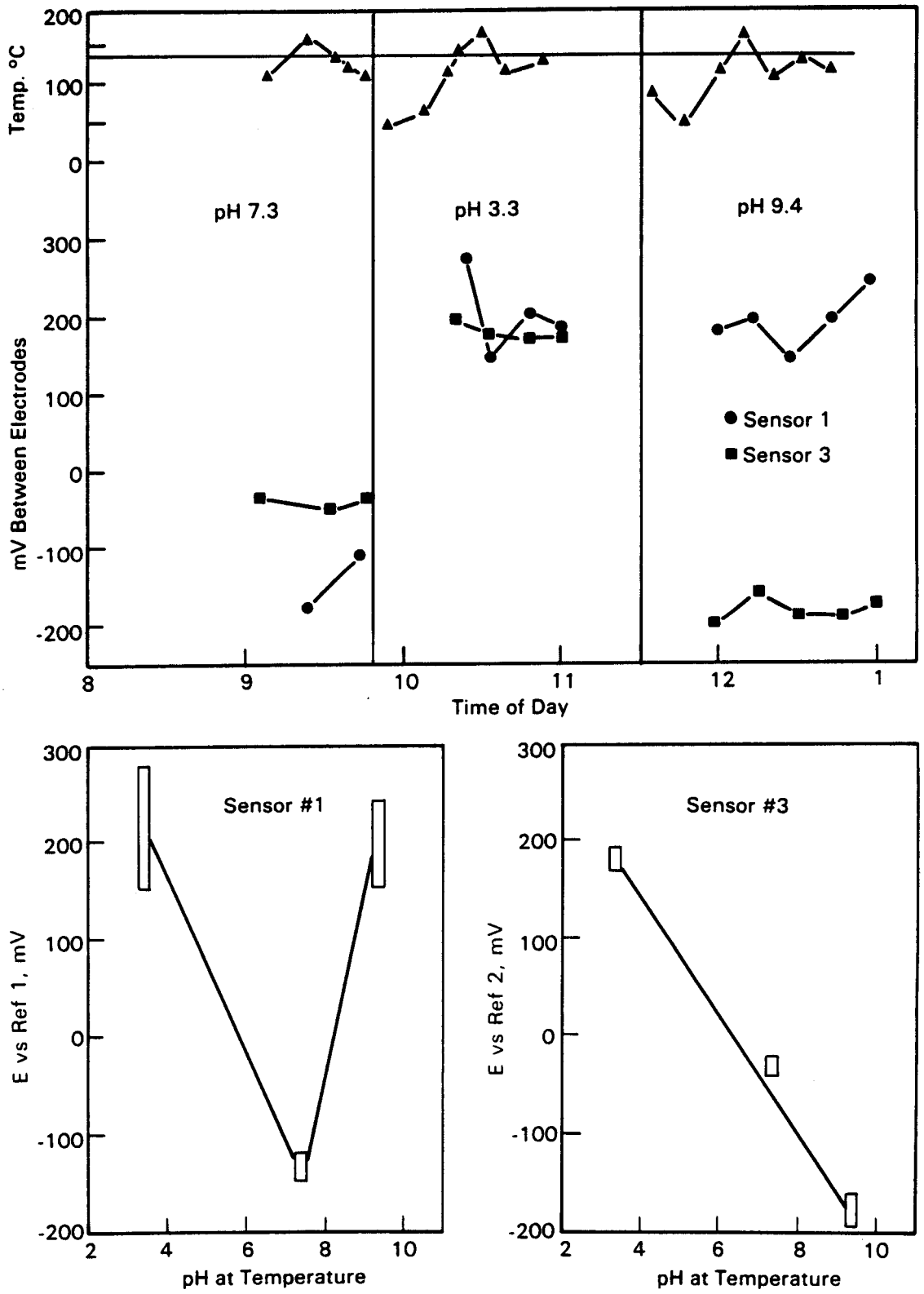

FIGURE 4.3.5. Data from First Field Test of pH Probes

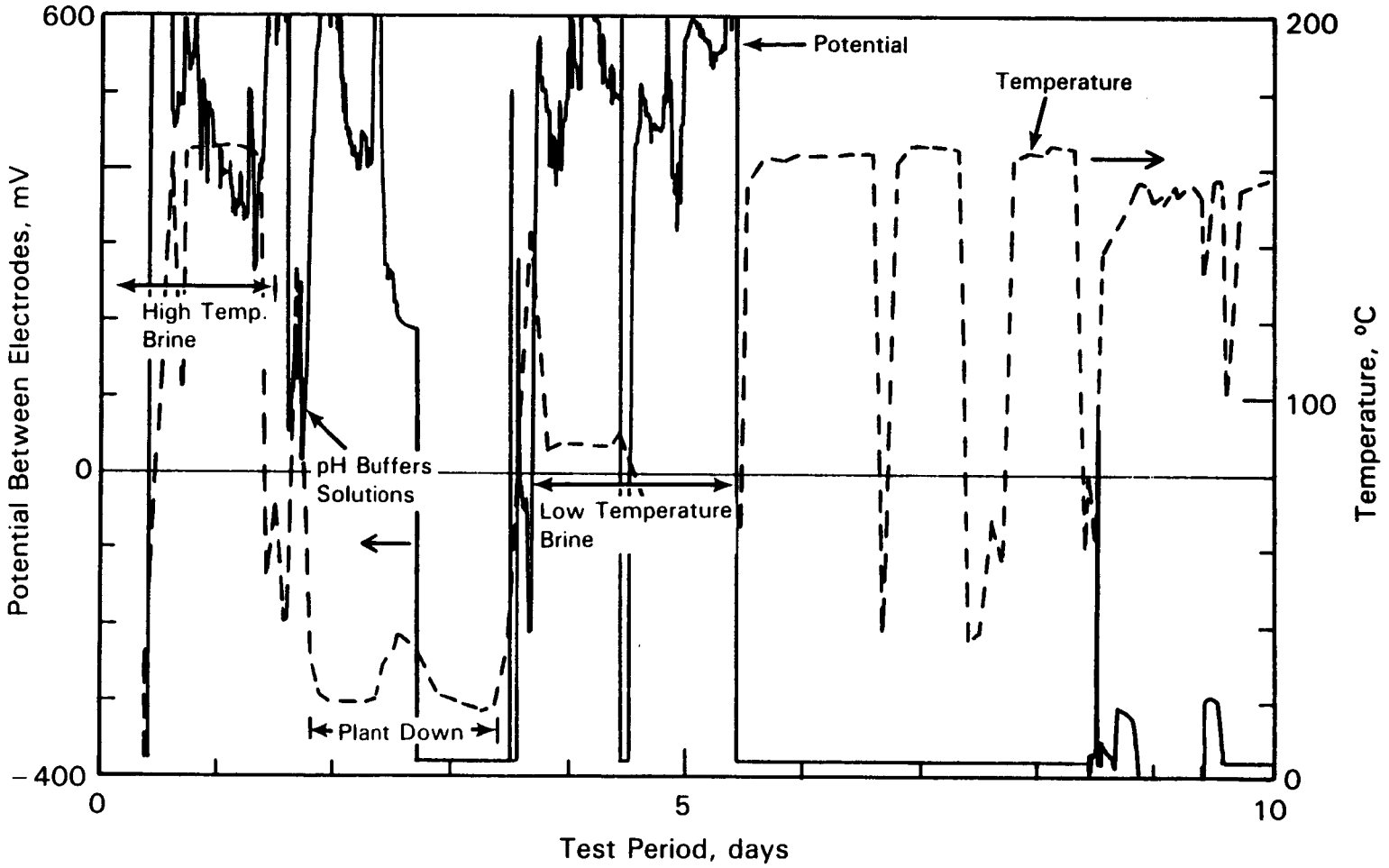

September 27, 1983

FIGURE 4.3.6. Ceramic PNL pH Probe Responses

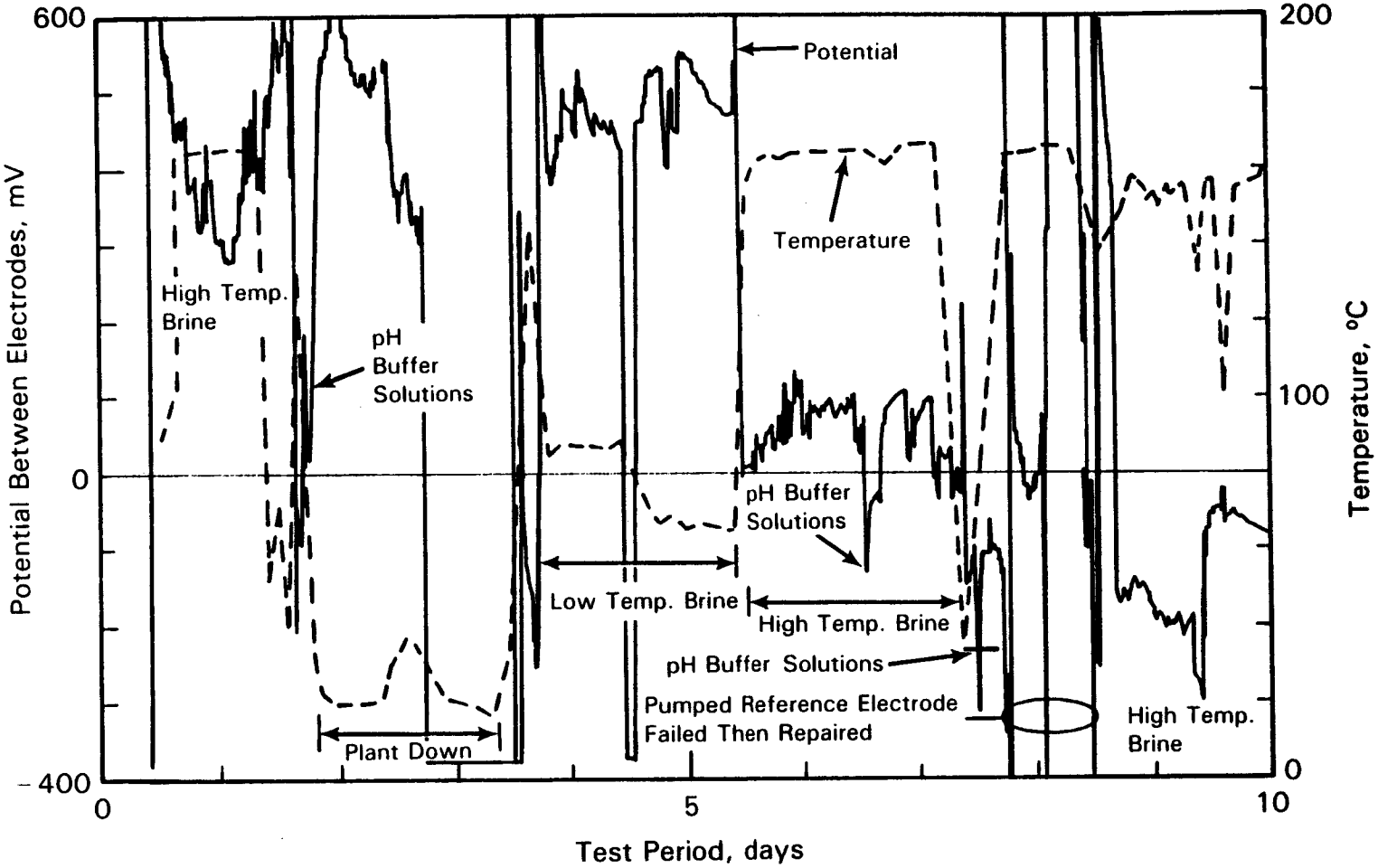

September 27, 1983

FIGURE 4.3.7. Response of Other PNL pH Probes

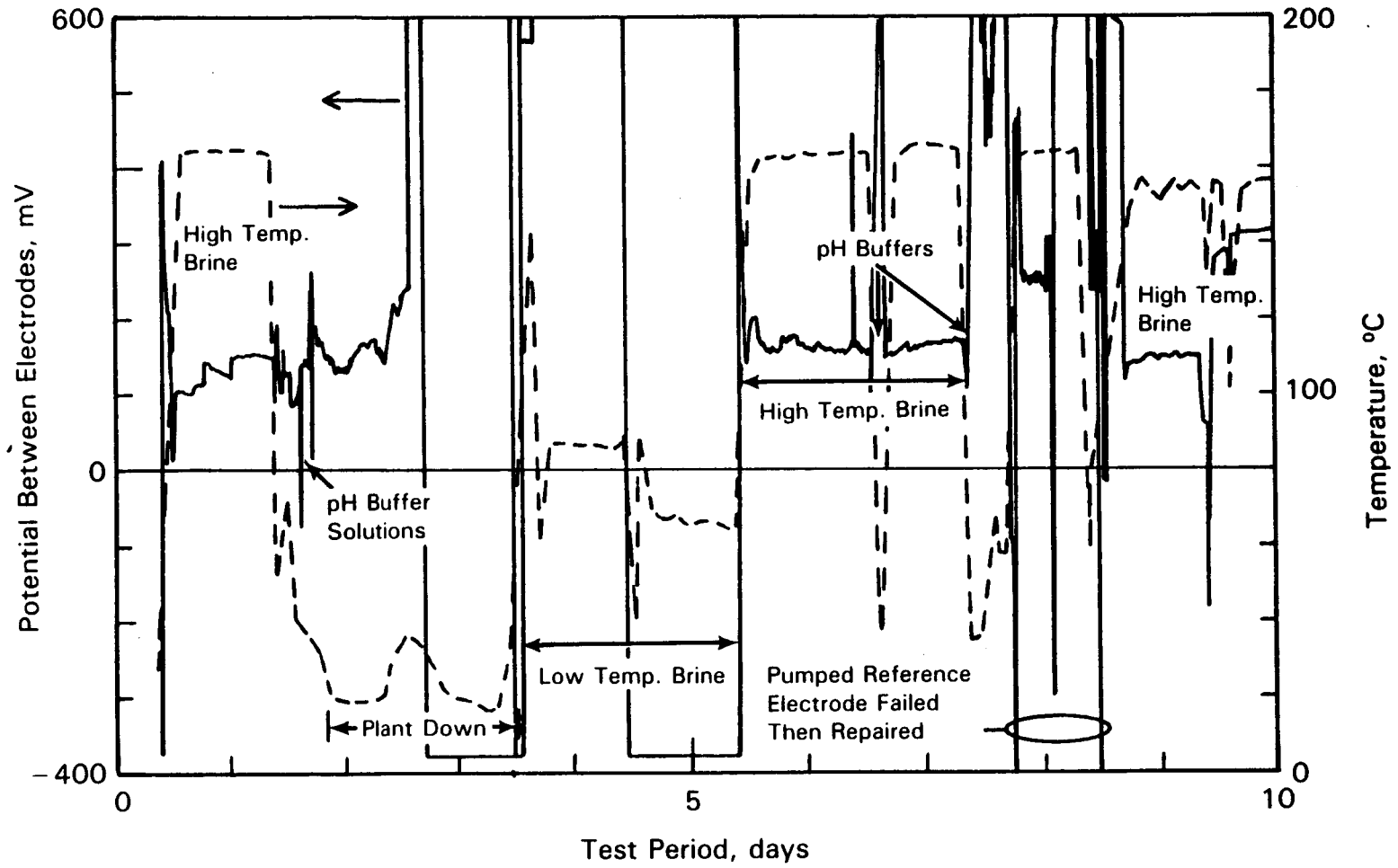

September 27, 1983

FIGURE 4.3.8. Response of Industrial (Y74-BJ) Ceramic pH Probe

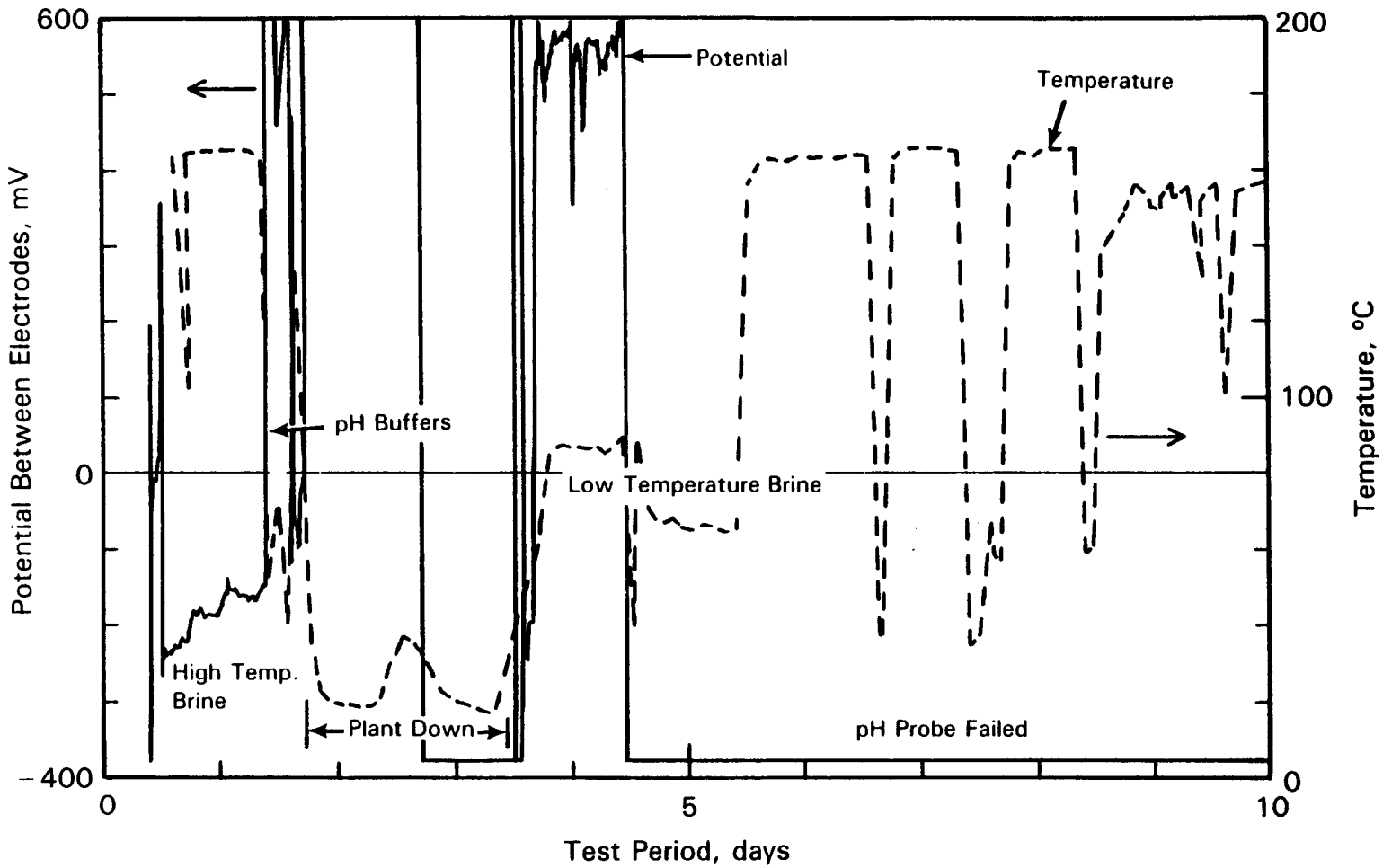

September 27, 1983

FIGURE 4.3.9. Response of Industrial (NGK-B4) Ceramic pH Probe

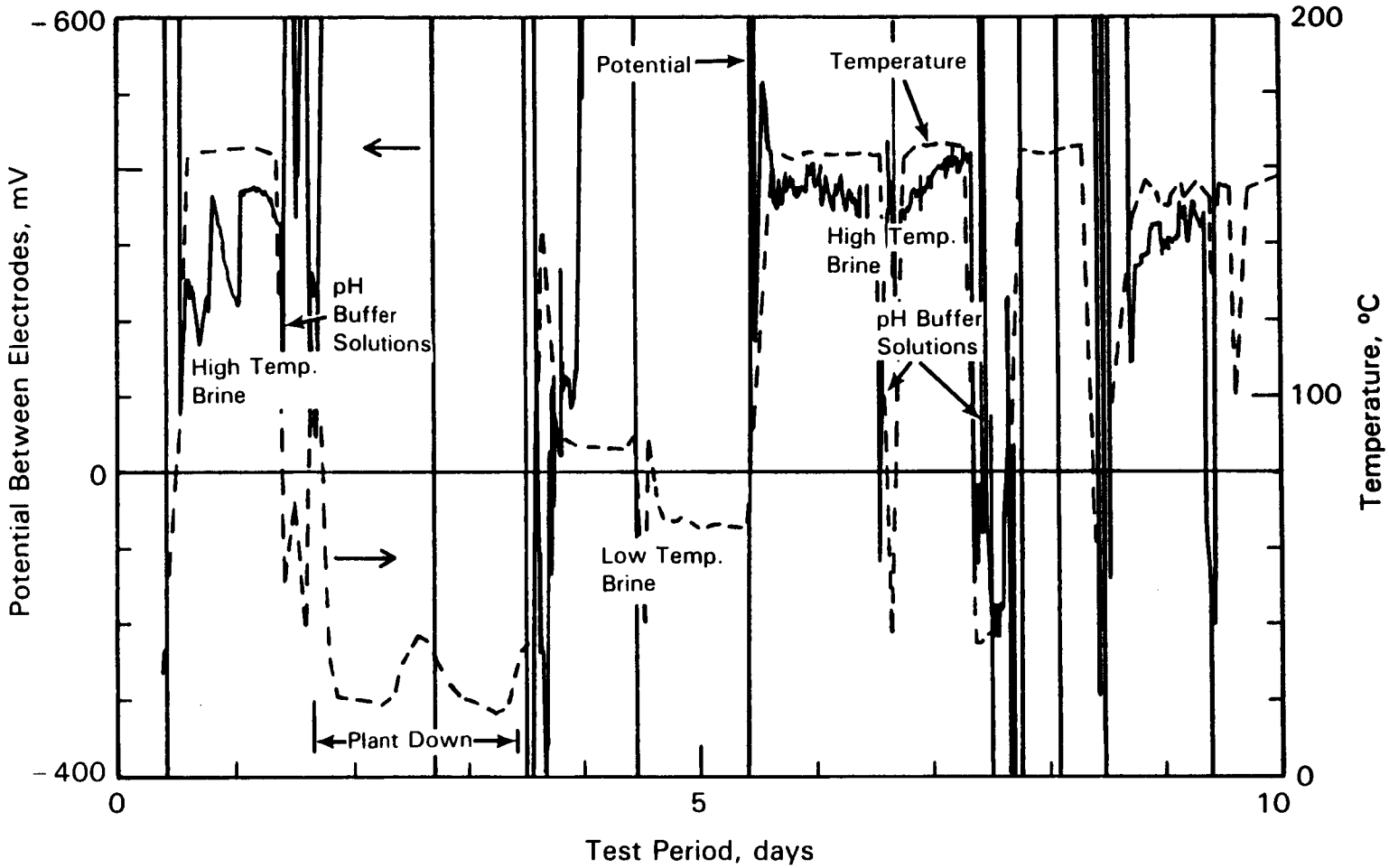

September 27, 1983

FIGURE 4.3.10. Response of Industrial (NGK-El-BJ) Ceramic pH Probe

the plant brine outlet temperature of 65-80°C. Laboratory testing had shown reasonable performance at 95-100°C.

Figures 4.3.11 and 4.3.12 show data for another ceramic probe that was paired with a ceramic Ag/AgCl-filled reference electrode. This electrode required no pumping. Three separate calibration intervals are traced in Figure 4.3.11; Figure 4.3.12 amplifies one of them. The millivolt jump from pH 5 buffer solution to pH 7 is reasonable. The intermediate level for the pH 3.2 buffer suggests a problem. The probe was left in the test loop and exposed to high-temperature brine. The readings returned to previous values. New calibration buffers were prepared and then circulated through the test loop. Again, anomalous behavior was observed. The reference electrode was removed and checked in the laboratory; it was good. The pH sensor was checked and a hairline crack was found near the mechanical seal. Exactly what fractured the sensor is unknown; overtightening is suspected to be the cause.

The lack of a good low-temperature (below 95°C) response on these probes is one serious drawback towards getting the design into commercial production. A second inherent flaw is the fragile nature of the probes. The final versions were all enclosed in protective metal cages to protect them from damage during insertion or removal as well as from velocity fluctuations during "steady" operation. Difficulty in sealing the inner workings of the probe from outside fluids plagued early versions, but the problem was being solved when testing stopped. The conclusion from this testing is that no commercial ceramic pH probes are suitable for service in geothermal brines at this time.

4.3.2 Solid-State pH Electrode Testing

Details of the design of the solid-state pH sensors are given in Phelan, Taylor, and Baxter (1980) and Taylor and Phelan (1980). The ion sensitive field effect transistor (ISFET) is a solid-state type FET-based sensor that has been specifically tailored for hydrogen ion detection. Details of the ISFET are shown in Figure 4.3.13 (Phelan, Taylor, and Kugler 1985). Its operation is depicted schematically in Figure 4.3.14 (Phelan, Taylor, and Kugler 1985). The gate coating, through surface interactions with the ions in solution, produces a field that changes the channel conductance of the FET in proportion to the concentration of ions. The coating material must be resistant to chemical attack to survive in geothermal environments. Alumina (Al_2O_3) and tantala (Ta_2O_5) were both shown to be gate materials with excellent

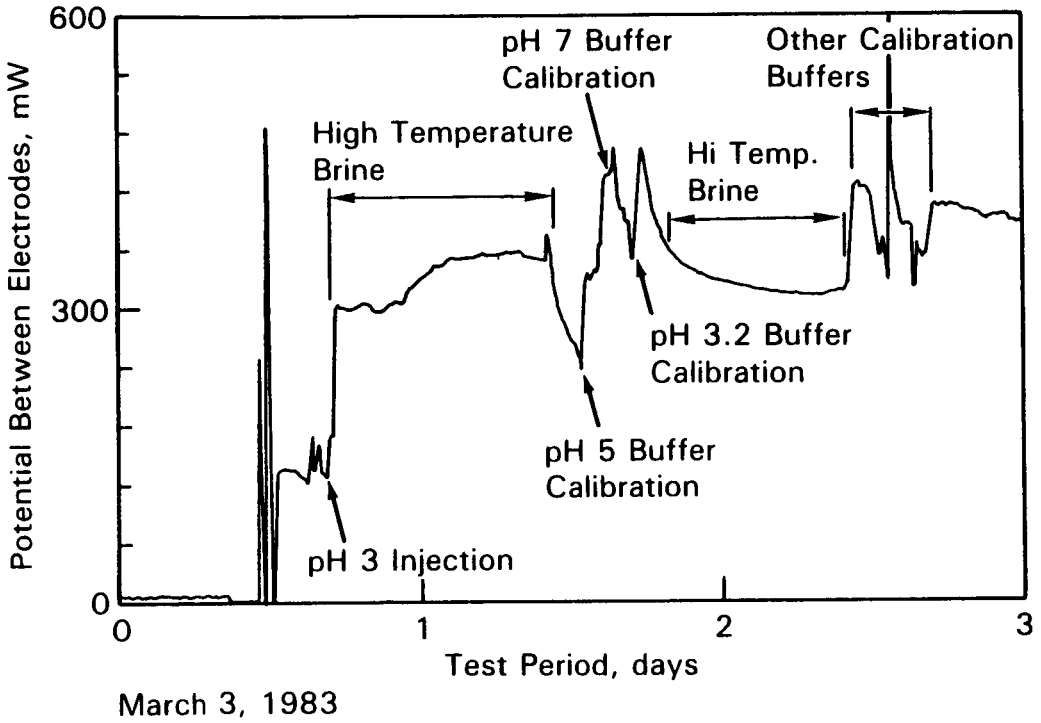

FIGURE 4.3.11. pH Probe Response to a Calibration Sequence

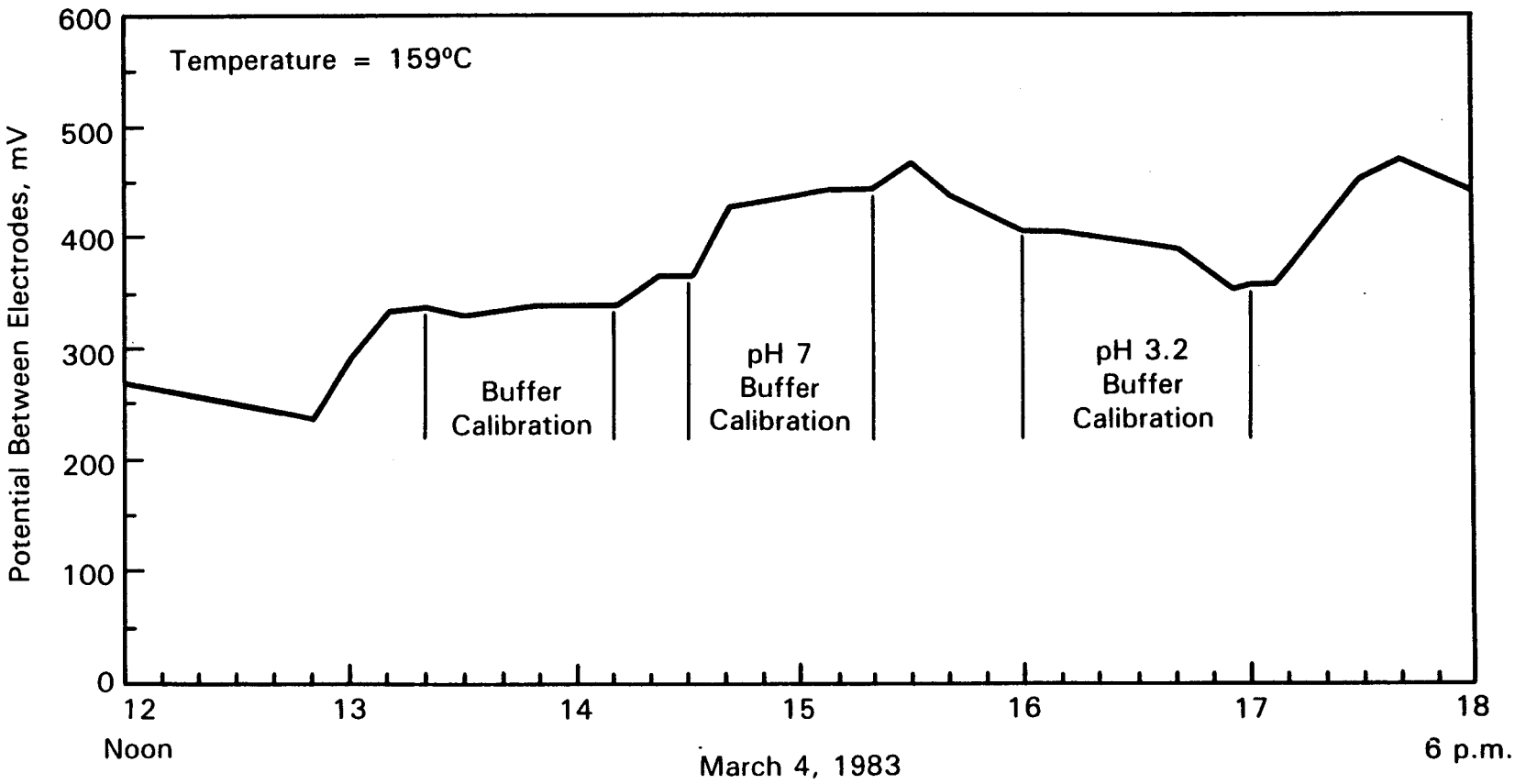

FIGURE 4.3.12. pH Probe Response to Buffer Solutions

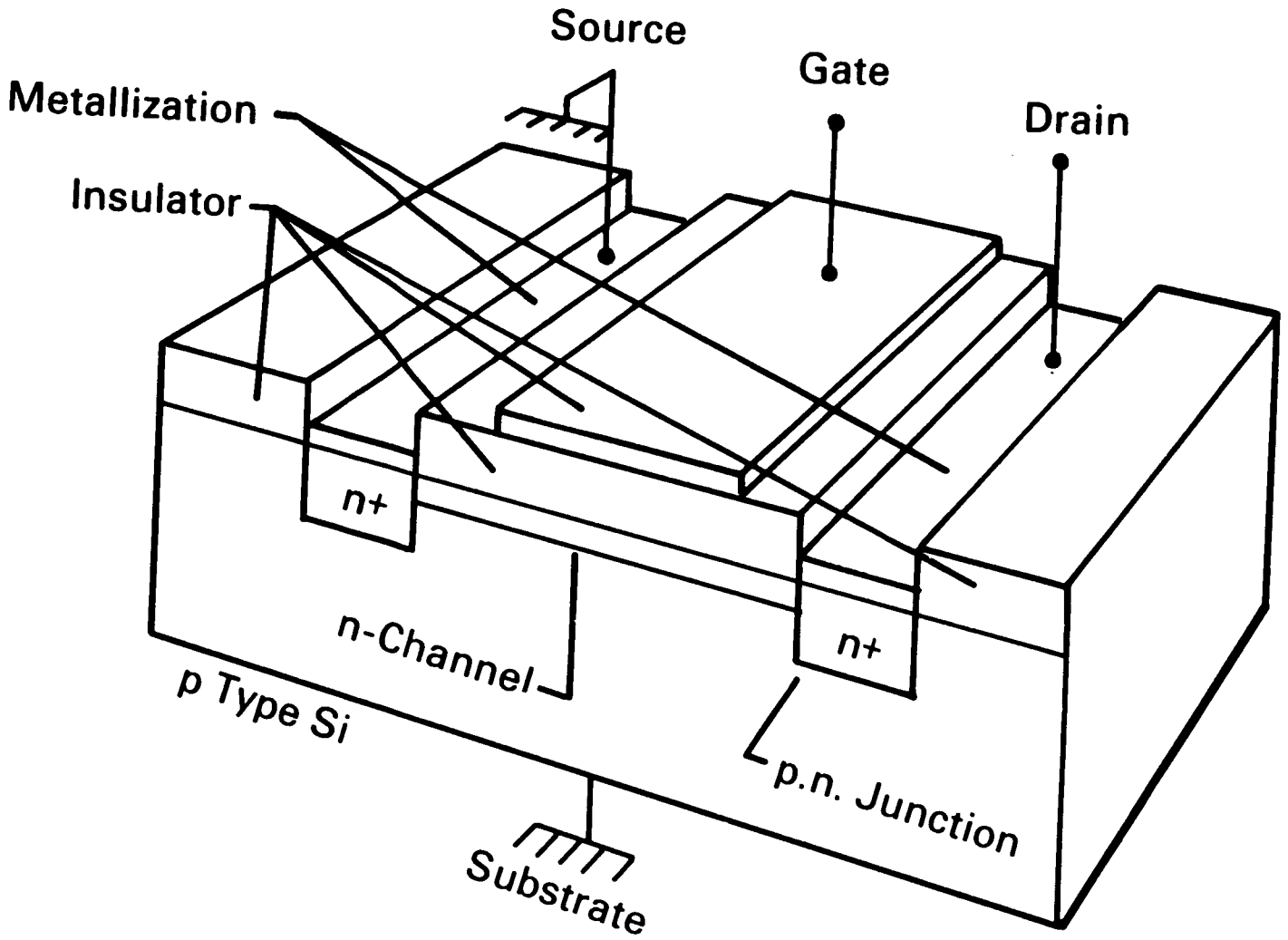

FIGURE 4.3.13. Structure of an Ion Sensitive Field Effect Transistor (ISFET)

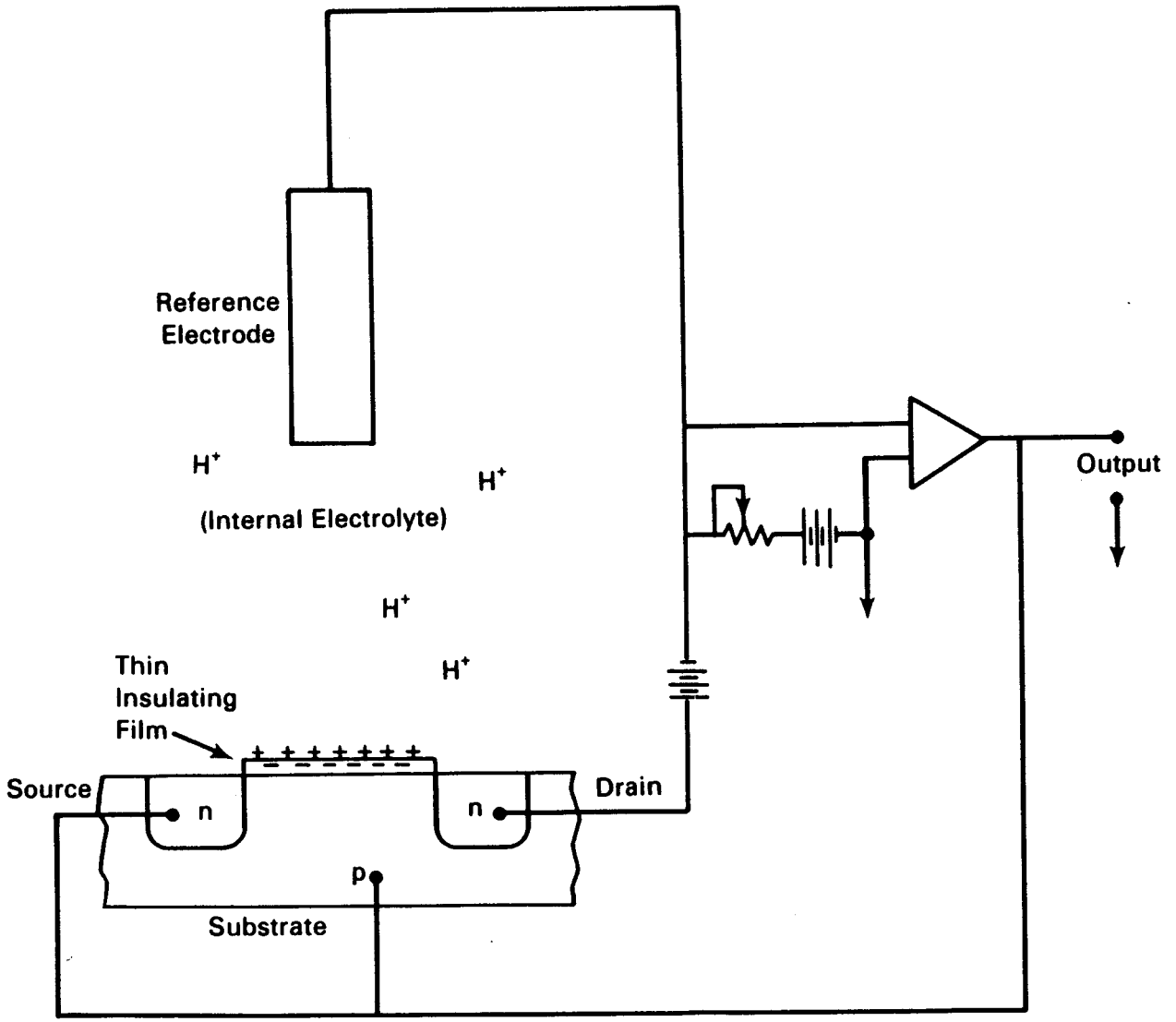

FIGURE 4.3.14. Schematic of ISFET Operation

chemical resistance. Both materials were tested in the laboratory and in the field. Laboratory test results are summarized by Phelan, Taylor, and Kugler (1985) and Taylor and Phelan (1980).

The goal of the field tests was to have the sensors respond reliably for 24 hours. Only two of four sensors were tested. Both sensors ultimately failed from seal failures that wet the ISFET leads. The two probes had responded to calibration solutions and were monitoring low-temperature brine overnight when the pumped reference electrode failed. Figures 4.3.15 and 4.3.16 show averaged responses for two buffers and two brine streams (plant inlet and plant outlet). Probe 1 gave reasonable values and the averaged ones shown were quite stable with time. Probe 2 gave stable and reasonable values for the buffer solutions, but the brine pH values are not logical. The high-temperature brine readings were obviously erroneous. (Room temperature brine pH values are 5.3 to 5.5. At higher temperatures, values should rise.) It is speculated that the seal failure developed sometime between the calibration tests and the monitoring of the geothermal brines. The failure of the pumped reference did not coincide with bad readings for hot geothermal brine.

Although the test interval was short, the response of the ISFET probes was encouraging. They had a low-temperature response in the range of interest to geothermal plants. Also, no chemical or mechanical degradation was noticed. The housing for these probes was rugged enough to withstand plant operator handling and mechanical abuse from the process. More work is needed to solve the seal problem and demonstrate longer-term service.

4.4 OXIDATION-REDUCTION POTENTIAL CELL (ORP PROBE)

Geothermal fluids are normally in a strongly chemically reduced state because of the H_2S present. The ORP cell is sold by many companies, but none of the commercial designs will work at 400°F and 1000 psi. The PNL design in Figure 4.4.1 was used successfully for a year in field conditions. It uses commercial electronics but PNL-designed electrodes. The cell uses a platinum electrode and high-temperature silver/silver chloride reference electrode to detect changes in oxidation state of the brine. It is very sensitive to the presence of oxygen. It also responds to changes in Fe^{++}/Fe^{+++} ratios, which are affected by additional gases such as H_2S. Figure 4.4.2 illustrates response of the ORP probe to a seven-minute injection of oxygen. Calculations

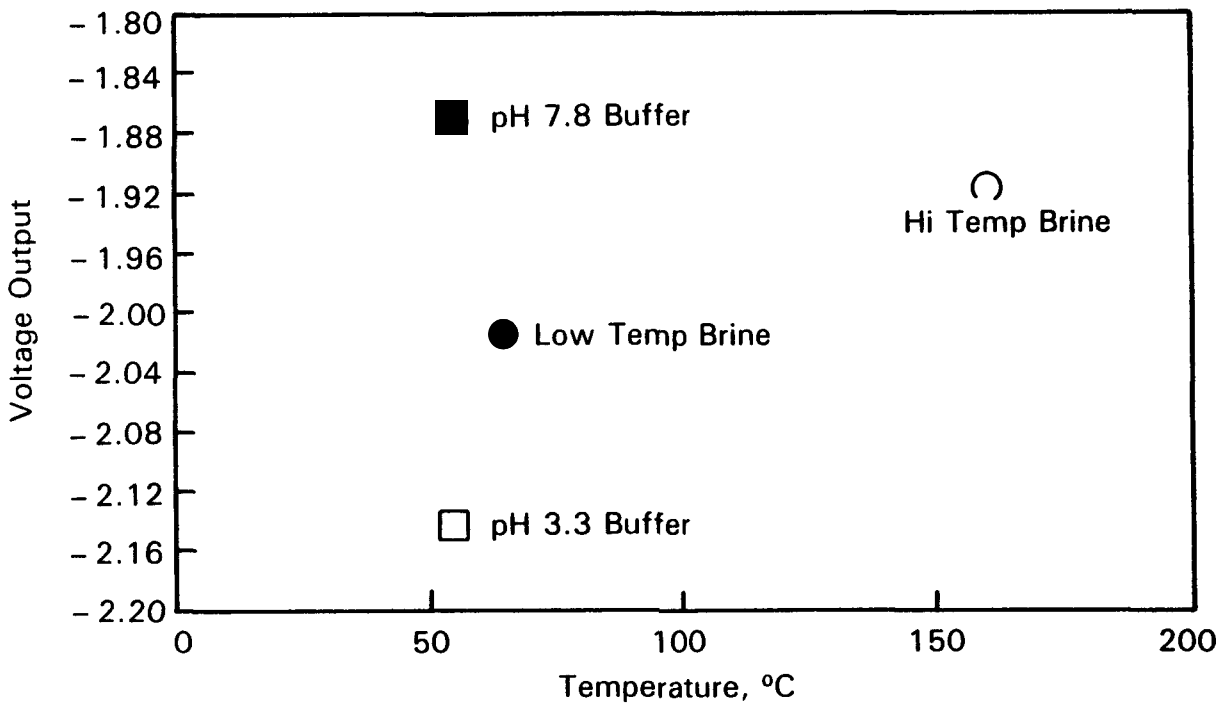

FIGURE 4.3.15. Solid State pH Probe (1) Response

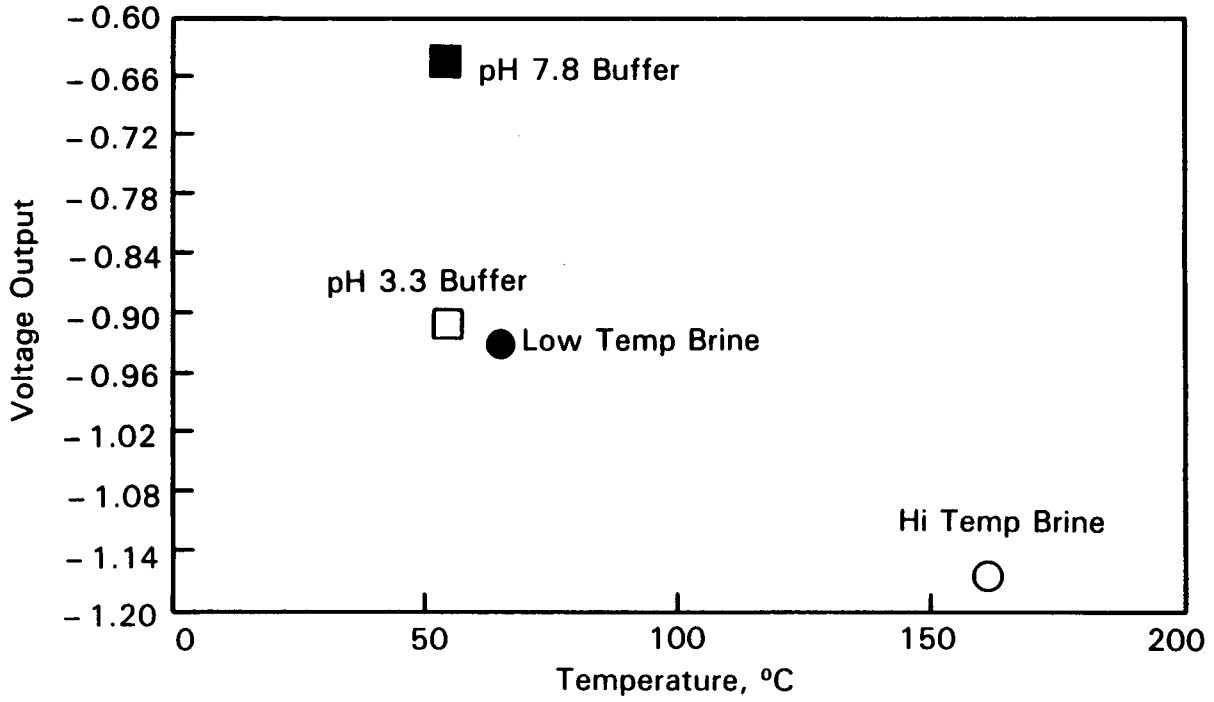

FIGURE 4.3.16. Solid State pH Probe (2) Response

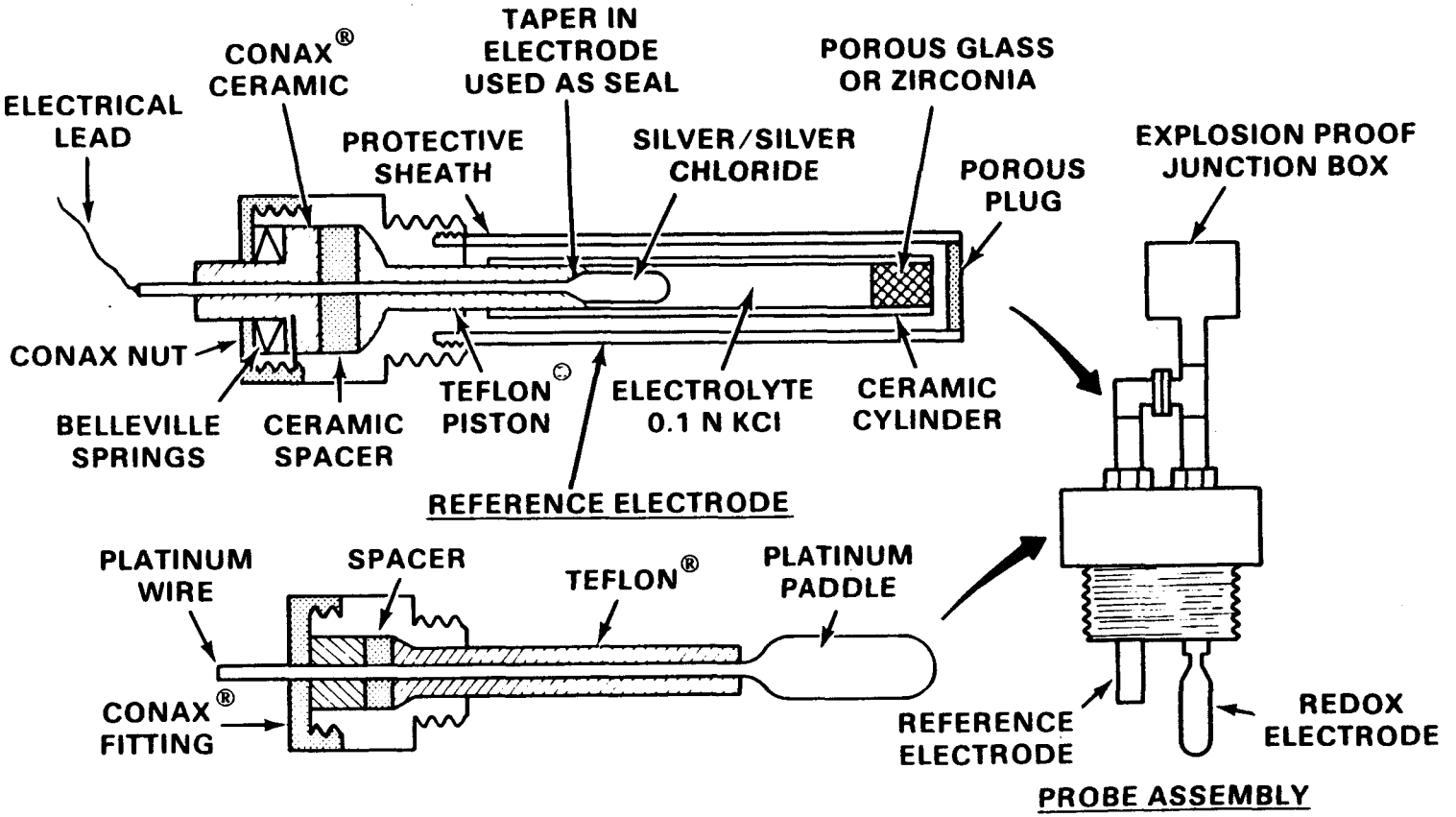

FIGURE 4.4.1. Oxidation Reduction Potential Probe

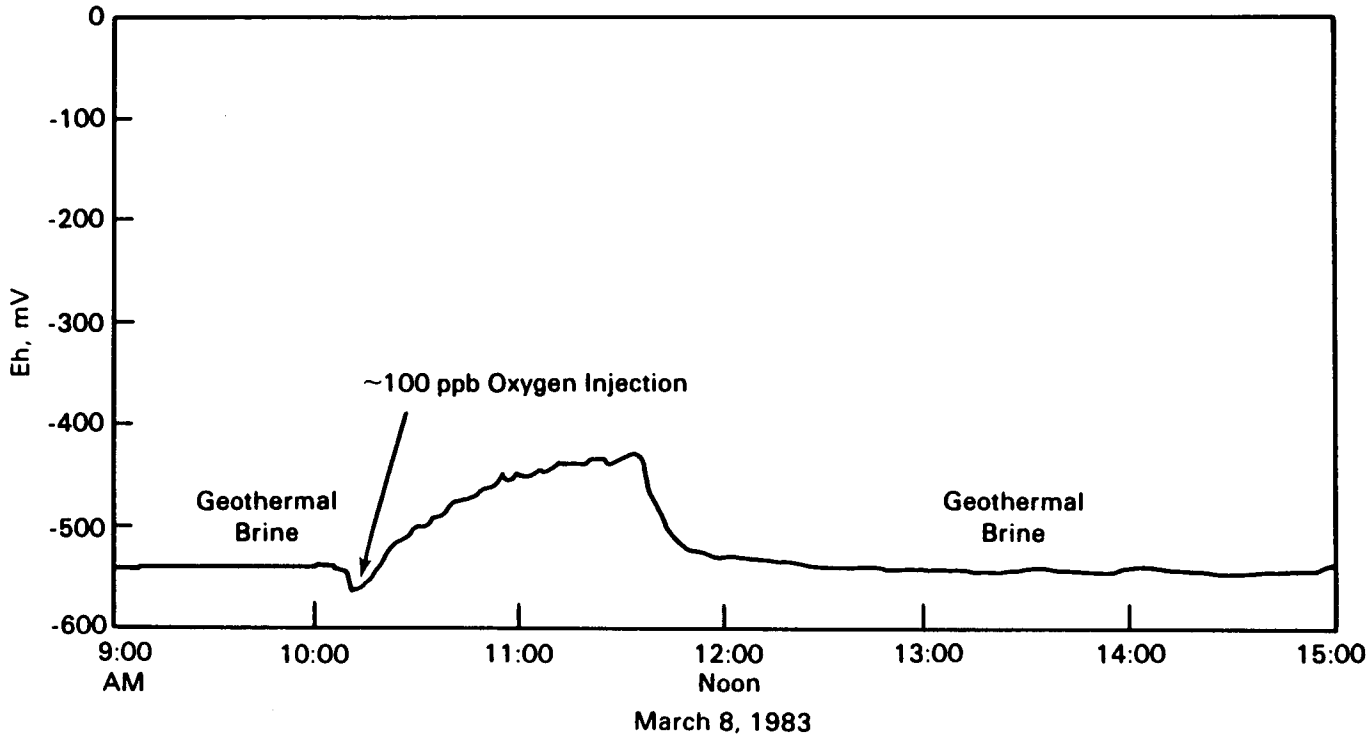

FIGURE 4.4.2. ORP Probe Response to Oxygen Injection

indicated the oxygen concentration was 100 parts per billion (ppb) at the probe. A measured value taken just upstream of the probe using a manual analysis kit was 40 ppb. The decay part of the curve just after 11:30 shows recovery time when the oxygen is shut off.

Figure 4.4.3 shows several important operating characteristics of the cell at the plant inlet. Normal operating voltages vary between -500 and -700 mV. Outputs below -700 mV usually indicate saturated electronics. Outputs above -500 mV could mean oxygen was present or some component was failing. An erratic response usually means some component is failing.

The initial response in Figure 4.4.3 is normal for the brines being tested. On February 9, 1983, the reference electrode failed. On February 12, 1983, the reference electrode was replaced. For about one week the cell was giving slightly low readings while the reference electrode became "conditioned." After "conditioning," the cell worked well for about one month. This "conditioning" period for the reference electrode varied from minutes to days. (The same design was used occasionally with the pH probes and is discussed in Section 4.3.) Since the reference electrodes were not commercial devices, some variation in performance was expected but not entirely explainable.

The trace in Figure 4.4.4 was recorded at the plant outlet. The three spikes in the plot correspond to times when the plant came down suddenly, then soon returned to operation. Our best guess is the ORP probe indeed did see trace amounts of oxygen entering the brine. The source of the air leak was never identified, however.

At various times the ORP probes were also paired with the quasi-reference electrode described earlier. As long as the electrolyte flow remained constant, the reference voltage was stable and the ORP probe functioned reliably. Often, however, the electrolyte pumps failed and the probe readings were meaningless.

A reliable pumped reference electrode could find successful application in industry. The model we tested requires too much attention to be accepted by industry.

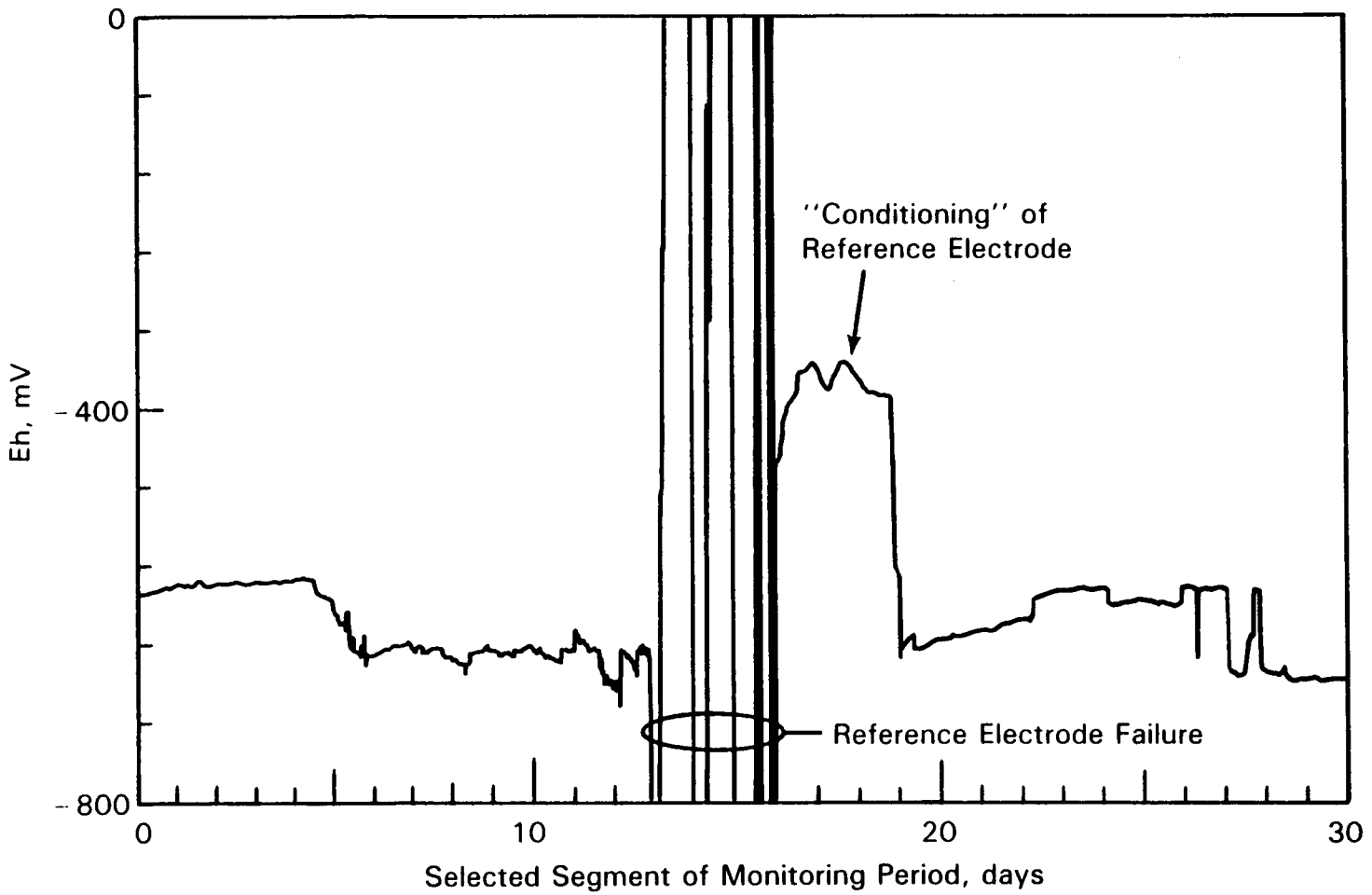

January 27, 1983

FIGURE 4.4.3. Plant Inlet Oxidation/Reduction Potential

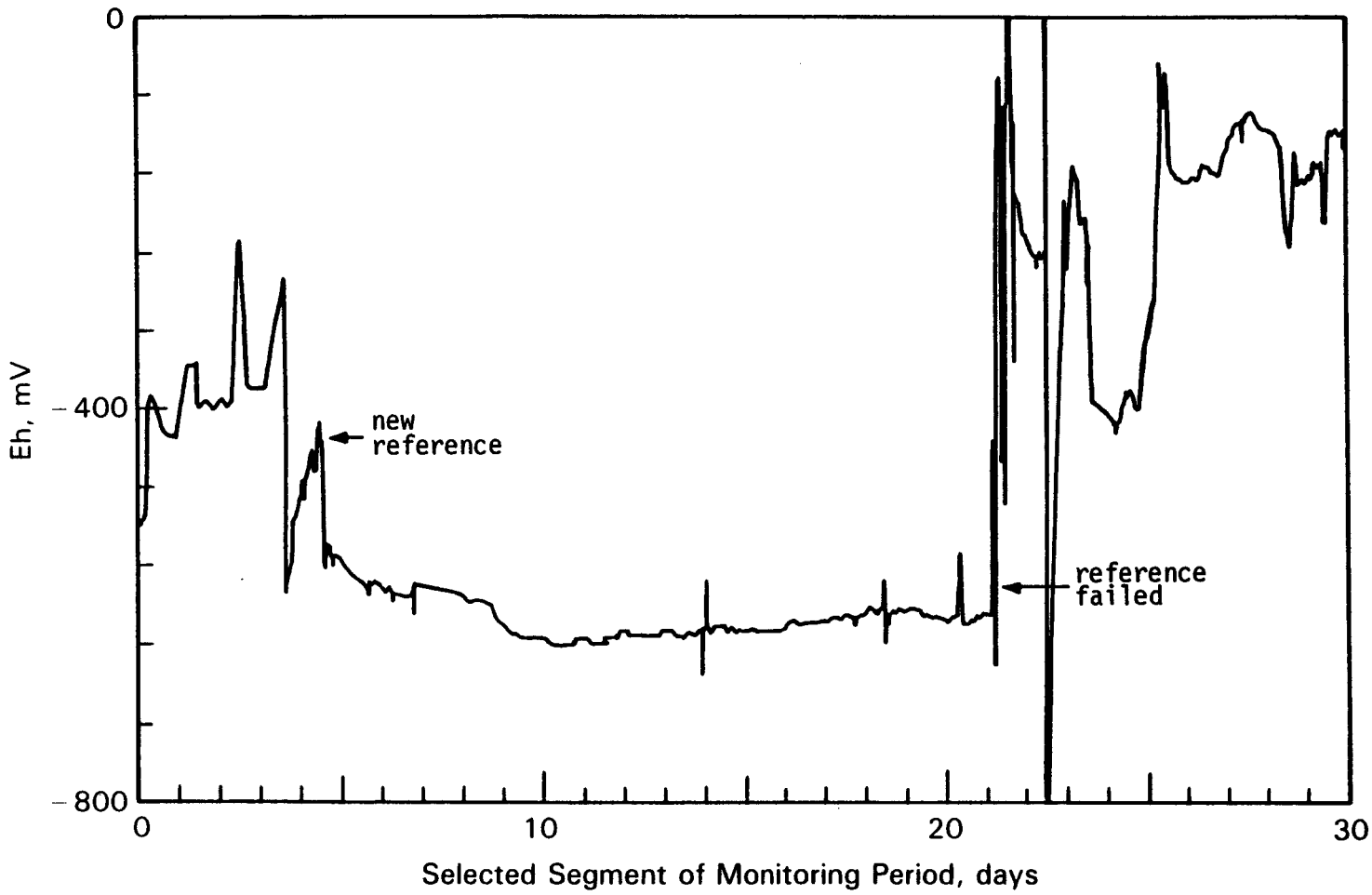

November 17, 1982

FIGURE 4.4.4. Plant Outlet Oxidation/Reduction

4.5 CONDUCTIVITY

Electrical conductivity is an excellent continuous measure of brine salinity. If foreign materials such as well-kill fluids, drilling mud, oils, or gases come through the plant, the conductivity cell registers the change from normal salinity, alerting the operators that something has changed. Conventional electrode-type cells quickly develop a film of scale and fail in geothermal systems. When the project started, there were no commercial sources of high-temperature, high-pressure electrodeless cells, so PNL built the unit shown in Figure 4.5.1. This cell can be built as either an insertion probe or as the flow-through type shown in Figure 4.5.2. A voltage spike is applied to one toroid (about 400 times/s), then the signal is picked up in the second toroid and converted to a voltage in special time-gating electronics (Danielson and Koski 1979b). The principle is similar to an ac transformer, with the brine forming the conductivity path. Similar instruments are now available commercially for lower temperature, but they were not tested. The PNL cell has special features to seal the toroids against leaks during rapid temperature and pressure cycles, and this design worked successfully for over two years at temperatures of 350°F and pressures up to 600 psig. Details of the design have been reported by Danielson and Koski (1979b). The flow-through cell has been designed to work with commercial electronics.

Laboratory testing of the cells was completed in autoclaves using 0.10 M KCl as the electrolyte. Test temperatures as high as 250°C were used. Temperature cycling between 25 and 250°C did not affect repeatability of the measurements. Figure 4.5.3 compares literature values and the experimental points from autoclave testing.

The conductivity probes were originally developed to prove the reliability of electrodeless conductivity cells in geothermal brines. That was accomplished. (Automatic temperature compensation was not built into the commercial electronics we used, but could be incorporated in future models.)

Later the instrument was able to detect gas bubbles in the brine. (Some modifications to the electronics were made to aid understanding of the instrument's response.) Gas bubbles are generally carbon dioxide. If carbon dioxide flashes out of the brine, a very rapid deposition of calcium carbonate scale follows. The gas breakout can be stopped by increasing system pressure. The secret to avoiding scale formation is to detect early any CO_2 evolution.

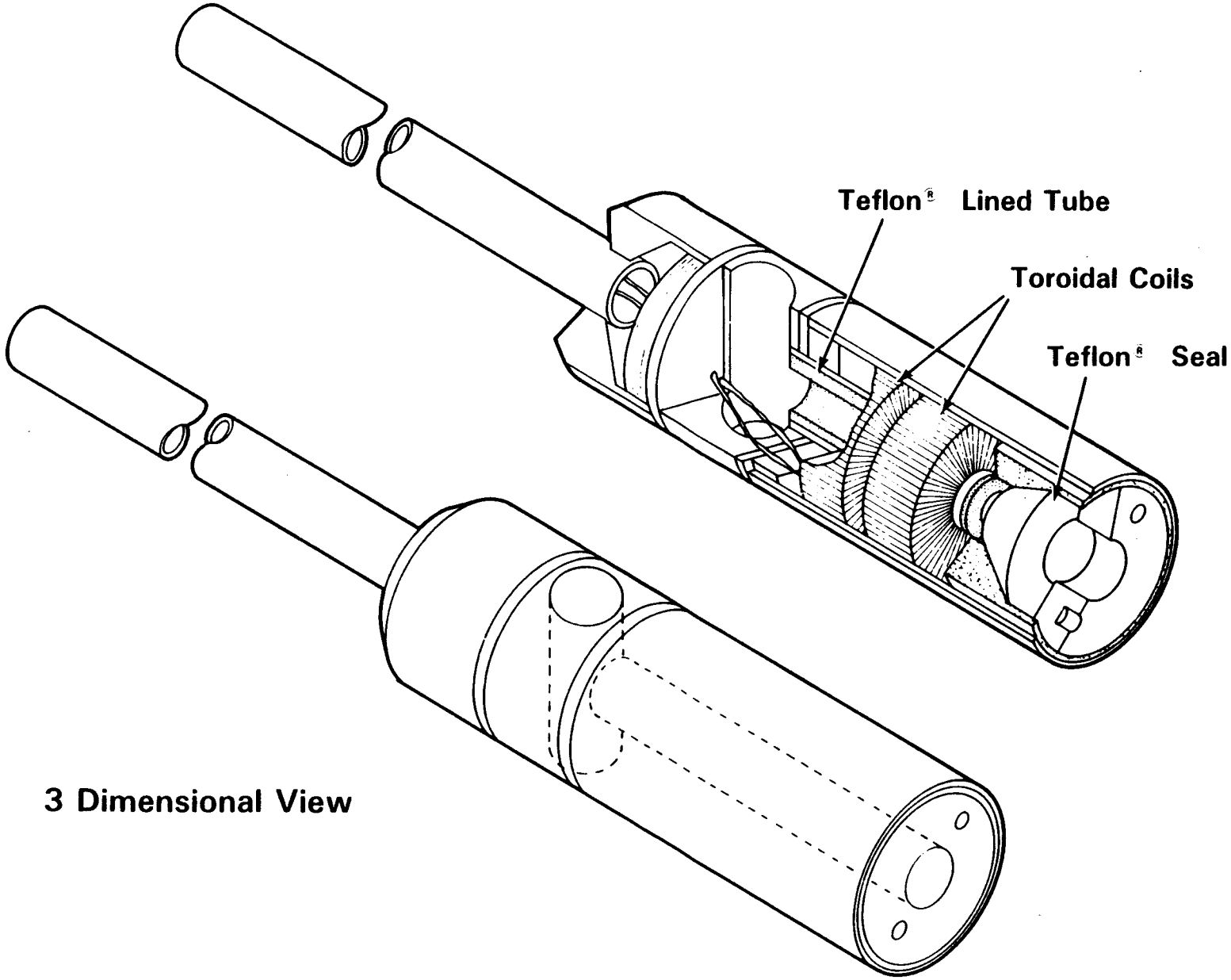

FIGURE 4.5.1. Submersible Electrodeless Conductivity Cell

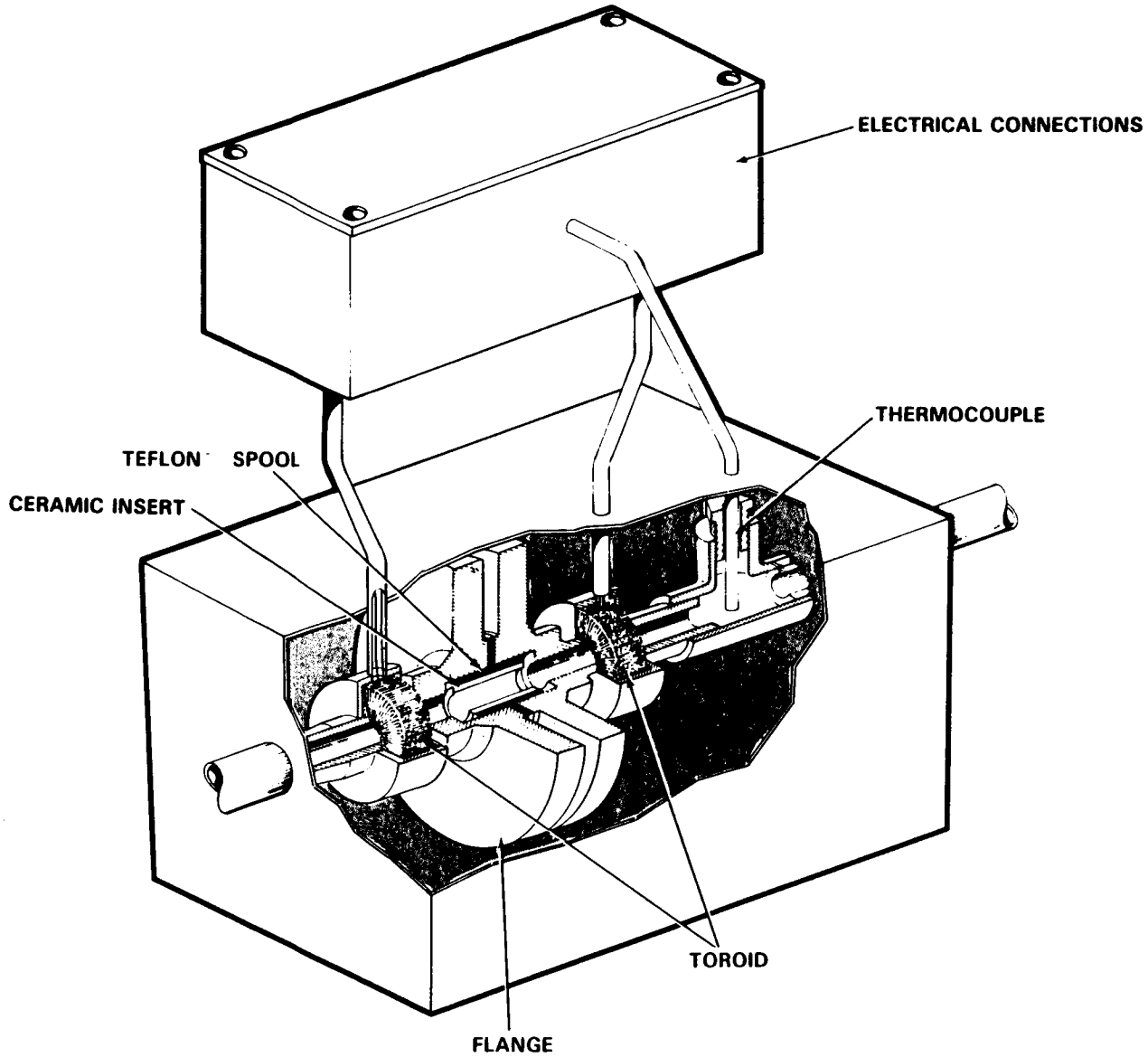

FIGURE 4.5.2. High-Pressure/High-Temperature Electrodeless Flow-Through Conductivity Cell

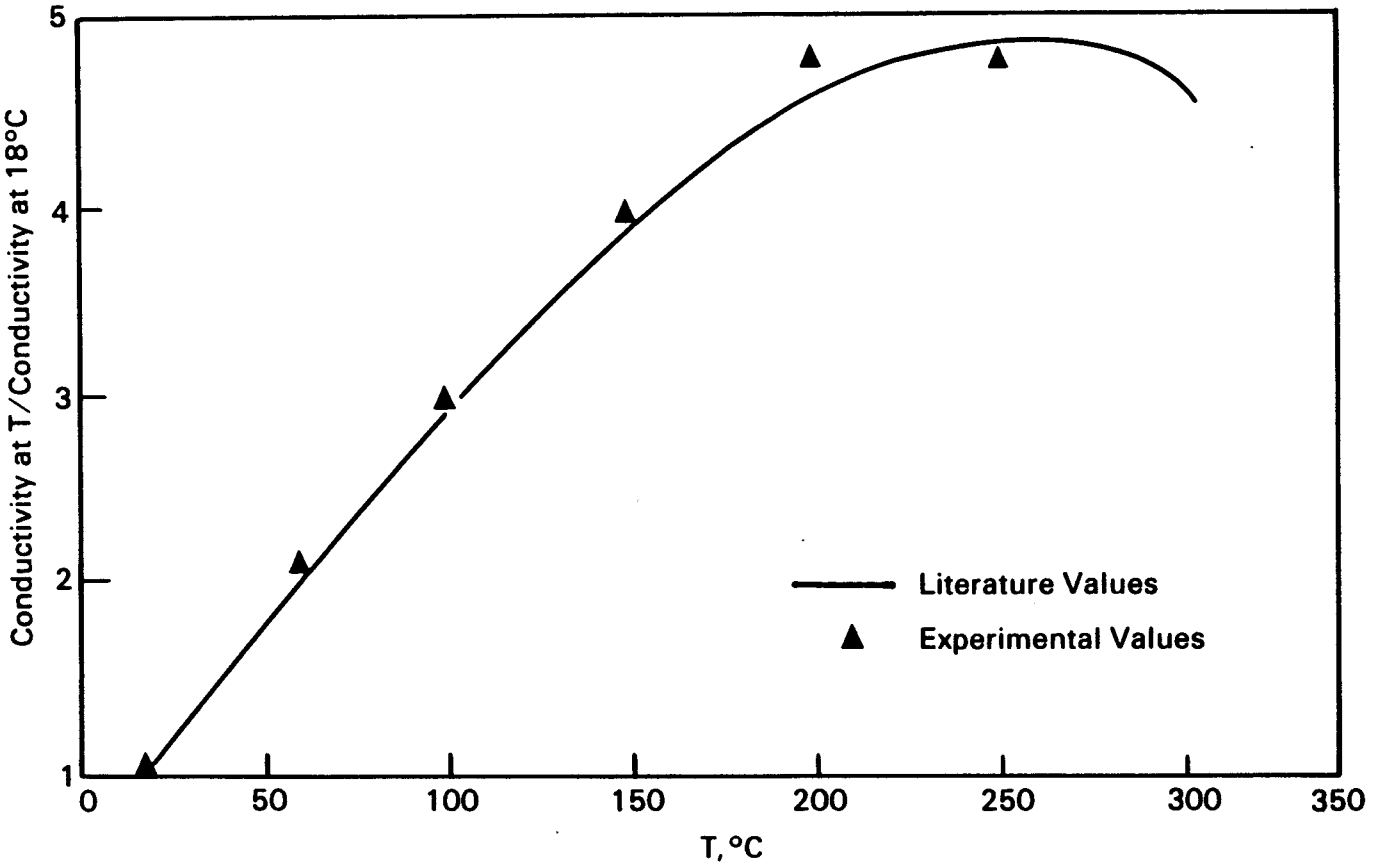

FIGURE 4.5.3. Literature and Experimental Conductivity Values

If bubbles are forming, the conductivity of the solution drops rapidly and should be detected by the meter. Figure 4.5.4 shows recorder traces from the meter when gas bubbles were generated by injecting gases into circulating fluid of 0.1 N KCl. Similar recorder traces were obtained by dropping brine pressure in the test loop and monitoring CO_2 gas breakout. Funding limitations prevented establishing detection limits for the cell or even optimizing the cell dimensions for bubble detection. Enough work was done, however, to demonstrate that the unit could be a valuable tool for plant operators to determine when CO_2 breakout was occurring.

The rapidly oscillating line in Figure 4.5.4 is the typical raw voltage output from the cell. The smoother line is an integrated value of departures from the baseline. The integration interval was adjustable, but typically set to 15 seconds. The trace of integrated voltages was the more sensitive indicator of bubble formation since most of the signal noise was filtered out by the integrating circuit. (A quartz window was installed in the test loop just downstream of the conductivity cell. This allowed visual verification of bubbles in the line.)

The traces shown in Figures 4.5.5 and 4.5.6 were produced from data taken at 15 min intervals. They illustrate several potential data interpretation errors. A normal voltage should be near -5 volts. The trace in Figure 4.5.5 shows a corrected version of data that was originally deemed good, i.e., instrument working properly. Earlier plots were made with an outdated conversion factor in the computer data reduction program. When the conversion factor was corrected (as shown in Figure 4.5.5), it was obvious the instrument had not been working for some time. This emphasizes the need for meticulous documentation of hardware as well as computer software changes.

Most of the responses in Figure 4.5.6 correspond to real events. Early in the plot the cooled stagnant brine shows a different output than the flowing outlet brine. The erratic responses on February 8 and 9, 1983, occurred because sudden cooling and heating had caused some seals to leak and changed the conductivity path through the cell. The cell's response from February 12 through February 19 reflected the changed operating condition where flow was stopped through the test loop but the cell was left filled with water (not brine). The slight voltage fluctuations are merely responses to ambient (hence fluid) temperature changes.

REPRODUCED FROM
BEST AVAILABLE COPY

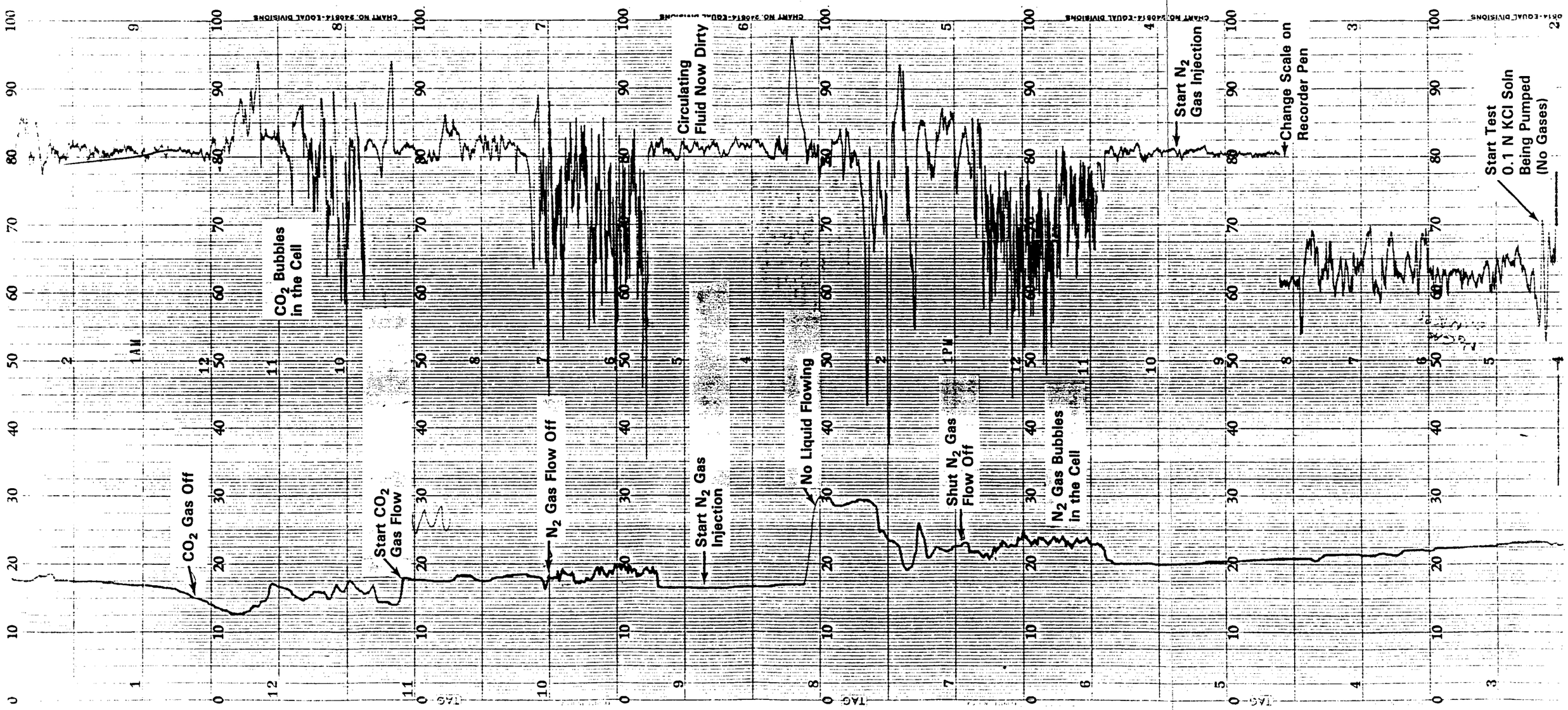

FIGURE 4.5.4 Recorder Trace From Conductivity Cell

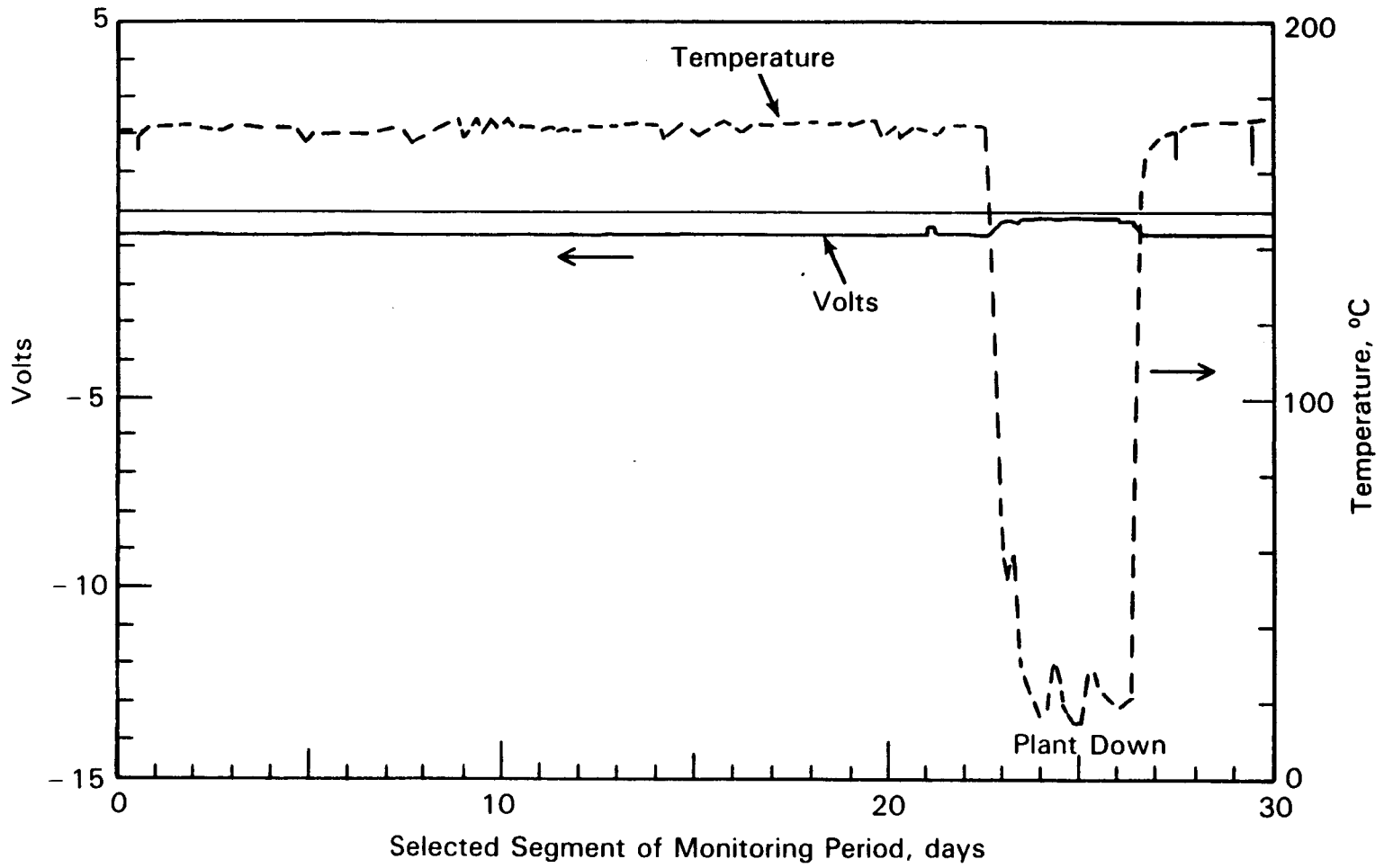

January 20, 1983

FIGURE 4.5.5. Plant Inlet Conductivity

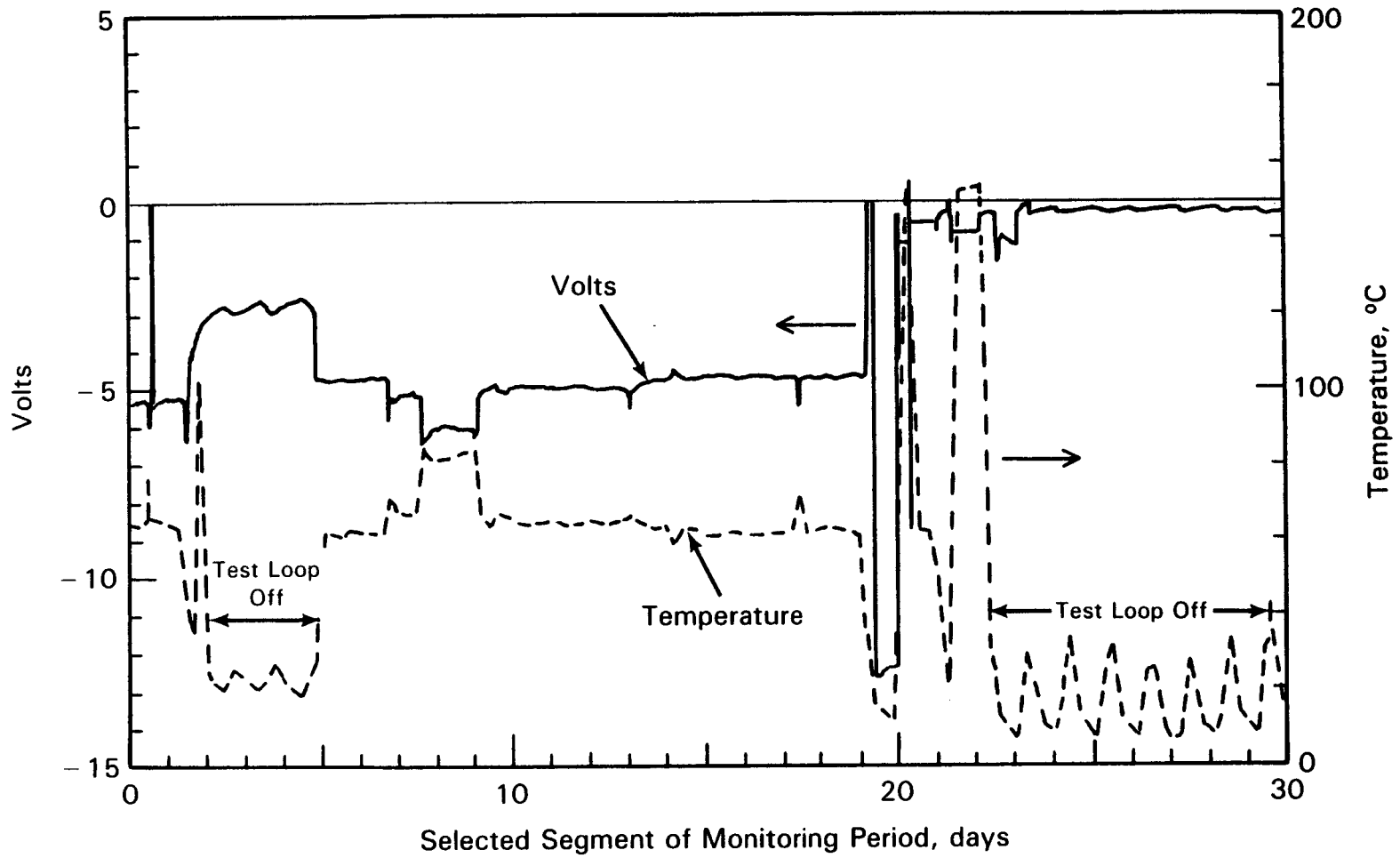

January 20, 1983

FIGURE 4.5.6. Plant Outlet Conductivity

5.0 REFERENCES

Callow, L., J. Richardson, and J. Dawson. 1976. British Corrosion Journal 11(3):123-139.

Danielson, M. J. 1979. "The Construction and Thermodynamic Performance of an Ag-AgCl Reference Electrode for Use in High-Temperature Aqueous Environments Containing H_2 and H_2S." Corrosion 35(5):200-204.

Danielson, M. J., and O. H. Koski. 1979. "Application of Linear Polarization Techniques to the Measurement of Corrosion Rates in Simulated Geothermal Brines." ASTM Special Publication 717, Geothermal Scaling and Corrosion, 1981. American Society for Testing and Materials, Philadelphia, Pennsylvania, pp. 41-56.

Danielson, M. J., and O. H. Koski. 1979. "Design and Construction of a High Temperature and Pressure Electrodeless Conductivity Probe." Rev. Sci. Instrum. 50(11):1433-1436.

Fontana, M., and R. Staehle, Eds. 1970. Advances in Corrosion Science and Technology, Vol. 6, Plenum Press, New York, New York, pp. 163-262.

National Materials Advisory Board (NAS-NAE). 1978. Assessment of the Characterization (In Situ-Downhole) of Geothermal Brines. NMAB-344, National Academy of Sciences, Washington, D.C., January.

Niedrach, L. W., and W. H. Stoddard. 1981. The Development of a High-Temperature pH Electrode for Geothermal Fluids - Task 1. PNL-3857. Prepared for the U.S. Department of Energy by Pacific Northwest Laboratory, Richland, Washington, March.

Niedrach, L. W., and W. H. Stoddard. 1983. The Development of a High-Temperature pH Electrode for Geothermal Fluids - Task 3. PNL-4651. Prepared for the U.S. Department of Energy by Pacific Northwest Laboratory, February.

Niedrach, L. W., and W. H. Stoddard. 1984. "Development of a High-Temperature pH Electrode for Geothermal Fluids." J. Electrochem. Soc.: Electrochemical Science and Technology, May, pp. 1017-1026.

Phelan, D. M., R. M. Taylor, and R. D. Baxter. 1980. "Detailed Conceptual Design of a High-Temperature CO_2 Sensor for Geothermal Application, Final Report Task 1." Prepared for the U.S. Department of Energy, Division of Geothermal Energy, by Pacific Northwest Laboratory, Richland, Washington.

Phelan, D. M., R. M. Taylor, and G. C. Kugler. 1985. "Detailed Conceptual Design of a High-Temperature CO_2 Sensor for Geothermal Fluids, Final Report Task 2." Prepared for the U.S. Department of Energy, Division of Geothermal Energy, by Pacific Northwest Laboratory, Richland, Washington, June.

Shannon, D. W. 1978. "The Role of Chemical Components in Geothermal Brines on Corrosion." National Association of Corrosion Engineers Paper No. 57, Corrosion/78 National Meeting, Houston, Texas, March 6-10.

Shannon, D. W., R. P. Elmore, and D. D. Pierce. 1981. Monitoring the Chemistry and Materials of the Magma Binary Cycle Generating Plant. PNL-4123. Prepared for the U.S. Department of Energy by Pacific Northwest Laboratory, Richland, Washington, October.

Taylor, R. M., and D. M. Phelan. 1980. Detailed Conceptual Design of High-Temperature Glass pH Electrode for Geothermal Applications, Final Report Task 2. PNL-3593. Prepared for the U.S. Department of Energy by Pacific Northwest Laboratory, Richland, Washington, March.

DISTRIBUTION

No. of Copies

OFFSITE

20 Gladys Hooper
Division of Geothermal Energy
U.S. Department of Energy
Washington, D.C. 20545

5 A. J. Adduci
U.S. Department of Energy
San Francisco Operations Office
1333 Broadway
Oakland, CA 94612

30 DOE Technical Information Center

H. K. Bishop
San Diego Gas & Electric Co.
P.O. Box 1831
San Diego, CA 92112

James Bresee, Manager
U.S. Department of Energy
Geosciences Team
1000 Independence Avenue SW
Washington, DC 20585

A. M. Cooper
Chevron
595 Market Street
P.O. Box 7147
San Francisco, CA 94120-7147

Dan Cubiciotti
Systems and Materials
Electric Power Research Institute
P.O. Box 10412
Palo Alto, CA 94303

Dennis Downs
Magma Electric Company
8 Miles East of Holtville
Evan Hewes Highway
Holtville, CA 92250

John Featherstone
2120 South 9th Street
El Centro, CA 92243

No. of Copies

Geo-Heat Utilization Center
Oregon Institute of Technology
Klamath Falls, OR 93003

Geothermal Resources Council
P.O. Box 1033
Davis, CA 95616

T. C. Hinrichs
Magma Electric Co.
993 Oak Lane
Escondido, CA 92025

Stu Johnson
Phillips Petroleum Company
655 East 4500 South
Salt Lake City, UT 84107

G. A. Kolstadt
U.S. Department of Energy
Division of Basic Energy Services
Washington, DC 20545

L. Kukacka
Brookhaven National Laboratory
Upton, NY 11973

Jim Kuwada
Geothermal Kinetics
3 Embarcadero Center No. 2045
San Francisco, CA 94111

W. Levers
Chevron Resources Company
P.O. Box 7147
San Francisco, CA 94120

Paul Lienau
Oregon Institute of Technology
Klamath Falls, OR 97601

Gil Lombard
San Diego Gas & Electric Company
P.O. Box 1831
San Diego, CA 92112

No. of Copies

2 Tiff Nelson
San Diego Gas & Electric Company
P.O. Box 1831
San Diego, CA 92112

Michael Pierce
Magma Power Company
P.O. Box 630
Calipatria, CA 92233

Lew Pratsch
U.S. Department of Energy
Heber R&D
1000 Independence Avenue SW
Washington, DC 20585

V. Roberts
Electric Power Research Institute
P.O. Box 10412
Palo Alto, CA 94304

B. Syrett
Materials Support Group
Electric Power Research Institute
P.O. Box 10412
Palo Alto, CA 94304

Technical Library
Union Oil Company of California
P.O. Box 7600
Los Angeles, CA 90017

Russ Tenney
Magma Power Company
P.O. Box 630
Calipatria, CA 92233

Don Thomas
Hawaii Institute of Geophysics
2525 Correa Road
Honolulu, Hawaii 96822

Paul Thrash
U.S. Department of Energy
San Francisco Operations Office
1333 Broadway
Oakland, CA 94612

No. of Copies

Victor Van Der Mast
Bechtel Group
50 Beale Street
San Francisco, CA 94105

J. H. Weare
University of California/San Diego
La Jolla, CA 92093

ONSITE

DOE Richland Operations Office

M. J. Anthony

32 Pacific Northwest Laboratory

R. L. Dillon
J. R. Divine
J. L. Duce
C. H. Kindle
O. H. Koski
D. B. Mackey
F. O. McBarron
D. D. Pierce
J. T. A. Roberts
R. J. Robertus (10)
D. W. Shannon (5)
R. G. Sullivan
Technical Information (5)
Publishing Coordination (2)